

FUNCTIONAL MRI STUDIES INTO THE NEUROANATOMICAL BASIS OF EYE MOVEMENTS

Functionele MRI Studies naar de
Neuro-Anatomische Basis van
Oogbewegingen

譚繼蓮

CAROLINE KAI LIN TAM

Cover design : A.W. Everaers and Caroline Tam
Layout : A.W. Everaers
Printed by : Offsetdrukkerij Haveka bv, Alblasserdam, The Netherlands
ISBN : 978-90-9023647-6

Copyright © 2008 Caroline Tam, Rotterdam, The Netherlands

All rights reserved. No part of this thesis may be reproduced, stored in a retrieval system or transmitted in any form or by any means, without written permission of the author, or, when appropriate, of the scientific journal in which parts of this thesis may have been published.

FUNCTIONAL MRI STUDIES INTO THE NEUROANATOMICAL BASIS OF EYE MOVEMENTS

Functionele MRI Studies naar de
Neuro-Anatomische Basis van
Oogbewegingen

PROEFSCHRIFT

ter verkrijging van de graad van doctor aan de
Erasmus Universiteit Rotterdam
op gezag van de
rector magnificus

Prof.dr. S.W.J. Lamberts

en volgens besluit van het College voor Promoties.

De openbare verdediging zal plaatsvinden op

WOENSDAG 7 JANUARI 2009 om 13:45 UUR

door

CAROLINE KAI LIN TAM

geboren te

HONG KONG, CHINA



PROMOTIECOMMISSIE

Promotor: Prof. dr. G. P. Krestin

Overige leden: Prof. dr. M. A. Frens

Prof. dr. P. Sillevius Smitt

Prof. dr. L. Feenstra

Copromotoren: Dr. A. van der Lugt

Dr. J. N. van der Geest

Dedicated to: Our Father, Dad, Mom, Kelvin, Ivy, Margaret, Bart, Doris and Emma

CONTENTS

Chapter 1	Introduction	9
PART 1	OPTOKINETIC AND SMOOTH PURSUIT EYE MOVEMENTS	23
Chapter 2	Differences between smooth pursuit and optokinetic eye movements: a functional magnetic resonance imaging study. (Accepted by Clinical Physiology and Functional Imaging)	25
Chapter 3	fMRI of optokinetic eye movements with and without a contribution of smooth pursuit. (J Neuroimaging, 2008, 18(2):158-167)	41
PART 2	SMOOTH PURSUIT AND FIXATION SUPPRESSION	57
Chapter 4	An fMRI study on smooth pursuit and fixation suppression of the optokinetic reflex using similar visual stimulation. (Exp Brain Research, 2008, 185(4):535-544)	59
PART 3	SACCADIC EYE MOVEMENTS	73
Chapter 5	Cortical and cerebellar activation induced by reflexive and voluntary saccades. (Exp Brain Research DOI 10.1007/s00221-008-1569-4)	75
Chapter 6	Cerebellar contributions to the processing of saccadic errors (Submitted)	97
PART 4	SUMMARY	117
Chapter 7	Summary	119
Chapter 8	Samenvatting	127
PART 5	APPENDIX	133
Appendix	List of publications	135
	Curriculum vitae	139
	About the author	141
	Acknowledgements	142

CHAPTER 1

INTRODUCTION

INTRODUCTION

Humans make eye movements to ensure proper processing of visual information. The study of eye movement control provides a window to the brain and can tell us how the brain processes information from the environment. Abnormal eye movement behavior can provide information about the functional deficits in certain parts of the brain. Moreover, eye movements are relatively easy to measure and the environment in which they are made is easy to manipulate.

This thesis presents five studies on the neuronal basis of human eye movement control investigated by functional magnetic resonance imaging (fMRI). This chapter provides a brief overview of the visual system, of eye movement behavior, and the techniques used in the experimental studies presented in this thesis.

ORGANIZATION OF THE VISUAL SYSTEM

The eye

Vision begins when light rays are reflected off an object and enter the eye through the cornea (Figure 1). The cornea and the lens refract the light onto the retina at the back of the eye. The primary function of the lens is to focus the visual image of the environment on the surface of the retina (Figure 2).

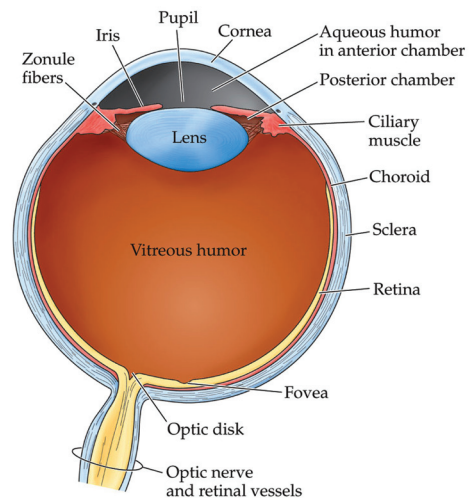


Figure 1: Schematic drawing of the human eye showing the cornea, the pupil, the iris, the lens, the retina and the optic nerve.

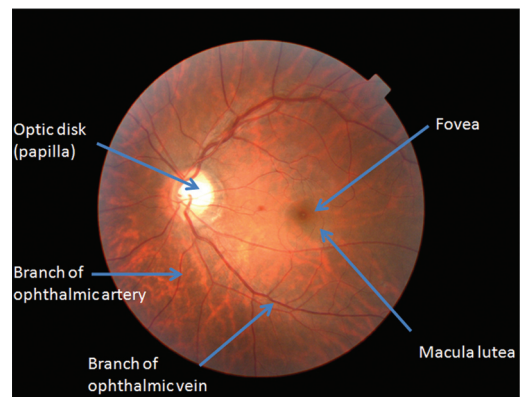


Figure 2: A photograph of the retinal surface showing the blood vessels, the fovea and the papilla (optic disk) where the optic nerve and the ophthalmic arteries and veins enter and leave the eye.

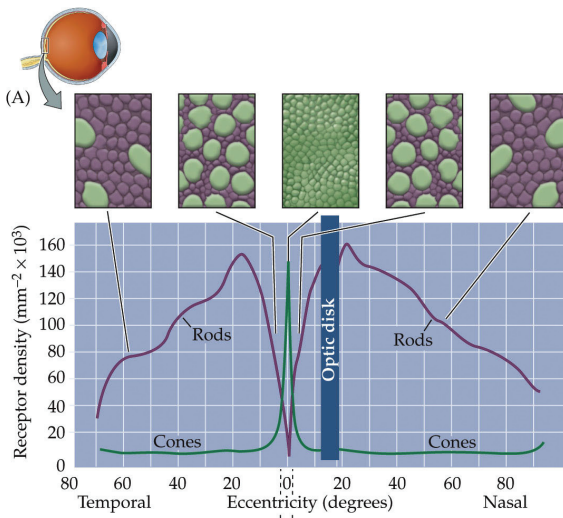


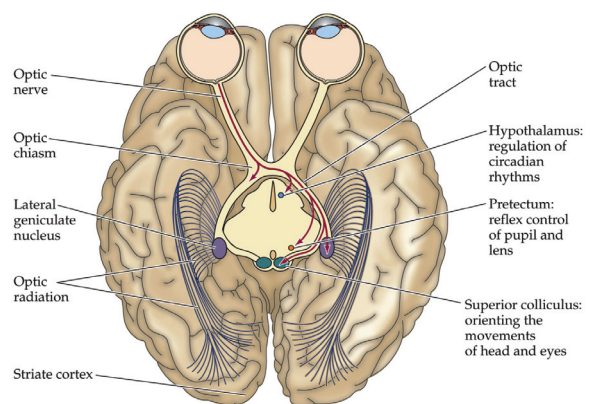
Figure 3: Distribution of rods and cones across the surface of the retina. Cones are present with a low density throughout the retina except at the center of the fovea. In contrast, rods are unevenly distributed across the retina. They are denser near to the fovea but not presented at the fovea. The image above illustrates the receptor density at various locations of the retina.

The inner surface of the retina consists of a thin layer of tissue containing millions of tiny light-sensing nerve cells called photoreceptors. These cells convert light into electrical signals, which are subsequently processed by retinal neurons and are finally conveyed by the ganglion cells to the brain through the optic nerve. Photoreceptors come in two types. Cones function optimally in bright light conditions and are involved in color vision. Rods can operate in dim light conditions as well. Photoreceptors are not uniformly distributed across the retina (Figure 3). The number of photoreceptors and hence visual acuity rapidly drops off from the center toward the periphery of the retina. Highest visual acuity is obtained at the fovea, which is dense with cones. The papilla (or optic disk) contains no photoreceptors at all and, being insensitive to light falling on it, is therefore known as the blind spot. It is the site where retinal axons leave the eye through the optic nerve (Figure 1).

The optic nerve is composed of the axons of the retinal ganglion cells and relays the visual information from the retina to several structures in the brain. The continuation of the optic nerve after the optic chiasm is the optic tract. The optic tract projects, among others, to the lateral geniculate nucleus (LGN) in the thalamus. The LGN relays the signals to the primary visual cortex (V1 or striate cortex) in the occipital lobe (Figure 4).

Visual cortex

The occipital lobe is the part of the cerebral cortex that is primarily responsible for processing visual information. The signals from the LGN enter the primary visual cortex (V1). From there on, the information is relayed to the other visual areas. In V1 the fovea is much more represented than the periphery which means that more processing capacity is available for the center of the visual field. Basically, there are two major cortical pathways for processing visual information. The ventral visual pathway, extending to V4, and



NEUROSCIENCE, Fourth Edition, Figure 12.1

© 2008 Sinauer Associates, Inc.

Figure 4: Central projections in the brain of retinal ganglion cells. Ganglion cell axons terminate in the lateral geniculate nucleus of thalamus (for visual processing), the superior colliculus (for reflexive eye and head movements), the pretectum (for reflex control of pupil and lens) and the hypothalamus (for regulation of circadian rhythms).

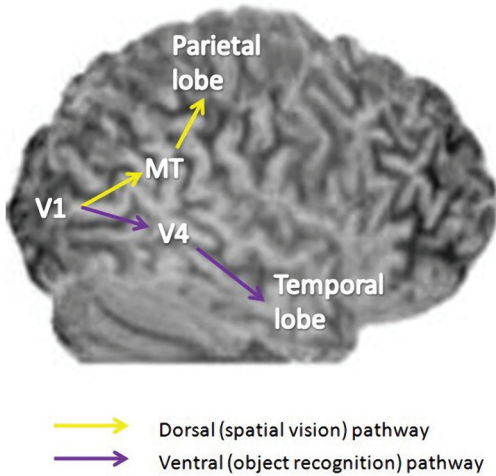


Figure 5: The two major cortical visual pathways illustrated in a human brain: the ventral pathway that leads to the temporal lobe is important for object recognition and the dorsal pathway that leads to the parietal lobe is important for spatial vision.

the temporal lobe is primary involved for color and object recognition. The dorsal visual pathway extends to the parietal lobe, and is involved in spatial processing of the visual environment. This pathway includes the middle temporal area (MT/V5) which is involved in the processing of visual motion (Figure 5).

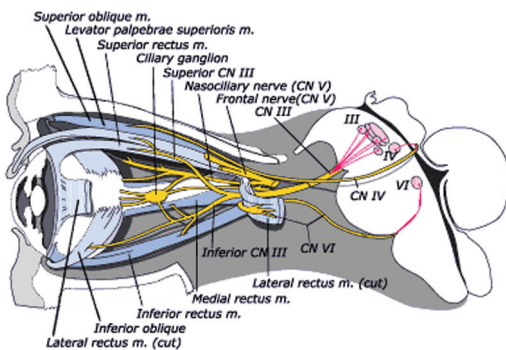


Figure 6: The location of the eye muscles (the superior rectus, the inferior rectus, the lateral rectus, the medial rectus, the superior oblique, and the inferior oblique muscles, the three cranial nerves for eye movement: (the oculomotor (CN III), the trochlear (CN IV) and the abducens nerve (CN VI)) and their brainstem nuclei [1].

EYE MOVEMENTS

The ability to make eye movements is important for two reasons. First, as indicated in the previous section, visual acuity is not homogenous across the visual field, being the highest at the center and far worse in the periphery. Eye movements are used to direct the fovea to new objects of interest, so that they can be processed in detail. Second, motion across the retina induces blurring and hampers detailed visual processing. Eye movements can be used to keep a stationary projection of the visual image in spite of motion of the visual scene or motion of the head.

Eye muscles and brainstem nuclei

The eye can be rotated in multiple directions within its socket by six different eye muscles. The muscles are innervated by cranial nerves which are controlled by oculomotor nuclei within the brainstem. The oculomotor nerve (CN III) exits from the rostral midbrain and innervates the superior, inferior and medial rectus muscle and the inferior oblique muscle. The trochlear nerve (CN IV) exits from the caudal portion of the midbrain and innervates the superior oblique muscle. The abducens nerve (CN VI) exits the brainstem from the junction between the pons and medulla and innervates the lateral rectus muscle.

TYPES OF EYE MOVEMENTS

The type of eye movements in humans can be divided into two broad categories: gaze stabilization and gaze aligning [2]. Gaze-stabilization movements are needed to stabilize the image on the fovea during movements of the observer relative to the visual world. These eye movements include the vestibule-ocular reflex (VOR) and the optokinetic reflex (OKR). Gaze-aligning movements are used to keep the projection of

a visual target on the fovea. These eye movements include smooth pursuit (SP), saccades and vergence.

1 The vestibular ocular reflex (VOR) occurs when the head is moving relative to the environment. It serves to stabilize the visual image on the retina during the motion of the head. VOR employs the inertial velocity sensors from the semi-circular canals in the inner ear to determine the speed and direction of the head movement. The vestibular signal is conveyed through the vestibular and oculomotor nuclei to generate an eye movement in the direction opposite to the direction of the head movement. The VOR is a very rapid reflex that moves the eyes within 10 ms after the onset of the head movement. During prolonged stimulation it gradually declines.

2 The optokinetic reflex (OKR) is evoked in response to a moving visual environment when the head is stationary. A familiar example is as our eyes follow the passing scenery from a moving vehicle. Similar to the VOR, it serves to stabilize the image on the fovea and in daily life the VOR and OKR operate in conjunction. The relative velocity of the image on the retina is used to induce eye movements in the same direction and with the same velocity as the moving environment. The OKR is largely driven by peripheral retinal stimulation, and is therefore optimally elicited by the movement of a large visual stimulus covering the visual field [2-4]. Since the maximum rotation of the eye is limited, a stimulus moving continuously in the same direction will elicit an eye movement pattern known as nystagmus, which consists of a combination of smooth tracking movements in the same direction as the moving stimulus (slow phases) and fast

resetting movements in the opposite direction (fast phases).

In a laboratory setting, the OKR response is readily evoked by showing a large moving pattern to the observer, for instance, stripes on a rotating drum. OKR has a latency of 60-100 ms, which is much longer than the VOR, due to the visual processing that is involved. The sensory signals that evoke the OKR response will not degrade over time and therefore OKR does not decline during prolonged stimulations.

3 Smooth pursuit eye movements (SP) are generated when we choose to follow a small moving object. These eye movements allow us to keep the image of that small object on the fovea, and to ignore the background on which it is moving. This enables us to see with great detail, for instance, watching a flying bird. The smooth pursuit system aims to match eye velocity to target velocity and is driven by the visual motion of a small target. Smooth pursuit has a latency of more than 100 ms. If the small object is moving too fast, smooth pursuit will fall behind and the smooth pursuit is interspersed with quick sudden movements, known as catch-up saccades.

Fixations occur when our eyes are looking at a small stationary target. This behavior can be considered as smooth pursuit of a target with zero velocity. During fixation at a stationary target, the background may move. Normally, a moving background could evoke an optokinetic eye movement response (OKR). The suppression of a moving background during fixation on a stationary target is called **fixation suppression of the OKR**.

4 Saccadic eye movements, or saccades, are used to direct the eye rapidly to a new position in the visual scene. The purpose of saccades is to increase the effective visual resolution of a scene. Since only objects presented at the fovea can be processed in detail, we make saccadic eye movements to direct gaze to various parts of the visual scene. With the help of visual memory, a perception of the whole visual scene can be obtained [5-8].

Saccades can be classified into two broad categories: reflexive and higher-order saccades [2, 9, 10]. Reflexive saccades are saccades toward suddenly appearing targets. The fast phases during nystagmus and the catch-up saccades during smooth pursuit are also examples of reflexive saccadic eye movements. Higher-order saccades are more volitional in nature and include voluntary, memory-guided and delayed saccades. Such saccades are made with a cognitive judgment in order to determine when and where to move gaze. They occur, for instance, during reading in which the words of a text are looked at in order [2, 9, 10].

Saccades are fast eye movements. The peak angular speed of the eye during a saccade reaches up to 600 degrees per second [11]. Saccades last from about 20 to 200 ms. Both the speed and the latency are related to the amplitude of the saccade. These relationships between saccade amplitude, duration and peak velocity are known as the saccade main sequence. Furthermore, saccades are ballistic, that is, their direction and amplitude are specified in advance, and can hardly be altered during the ongoing saccade. Normal saccades are highly accurate.

5 Saccadic adaptation is a process to modify the amplitudes of a saccade when saccades are becoming inaccurate, for example, due to a decrease in muscle strength from aging or due to brain damage. When a saccade is inaccurate, the amplitudes or directions of saccades can be adjusted [12]. The amplitude of the saccade is modified in order to maintain a high accuracy with respect to the visual environment. Saccadic accuracy can be artificially reduced in the laboratory using a so-called saccade adaptation paradigm, in which the onset of a saccade triggers an intra-saccadic shift of the target to a new position [13]. In a saccadic adaptation paradigm, systematic post-saccadic visual errors induce a gradual change of saccadic amplitudes [14, 15].

6 In the eye movements described above, both eyes move in the same direction. **Vergence** moves the eyes simultaneously in different directions, producing a convergence or divergence of each eye's visual axis to focus an object that is near or far. These vergence eye movements serve to obtain a similar sharp image for both eyes simultaneously in order to maintain proper binocular vision. Vergence movements are small (less than 5 degrees) and slow (need 1 s for completion) with a relatively long latency of about 150-200 ms.

Brain areas involved in eye movement control

The nuclei in the brainstem, which innervate the eye muscles through the cranial nerves, receive input from several cortical and subcortical brain areas (Figures 7 and 8).

The superior colliculus (SC) and the frontal eye fields (FEF) project directly to the oculomotor nuclei in the brain stem. The SC is located below

the thalamus and receives input from cortical areas, as well as direct input from the retina (Figure 4). The frontal eye field (FEF: Brodmann Area 8 and 9) is located in the posterior extremity of the middle frontal gyrus and the precentral sulcus, anterior to the motor cortex.

Several other areas also have direct or indirect connections with the oculomotor brainstem nuclei. The supplementary eye field (SEF: Brodmann Area 6) is located in the medial anterior part of the supplementary motor area (SMA). The parietal eye field (PEF: Brodmann Area 5, 7, 39 and 40) is located in the intra-parietal sulcus (superior parietal and inferior parietal gyrus). The motion-sensitive area (MT/V5: Brodmann Area 21) is located in the middle temporal and superior middle temporal gyri. The oculomotor areas in the cerebellum includes (1) the oculo-

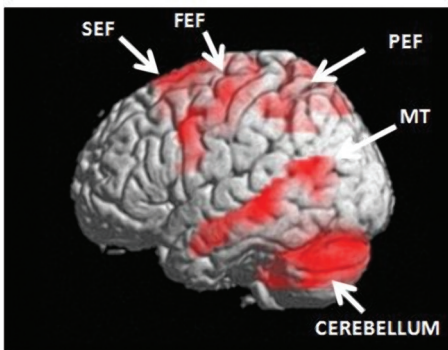
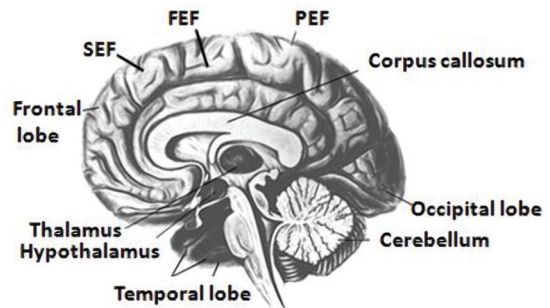


Figure 7 (left): The major oculomotor areas include: the frontal eye field (FEF, the precentral gyrus); the supplementary eye field (SEF, the supplementary motor area), the parietal eye field (PEF, the superior and inferior parietal gyri), the motion-sensitive area (MT/V5, the middle temporal gyrus) and the cerebellum.

Figure 8 (right): A schematic diagram of the major oculomotor areas [17].



TECHNIQUES TO STUDY THE NEURAL BASIS OF EYE MOVEMENTS

The neuronal basis of eye movements can be studied by several different techniques with their own characteristics and advantages and disadvantages.

1 Eye tracking. Eye movement control can be studied by measuring eye movements in response to particular stimulation. Measuring eye movements, also known as eye tracking, can be done using a variety of techniques, for instance video-oculography [18] or scleral search coils [19]. Using eye tracking the behavioral properties of eye movements like the velocity and the amplitude of saccadic eye movements can be accessed.

motor vermis and paravermis (cerebellar lobules V, VI – declive and VII – folium and tuber vermis), (2) the uvula and nodulus, (3) the flocculus and paraflocculus and (4) Crus I and II, which are laterally connected to lobule VII [16].

2 Animal lesion studies. Distinct brain regions, nerves or tracts in animals can purposely be damaged. The effect of a lesion can be studied by evaluating changes in eye movement behavior. For example, lesions in vermal areas V-VIII, including the oculomotor vermis, will impair the initiation, accuracy and dynamics of saccades [20, 21].

3 Human lesion studies. In humans, purposely damaging regions is not an option. Nevertheless, brain lesions can occur by trauma, infarct, infections or therapeutic intervention. This allows studying the behavioral consequences of lesions in a particular brain region. For example, patients with lesion at the frontal eye field will have deficits in saccade initiation and latency [22].

4 Electrophysiological recording. Neuronal recordings can be obtained in animals while an eye movement stimulus is presented. The correlation of the activity of different brain regions to the eye movement can then be analyzed [23].

5 Neurophysiological stimulation. Stimulation with electrodes can be applied at certain brain regions and the effects on eye movement behaviors can be observed. For example, stimulation of vermis VI and VII in the alert monkey induce and influence saccadic eye movements [24].

6 Electroencephalography (EEG). In humans and animals, EEG can be used to look at brain activity in relation to behavior. Electrical signals produced by the brain can be measured by electrodes that are placed on the skull of the subject. EEG allows us to follow electrical impulses across the surface of the brain and observe changes over split seconds of time. Although EEG allows for recording with millisecond resolution, it provides only a fairly crude estimate of the spatial location of brain areas that are involved in eye movement control [25].

7 Functional imaging. With functional imaging the location of brain activation involved in a specific task can be assessed. Commonly used techniques are positron emission tomography (PET), single photon emission computed tomography (SPECT), and magnetic resonance imaging (MRI).

In the present thesis video-oculography (VOG) and functional MRI are combined to investigate the neuronal basis of particular

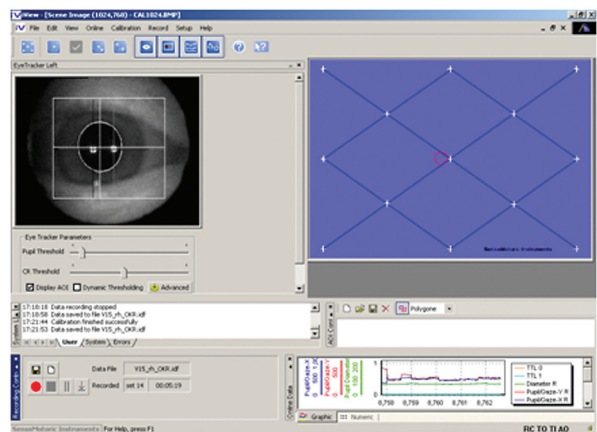


Figure 9: A screen image of the interface of the eye tracker used in the present thesis. The left eye of the subject is being monitored during the eye movement experiment. The position and the timing of the eye movement can be monitored on line. The data could be recorded for further analyses.

kinds of eye movements in healthy volunteers. During specific eye movement behavior, which was measured with VOG, the involvement of specific brain areas was assessed with fMRI.

8 Video-oculography. Video-oculography is a method for measuring eye movements using video images of the eyes. The position of the pupil is detected by image processing algorithms and used to calculate the rotation angles of the eye, by measuring the position of the pupil relative to the camera. The MR-compatible eye tracker had a sam-

pling rate of 50 Hz, tracking resolution of 0.1 degree and a gaze position accuracy of 0.5 to 1 degree.

FUNCTIONAL MAGNETIC RESONANCE IMAGING (fMRI)

An MRI scanner uses a huge magnet to create a uniform magnetic field. Normally, atomic nuclei are randomly oriented. Placed in a magnetic field the nuclei become aligned with the direction of the field. When pointing in the same direction, the magnetic signals from individual

of oxygen consumption and hence causes a significant increase in the local oxygen concentration. As a result the ratio between oxygenated and deoxygenated blood is changed. Deoxygenated blood contains the inherent substance (de-oxyhemoglobin), which distorts the magnetic field. Because of the relative decrease in concentration of the de-oxyhemoglobin, the uniformity of the magnetic field is increased, with a subsequent increase in signal.

Typically, a BOLD response can be divided into three sections (Figure 10). The initial dip, a very subtle effect immediately after the onset of the stimulus which last for about

0.5 to 1 second, causes the signal to go slightly below the baseline. Immediately after that is the positive BOLD response. BOLD response rises from the negative value to its highest positive value and forms a so-called overshoot. It takes 6-9 seconds to slowly rise to its peak and it takes 8 to 20 seconds to return to the baseline intensity after cessation of the stimulus. The period in between is referred to as the steady-state period.

The duration of the steady-state period depends on the duration of the stimulation. Due to the residual metabolic processes that continue after the cessation of the stimulation and blood flow increases, a post stimulus undershoot is observed, in which the response passes through the baseline and goes negative for several tens of seconds before it returns to its baseline [26, 27].

The signal changes during BOLD-fMRI are very small. Therefore, relative signal intensity changes are used in fMRI. The most popular approach for

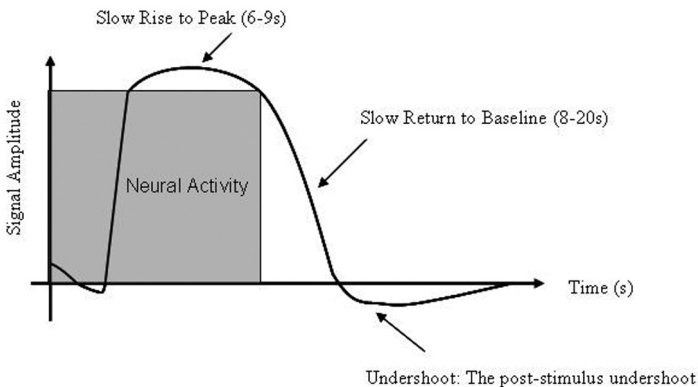


Figure 10: Schematic representation of the BOLD response with and without continuous stimulus.

nuclei add up resulting in a signal that is large enough to measure. The strength of the signal coming from a specific location depends on (besides various other factors) the type of tissue that is present.

Blood oxygenation level dependent (BOLD)-fMRI relies on the sensitivity of the MR signal to changes in oxygen levels within the blood circulation. The oxygen in the blood is extracted by the brain cells and used for cell metabolism. During brain activation, increasing demand of oxygen leads to a local increase in blood flow. The increase in blood flow exceeds the increase

comparing brain responses to different tasks is the block design. It consists of at least two states, an active task and a rest task. Subjects are asked to perform an active task related to the study purpose which is alternated with a rest task with respect to the active task being studied.

Extensive statistical analysis is performed to identify imaging voxels that show significant signal changes which vary with the changing brain states (active versus rest).

OUTLINE OF THE THESIS

The overall aim of the studies described in this thesis is to elucidate the cerebral and cerebellar contributions to the generation of several types of eye movements in humans. We used specific visual stimulations to investigate smooth pursuit, optokinetic and saccadic eye movements. The main focus of the thesis is the assessment of differences in activation patterns between different types of eye movements.

Part 1 – Smooth Pursuit and OKR

Oculomotor studies in foveated animals (e.g., monkeys) have shown that neurons can be specifically responsive to optokinetic and/or smooth pursuit eye movement responses [28-31]. Furthermore, clinical studies suggest that the OKR (optokinetic reflex) eye movement system and the smooth pursuit system may be impaired selectively [32, 33]. These studies suggest that the smooth pursuit eye movement and the OKR eye movement systems are controlled by distinct brain areas. However, functional imaging studies have failed to show differences in brain activation patterns for the two eye movement systems [34-39].

We investigated to what extent the brain areas for smooth pursuit and OKR eye movements can

be isolated. In **Chapter 2** we explored the OKR system by using an OKR stimulus consisting of a random pattern of dots with a limited lifetime. In such a stimulus each dot is repositioned every 50 ms, which is too short to evoke a smooth pursuit eye movement response, which is mediated by foveal stimulation. Hence this stimulus would effectively eliminate the smooth pursuit system, but still evokes a smooth optokinetic response. In this way we aimed to unravel the brain activations associated with the smooth pursuit and optokinetic eye movement systems.

In **Chapter 3** we investigated the contribution of the smooth pursuit system on the brain activations during OKR eye movements with the commonly used stimulus, i.e. a moving pattern of black and white stripes. One can argue that the movement of a large pattern of static elements does not only target the OKR system but also the smooth pursuit system. This confounding between smooth pursuit and OKR stimulation might explain the fact that in previous imaging studies no differences were found in activated brain areas between OKR and smooth pursuit stimulation, even when the two systems were compared directly. We assessed the difference in activation pattern between OKR eye movements elicited by limited lifetime dots and a moving pattern of black and white stripes.

Part 2 – Smooth pursuit and fixation suppression of the OKR

In the second part of this thesis we studied the differences between smooth pursuit and fixation suppression of OKR. Neurophysiological studies suggest that smooth pursuit and fixation suppression of OKR share many properties but can be regarded as two independent systems with overlapping pathways [31, 40-42]. For example, electrophysiological studies suggest that certain parietal lobe neurons discharge during fixations but not during smooth pursuit [41].

However, imaging studies suggest that the observed pattern of brain activations in humans induced by smooth pursuit of a single target is quite similar to the observed activity patterns during fixation suppression of OKR [34, 36, 38, 39, 43-46]. Differing from these studies, we developed a paradigm that induced the same retinal stimulation in both eye movement tasks. For smooth pursuit, the target moved against a stationary background that consists of a pattern of stripes, whereas during fixation suppression of OKR the target will be stationary and the background pattern will move. So, in both cases the visual background that is moving relative to the smooth pursuit or fixation target needs to be suppressed. The main question addressed in **Chapter 4** is whether smooth pursuit and fixation suppression of OKR yield differences that are related to the type of eye movement that is generated, despite the fact that the retinal stimulation is the same.

Part 3 – Saccadic eye movements

The final section of this thesis deals with brain activations induced by saccadic eye movements. It has been suggested that there are two separate and largely independent mechanisms involved in the generation of reflexive saccades and voluntary saccades [47]. For example, behavioral studies show that modification of the amplitudes of reflexive saccades in a saccade adaptation paradigm does not influence the amplitudes of voluntary saccades and vice versa [48-50]. In **Chapter 5** we investigate possible differences in cerebral and cerebellar activation patterns between reflexive and voluntary saccadic eye movements. Two experiments using the same experimental paradigm were performed. In the first experiment, we aimed to assess cerebral activations of saccadic eye movements and to compare the results with data from existing literature. In the second experiment, we focused on the cerebellum, specifically obtaining more

detailed activation within this brain structure. Would the differences between reflexive and voluntary saccadic eye movements be reflected by differences in cerebral as well as in cerebellar activation patterns?

In a classical saccadic adaptation paradigm, systematic post-saccadic visual errors induce a gradual change of saccadic amplitudes [14, 15]. In this paradigm, the processing of post-saccadic errors and the actual modification of saccadic amplitudes are confounded: changes in saccadic amplitude will induce a change in the post-saccadic error. In order to separate the processing of post-saccadic errors from the actual modification of saccadic amplitudes, other groups have implemented a paradigm in which the intra-saccadic target step was variable [51]. It was shown that variable intra-saccadic target steps do induce post-saccadic errors and corrective eye movements, but this so-called random paradigm does not lead to a gradual modification of saccadic amplitudes over a series of trials. Using PET imaging, no cerebral or cerebellar activations were observed when the condition with variable intra-saccadic target steps was compared to the condition without intra-saccadic target steps [51]. This is unexpected, since behavioral research has shown that the visual error is essential for saccade adaptation to occur [15]. It is conceivable that the neuronal activity related to the post-saccadic visual error processing is simply too small to detect with PET. In **Chapter 6** we investigate the activations in the cerebrum and the cerebellum related to the processing of post-saccadic errors. In order to induce post-saccadic errors without saccadic adaptation, we used variable forward and backward intra-saccadic target steps.

REFERENCES

1. The location of the eye muscles. [cited; Available from: http://www.childrenshospital.org/cfapps/research/data_admin/Site339/mainpageS339P18sublevel19.html].
2. Leigh, R.J. and D.S. Zee, *The Neurology of Eye Movements*. Third ed. 1999, New York: Oxford University Press.
3. Carpenter, R.H.S., *Movements of the Eyes*. Second ed. 1988, London: Pion Ltd.
4. Galati, G., et al., Cortical control of optokinetic nystagmus in humans: a positron emission tomography study. *Exp Brain Res*, 1999. 126(2): p. 149-59.
5. Amlot, R. and R. Walker, Are somatosensory saccades voluntary or reflexive? *Exp Brain Res*, 2006. 168(4): p. 557-65.
6. Hayakawa, Y., et al., Human cerebellar activation in relation to saccadic eye movements: a functional magnetic resonance imaging study. *Ophthalmologica*, 2002. 216(6): p. 399-405.
7. Schall, J.D., Neural basis of saccade target selection. *Rev Neurosci*, 1995. 6(1): p. 63-85.
8. Schiller, P.H. and E.J. Tehovnik, Neural mechanisms underlying target selection with saccadic eye movements. *Prog Brain Res*, 2005. 149: p. 157-71.
9. Straube, A. and H. Deubel, Rapid gain adaptation affects the dynamics of saccadic eye movements in humans. *Vision Res*, 1995. 35(23-24): p. 3451-8.
10. Walker, R., et al., Control of voluntary and reflexive saccades. *Exp Brain Res*, 2000. 130(4): p. 540-4.
11. Becker, W., S. Raab, and R. Jurgens, Circular vection during voluntary suppression of optokinetic reflex. *Exp Brain Res*, 2002. 144(4): p. 554-7.
12. Zuber, B.L., L. Stark, and M. Lorber, Saccadic suppression of the pupillary light reflex. *Exp Neurol*, 1966. 14(3): p. 351-70.
13. McLaughlin, S.C., Parametric adjustment in saccadic eye movements. *Percept Psychophys*, 1967. 2: p. 359-362.
14. Robinson, F.R., C.T. Noto, and S.E. Bevans, Effect of visual error size on saccade adaptation in monkey. *J Neurophysiol*, 2003. 90(2): p. 1235-44.
15. Wallman, J. and A.F. Fuchs, Saccadic gain modification: visual error drives motor adaptation. *J Neurophysiol*, 1998. 80(5): p. 2405-16.
16. Voogd, J. and N.H. Barmack, Oculomotor cerebellum. *Prog Brain Res*, 2005. 151: p. 231-68.
17. Major oculomotor areas. [cited; Available from: <http://www.niaaa.nih.gov/Resources/GraphicsGallery/Neuroscience/brainp127.htm>].
18. van der Geest, J.N. and M.A. Frens, Recording eye movements with video-oculography and scleral search coils: a direct comparison of two methods. *J Neurosci Methods*, 2002. 114(2): p. 185-95.
19. Collewyn, H., F. van der Mark, and T.C. Jansen, Precise recording of human eye movements. *Vision Res*, 1975. 15(3): p. 447-50.
20. Barash, S., et al., Saccadic dysmetria and adaptation after lesions of the cerebellar cortex. *J Neurosci*, 1999. 19(24): p. 10931-9.

21. Takagi, M., D.S. Zee, and R.J. Tamargo, Effects of lesions of the oculomotor vermis on eye movements in primate: saccades. *J Neurophysiol*, 1998. 80(4): p. 1911-31.
22. Lynch, J.C., Saccade initiation and latency deficits after combined lesions of the frontal and posterior eye fields in monkeys. *J Neurophysiol*, 1992. 68(5): p. 1913-6.
23. Electrophysiological recording. [cited; Available from: <http://www.yorku.ca/eye/electrop.htm>].
24. Ron, S. and D.A. Robinson, Eye movements evoked by cerebellar stimulation in the alert monkey. *J Neurophysiol*, 1973. 36(6): p. 1004-22.
25. EEG. [cited; Available from: <http://en.wikipedia.org/wiki/Electroencephalography>].
26. Buckner, R.L., et al., Detection of cortical activation during averaged single trials of a cognitive task using functional magnetic resonance imaging. *Proc Natl Acad Sci U S A*, 1996. 93(25): p. 14878-83.
27. Cohen, J.D., et al., Temporal dynamics of brain activation during a working memory task. *Nature*, 1997. 386(6625): p. 604-8.
28. Bremner, F., C. Distler, and K.P. Hoffmann, Eye position effects in monkey cortex. II. Pursuit- and fixation-related activity in posterior parietal areas LIP and 7A. *J Neurophysiol*, 1997. 77(2): p. 962-77.
29. Churchland, A.K. and S.G. Lisberger, Discharge properties of MST neurons that project to the frontal pursuit area in macaque monkeys. *J Neurophysiol*, 2005.
30. Ilg, U.J. and P. Thier, Visual tracking neurons in primate area MST are activated by smooth-pursuit eye movements of an "imaginary" target. *J Neurophysiol*, 2003. 90(3): p. 1489-502.
31. Komatsu, H. and R.H. Wurtz, Relation of cortical areas MT and MST to pursuit eye movements. I. Localization and visual properties of neurons. *J Neurophysiol*, 1988. 60(2): p. 580-603.
32. Barratt, H., M.A. Gresty, and N.G. Page, Neurological evidence for dissociation of pursuit and optokinetic systems. *Acta Otolaryngol*, 1985. 100(1-2): p. 89-97.
33. Hutton, S.B., et al., Smooth pursuit eye tracking over a structured background in first-episode schizophrenic patients. *Eur Arch Psychiatry Clin Neurosci*, 2000. 250(5): p. 221-5.
34. Konen, C.S., et al., An fMRI study of optokinetic nystagmus and smooth-pursuit eye movements in humans. *Exp Brain Res*, 2005. 165(2): p. 203-16.
35. O'Driscoll, G.A., et al., Differences in cerebral activation during smooth pursuit and saccadic eye movements using positron-emission tomography. *Biol Psychiatry*, 1998. 44(8): p. 685-9.
36. Petit, L. and J.V. Haxby, Functional anatomy of pursuit eye movements in humans as revealed by fMRI. *J Neurophysiol*, 1999. 82(1): p. 463-71.
37. Rosano, C., et al., Pursuit and saccadic eye movement subregions in human frontal eye field: a high-resolution fMRI investigation. *Cereb Cortex*, 2002. 12(2): p. 107-15.
38. Dieterich, M., et al., Horizontal or vertical optokinetic stimulation activates visual motion-sensitive, ocular motor and vestibular cortex areas with right hemispheric dominance. An fMRI study. *Brain*, 1998. 121 (Pt 8): p. 1479-95.
39. Tanabe, J., et al., Brain activation during smooth-pursuit eye movements. *Neuroimage*, 2002. 17(3): p. 1315-24.

-
40. Krauzlis, R.J. and F.A. Miles, Role of the oculomotor vermis in generating pursuit and saccades: effects of microstimulation. *J Neurophysiol*, 1998. 80(4): p. 2046-62.
 41. Lynch, J.C. and J.W. McLaren, Deficits of visual attention and saccadic eye movements after lesions of parietooccipital cortex in monkeys. *J Neurophysiol*, 1989. 61(1): p. 74-90.
 42. May JG, K.E., Crandall J, Changes in eye velocity during smooth pursuit tracking induced by microstimulation in the dorsolateral pontine nucleus of the macaque. *Soc Neurosci Abstr*, 1985. 11(79).
 43. Bense, S., et al., Direction-dependent visual cortex activation during horizontal optokinetic stimulation (fMRI study). *Hum Brain Mapp*, 2005.
 44. Berman, R.A., et al., Cortical networks subserving pursuit and saccadic eye movements in humans: an fMRI study. *Hum Brain Mapp*, 1999. 8(4): p. 209-25.
 45. Bucher, S.F., et al., Sensorimotor cerebral activation during optokinetic nystagmus. A functional MRI study. *Neurology*, 1997. 49(5): p. 1370-7.
 46. O'Driscoll, G.A., et al., Functional neuroanatomy of smooth pursuit and predictive saccades. *Neuroreport*, 2000. 11(6): p. 1335-40.
 47. Deubel, H., Separate adaptive mechanisms for the control of reactive and volitional saccadic eye movements. *Vision Res*, 1995. 35(23-24): p. 3529-40.
 48. Alahyane, N., et al., Oculomotor plasticity: are mechanisms of adaptation for reactive and voluntary saccades separate? *Brain Res*, 2007. 1135(1): p. 107-21.
 49. Erkelens, C.J. and J. Hulleman, Selective adaptation of internally triggered saccades made to visual targets. *Exp Brain Res*, 1993. 93(1): p. 157-64.
 50. Gaveau, V., et al., Self-generated saccades do not modify the gain of adapted reactive saccades. *Exp Brain Res*, 2005. 162(4): p. 526-31.
 51. Desmurget, M., et al., Functional adaptation of reactive saccades in humans: a PET study. *Exp Brain Res*, 2000. 132(2): p. 243-59.

PART 1

OPTOKINETIC AND SMOOTH PURSUIT EYE MOVEMENTS



香港

HONG KONG

CHAPTER 2

DIFFERENCES BETWEEN SMOOTH PURSUIT AND OPTOKINETIC EYE MOVEMENTS USING LIMITED LIFETIME DOT STIMULATION: A FUNCTIONAL MAGNETIC RESONANCE IMAGING STUDY

DIFFERENCES BETWEEN SMOOTH PURSUIT AND OPTOKINETIC EYE MOVEMENTS USING LIMITED LIFETIME DOT STIMULATION: A FUNCTIONAL MAGNETIC RESONANCE IMAGING STUDY

Accepted by Clinical Physiology and Functional Imaging

ABSTRACT

In this study we examined possible differences in brain activation between smooth pursuit and optokinetic reflexive (OKR) eye movements using functional magnetic resonance imaging (fMRI).

18 healthy subjects performed two different eye movement paradigms. In the first paradigm, smooth pursuit eye movements were evoked by a single moving dot. In the second paradigm, optokinetic eye movements without a smooth pursuit component were evoked by a foveal moving pattern of multiple dots with a limited lifetime.

As expected the two eye movement systems show overlapping network areas, but the direct comparison of the activation patterns between the two experiments showed that the FEF, MT/V5 and cerebellar area VI appear to be more activated during smooth pursuit than during optokinetic eye movements.

These results showed that the smooth pursuit and optokinetic eye movement systems can be differentiated with fMRI using limited lifetime dots as an effective OKR stimulus.

INTRODUCTION

Smooth pursuit and optokinetic reflexive (OKR) eye movements both aim to stabilize moving images on the retina and can be readily observed when a person is tracking a slowly moving stimulus in his field of view [1]. The main difference is that the execution of OKR depends on processing of global motion signals whereas the execution of pursuit depends on local motion signals. For a small moving object, the smooth pursuit eye movement system keeps the image of that object on the fovea where the retinal visual acuity is highest [2]. This enables an observer to see with great detail, for instance, a bird in flight. A large moving pattern on the other hand evokes a so-called OKR, for instance when an observer is looking out of a steadily moving train. OKR eye movement is needed for the observer to stabilize the image which produced by the relative movement between the environment and the observer onto the retina. The slow tracking movements during OKR eye movements are interspersed with saccadic-like resetting eye movements in the opposite direction, yielding the classical saw-tooth pattern known as optokinetic nystagmus [1, 3]. The smooth pursuit eye movement system is driven by the visual motion of the small target [4], whereas the OKR system seems to be driven mainly by the motion of a large stimulus on the whole retina [1, 3, 5]. In a laboratory setting, smooth pursuit eye move-

ment can be evoked by moving a small dot on a screen. OKR is usually elicited by a moving large homogeneous visual stimulus consisting of stripes or dots, for instance, mounted on an optokinetic drum, or generated by a computer program.

Oculomotor studies in foveated animals, e.g., monkeys, have shown that neurons, from the motion sensitive area especially the medial superior temporal neurons (MST) can be specifically responsive to either smooth pursuit or optokinetic eye movements [6-9]. Furthermore, a double dissociation between smooth pursuit and optokinetic eye movements have been found in patients with neurological damage [10]. They reported one patient with transient brainstem ischemia in whom pursuit was intact in the presence of severely impaired optokinetic responses and a second patient in whom optokinetic responses were intact in the presence of severely deranged pursuit. Study on first-episode schizophrenic patients revealed that, although the velocity of smooth pursuit eye tracking is reduced, the suppression of the OKR effect is not affected in these patients [11]. These patient studies suggest that the smooth pursuit and OKR eye movement systems may be impaired selectively, and are conceivably controlled by distinct brain structures. From the motion sensitive area especially the medial superior temporal neurons (MST) can be specifically responsive to either smooth pursuit or optokinetic eye movements.

There are several functional imaging studies of either the smooth pursuit or the OKR eye movement system using functional magnetic resonance imaging (fMRI) [12-19] or positron emission tomography (PET) [5, 20, 21]. These studies, in which either the smooth pursuit or the OKR eye movement system was investigated, showed similar brain activations for both eye movement

systems. These common activations included areas in the occipitotemporal, (occipito-)parietal and the frontal regions that functionally include the frontal eye fields (FEF), the supplementary eye fields (SEF), the parietal eye fields (PEF) and the middle temporal (V5) area. V5 is the homologue of the monkey middle temporal and middle superior temporal gyri [22].

Studies comparing the smooth pursuit and OKR systems directly are scarce. One fMRI study reported a large overlap in neural circuitry including the FEF, SEF, regions within ventrolateral premotor cortex, the posterior parietal cortex, the primary visual areas, the fusiform gyrus, MT/V5 and the cerebellum, for the two types of eye movements [14]. However, in this comparison study, as in many studies on OKR alone, the optokinetic eye movements were evoked by a moving pattern of black and white stripes. It is likely that such a pattern of moving stripes does not only induce continuous motion stimulation of the retinal periphery (driving the OKR response) but might also induce continuous motion stimulation of the fovea, which is typically needed to evoke a voluntary smooth pursuit response.

So far, previous functional imaging studies have failed to show differences in brain activation patterns for the two eye movement systems, despite the indications for a segregation suggested by animal electrophysiological and clinical studies. Although there are different kinds of OKR responses such as look nystagmus, stare nystagmus, circular vection, optokinetic after nystagmus, we did not investigate the diversities of the responses but only the look nystagmus similar to most of the previous OKR functional studies. In the present paper we investigated to what extent the brain areas for smooth pursuit and look OKR eye movements can be isolated by doing a direct comparison using fMRI. We

measured brain activation during the tracking of two types of moving stimuli that elicit either voluntary smooth pursuit or OKR eye movement responses. In contrast to previous imaging studies we used an OKR stimulus that does not target the voluntary smooth pursuit system component. Our OKR stimulus consisted of a random pattern of dots with a limited lifetime which was also used in our previous study. With this stimulus each dot was repositioned within 50 ms and since voluntary smooth pursuit has a latency of more than 100 ms, voluntary tracking of individual dots in our OKR stimulus by smooth pursuit eye movements is unlikely to play a role. Thus, this pattern effectively eliminates the voluntary smooth pursuit system, but still evokes a smooth optokinetic response [23, 24]. In this way we aimed to disentangle the brain activations associated with the voluntary smooth pursuit and optokinetic eye movement systems.

METHODS & MATERIALS

Subjects

Written informed consent was obtained from each participant prior to study, which was approved by the Institutional Review Board. Twenty healthy volunteers (9 men; average age of 27 years, range 22 to 37 years) participated in the study. None of the subjects had any known neurological or visual defects other than minor refractive anomalies. None of the subjects wore spectacle correction during the experiments but all reported good visual acuity during the experiment.

Data acquisition

For each subject the images were acquired on a 1.5T MRI scanner (Signa CV/I; General Electric, Milwaukee, USA) using a dedicated 8-channel head coil. For the anatomical image, a 3D high resolution FSPGR IR T1 weighted sequence (TR/

TE/TI 9.9/2.0/400 ms; ASSET factor 2; 512*512 matrix, field of view 22cm) covering the whole brain was acquired. Acquisition time was 3:10 minutes.

For functional imaging, a single-shot gradient-echo echo-planar imaging (EPI) sequence in transverse orientation was used that is sensitive to blood oxygenation level dependent (BOLD) contrast (TR/TE 3000/50 ms). The imaging volume covered the entire brain including the whole cerebellum (64*64 matrix with a field of view 22 cm, 4.5 mm slice thickness with no gap, 34 slices, voxel size of 3.4*3.4*4.5 mm³). Acquisition time was 5:15 minutes per scanning session (including 15 seconds of dummy scans that were discarded).

Stimuli

The experiments were performed in near darkness. The visual stimuli were binocularly presented by means of a goggle-based system (Silent VisionTM SV-7021 Fiber Optic Visual System; Avotec Inc., Stuart, Florida, USA). The optical components were mounted on top of the head coil. Screen resolution was 1024x768 pixels and the refresh rate 60 Hz.

Each subject participated in two experiments within one scanning session. In one experiment (Smooth Pursuit) the visual stimulus consisted of one continuously visible dot (size 0.4 degrees, luminance 1.8 cd/m²). In the other experiment (OKR) the visual stimulus consisted of a random pattern of 50 white dots (size 0.4 degrees, luminance 1.8 cd/m²) distributed across the field-of-view. The experiments are pseudorandomly performed. Each dot was repositioned every 50 ms to a new random location (random dot "limited lifetime" stimulation). All dots were white on a black background (background luminance: 0.4 cd/m², white-black contrast 100). The experiments were assigned

pseudo-randomly with half of the subject performing the smooth pursuit experiment first. The target motion for both smooth pursuit and OKR are predictable.

Task design

Both experiments consisted of a block design with two conditions (baseline and motion). The stimulus was either standing still (baseline), or was moving toward the right (motion), with respect to the observer, with a velocity of 10 degrees of visual angle per second. Each condition was alternated for 5 periods of 30 seconds during which 10 volumes were acquired. The total running time was 5 minutes. In the motion condition of the smooth pursuit experiment the dot moved repeatedly from 14 degrees on the left to 14 degrees on the right. In the motion condition of the OKR experiment a dot re-appeared on the left side, when it moved out of view at the right edge of the screen it. Subjects were instructed to look at and follow the movement of the stimuli. The baseline condition was also served as a rest period for the subject to resettle themselves from experiencing motion aftereffects from the motion condition. In a pilot study there appeared to be no difference between leftward and rightward movement of the stimuli, so we set out our investigations with one direction only.

Eye movement analysis

The online eye movement recordings were analyzed offline. Saccadic eye movements were extracted semi-automatically using a eye velocity criterion of 30 degrees/second and checked manually. The average eye velocities of the periods in between saccadic eye movements (fixations or slow-phases) were calculated. For each subject, the average number of saccades per second, and the gain (i.e., the ratio of eye velocity and target velocity; a gain of 1 indicates the eyes are moving as fast as the stimulus) were

calculated for each of the two conditions (baseline and motion) and each of the two experiments (smooth pursuit and OKR). Paired t-tests were used to assess differences between the two conditions and the two experiments.

The functional imaging data were analyzed using statistical parametric mapping software (SPM 2, distributed by the Wellcome Department of Cognitive Neurology, University College London, UK) implemented in MATLAB (Version 6.5, Mathworks, Sherborn, MA, USA). For both studies, motion correction and co-registration were done according to the methodology provided by SPM2. The time-series of images were realigned using a least square approach and a 6 parameter spatial transformation. The central image in the time-series was the reference to which all subsequent images were realigned. Motion parameters were checked for each subject to ascertain that no excessive motion (>3 mm translation or $>1.5^\circ$ rotation) has occurred. None of the scan sessions had to be discarded due to excessive motion [25]. Brain volumes were normalized to the standard space defined by the Montreal Neurological Institute (MNI) template. The normalized data had a resolution of $3 \times 3 \times 3$ mm³ and were spatially smoothed with a 3D isotropic Gaussian kernel, with a full width half maximum of 10 mm.

Statistical parametric maps for all conditions were calculated for each subject using the general linear model with hemodynamic convolution. Furthermore, fMRI is based on the Blood Oxygenation Level Dependent (BOLD) response, it takes about 5 seconds for the blood to catch up with the brain activation. In order to predict the activation, the hemodynamic response was convolved with the model to shape the true function and as well as the delay of response. Movement parameters resulting from the realignment pre-processing were included

as regressors of no interest to further reduce motion artifacts. The model was estimated with a high pass filter with a cut-off period of 128 seconds. For each subject, a t-contrast map was calculated between the motion condition and the baseline condition [motion > baseline].

The individual t-contrast maps were used for the second level random effects (group) analysis. One sample t tests were performed for each of the experiments separately: [motion > baseline]_{Smooth Pursuit} and [motion > baseline]_{OKR}. To investigate the differences in brain activation between the smooth pursuit experiment and the OKR experiment, corrected for the baseline activation, we used a paired t-test [motion > baseline]_{Smooth Pursuit} versus [motion > baseline]_{OKR} and vice versa. All tests were thresholded at $p < 0.05$ with false discovery rate (FDR) correction for multiple comparisons and with a minimum cluster size of 10 voxels.

Anatomic labeling of the observed areas of activation in SPM was done using the macroscopic anatomic parcellation procedure of the Montreal Neurological Institute (MNI) MRI single-subject brain.

RESULTS

Eye movements

Inspection of the eye movement responses showed that one subject did not fixate the dot continuously during the smooth pursuit experiment, and that the eye movements of another subject could not be recorded reliably. These two subjects were excluded from further analysis. The remaining 18 subjects made a clear smooth pursuit response when presented with a moving dot and adequate look optokinetic

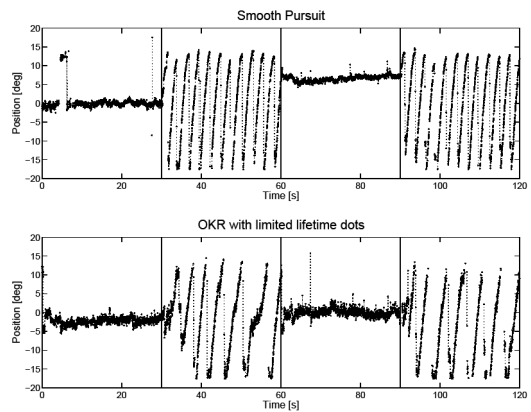


Figure 1: Examples of the eye movements made by one subject in the two experiments (smooth pursuit and OKR) during two baseline conditions and two motion conditions. In the motion condition subjects follow the movement of the stimuli in both experiments using smooth eye movements interspersed with saccades.

eye movement (OKR) responses during stimulation with limited lifetime dots. In both tasks, the eye movements were a mixture of saccades and fixations or slow phases. Note that the saccades occurred only when the moving dot jumped to the opposite side of the screen. None of the subjects experience any motion after effects.

Examples of the eye movements made in the two experiments are shown in figure 1. In both experiments more saccades were made in the motion than in the baseline condition (smooth pursuit: 1.9 ± 0.5 saccades/s during motion versus 1.2 ± 0.5 saccades/s during baseline, $p < 0.001$; OKR: 1.6 ± 0.8 saccades/s during motion versus 0.8 ± 0.6 saccades/s during baseline, $p < 0.001$). No differences in the average number of saccades were observed between the two experiments for the motion and baseline condition ($p > 0.05$). As expected, the gains of the smooth eye movement responses in between saccades (slow phases) were higher in the motion condition than in the baseline condition of both experiments (smooth pursuit: 1.1 ± 0.2 during motion versus 0.0 ± 0.1 during baseline, $p <$

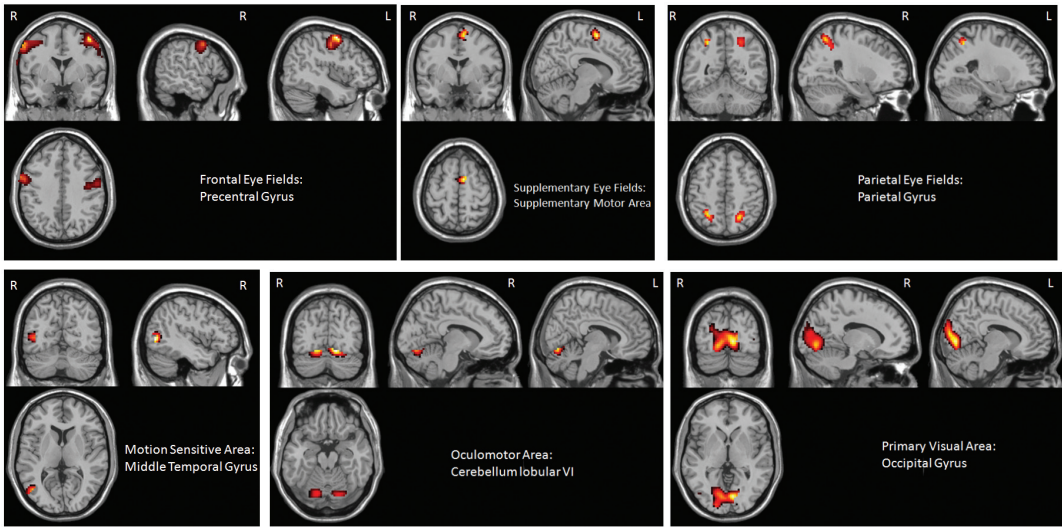


Figure 2: Activated clusters in the smooth pursuit experiment. All areas were thresholded at $p < 0.05$ with FDR correction for multiple comparisons and with a minimum cluster size of 10 voxels.

0.001; OKR: 0.6 ± 0.2 during motion versus 0.0 ± 0.0 degrees/s during baseline, $p < 0.001$). The gain during the motion condition was higher in the smooth pursuit experiment than in the OKR experiment ($p < 0.001$).

fMRI analysis

The results of the random effects group analysis comparing the motion condition with baseline in each experiment are shown in table 1 and 2.

The analysis of the smooth pursuit experiment (figure 2) revealed bilateral activation in the pre-

central gyrus (FEF), unilateral activation in the left supplementary motor area (SEF) and bilateral activation in the superior and inferior parietal gyri (PEF). Unilateral activation was found in the right middle temporal gyrus (motion-sensitive area MT/V5). Cerebellar activation was found bilaterally in area VI and unilaterally in the left crus I area and in the vermis VI. Bilateral activation was also found in the fusiform gyrus (visual area V4) and in the primary visual areas (PVA/V1: calcarine gyrus, cuneus gyrus, lingual gyrus and the superior occipital gyrus).

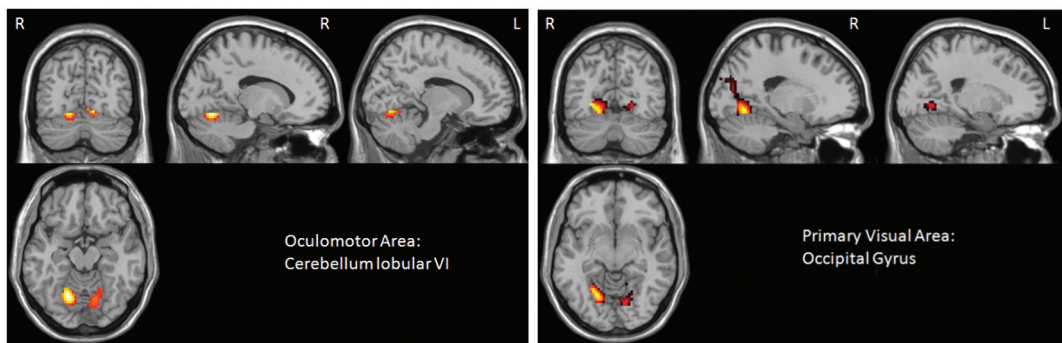


Figure 3 Activated clusters in the OKR experiment. All areas were thresholded at $p < 0.05$ with FDR correction for multiple comparisons and with a minimum cluster size of 10 voxels.

Cluster size	T-value	MNI coordinate (mm)			Anatomic area	side	%*	Functional Area
		x	y	z				
4730	10.37	24	-90	15	Middle Temporal Gyrus	R	1.63	MT/V5
					Cerebellum VI	L	3.45	Oculomotor Vermis
					Cerebellum VI	R	3.28	Oculomotor Vermis
					Vermis VI		1.16	Oculomotor Vermis
					Cerebellum Crus I	L	1.12	Oculomotor Vermis
					Lingular Gyrus	R	10.23	PVA/V1
					Calcarine Gyrus	R	8.9	PVA/V1
					Calcarine Gyrus	L	8.65	PVA/V1
					Lingular Gyrus	L	8.58	PVA/V1
					Middle Occipital Gyrus	L	7.53	PVA/V1
					Superior Occipital Gyrus	R	5.92	PVA/V1
					Cuneus	L	5.26	PVA/V1
					Superior Occipital Gyrus	L	5.12	PVA/V1
					Middle Occipital Gyrus	R	4.99	PVA/V1
					Cuneus	R	4.71	PVA/V1
291	5.94	-45	-3	57	Precentral Gyrus	L	63.57	FEF
					Postcentral Gyrus	L	29.9	FEF
204	5.37	57	3	48	Middle Frontal Gyrus	L	2.41	FEF
					Precentral Gyrus	R	54.9	FEF
					Middle Frontal Gyrus	R	27.54	FEF
112	5.27	-9	0	60	Postcentral Gyrus	R	5.39	FEF
					Supplementary Motor Area	L	57.14	SEF
66	4.83	-21	-63	57	Superior Frontal Gyrus	L	23.12	
					Middle Frontal Gyrus	L	1.79	
49	4.45	-39	51	-12	Superior Parietal Gyrus	L	84.85	PEF
					Inferior Parietal Gyrus	L	15.15	PEF
38	4.18	27	-54	48	Inferior Orbital Gyrus	L	57.14	
					Middle Orbital Gyrus	L	14.29	
					Inferior Parietal Gyrus	R	28.95	PEF
					Superior Parietal Gyrus	R	28.95	PEF
					Angular Gyrus	R	2.63	PEF

Table 1: Activation areas for the smooth pursuit experiment with cluster size, t-values of local maximum, Montreal Neurological Institute (MNI) coordinates, anatomical labels, % of cluster size and functional labels are included. All areas were thresholded at $p < 0.05$ with FDR correction for multiple comparisons and with a minimum cluster size of 10 voxels.

(L: left hemisphere, R: right hemisphere; FEF: frontal eye fields, SEF: supplementary eye fields, PEF: parietal eye fields, V4: visual area 4, V5: motion-sensitive area, PVA/V1: primary visual areas (V1)) *The unassigned areas for each cluster are not listed in the table.

Cluster size	T-value	MNI coordinate (mm)			Anatomic area	side	%*	Functional Area
		x	y	z				
1214	8.94	27	-60	-6	Cerebellum VI	R	2.22	Oculomotor Vermis
					Lingual Gyrus	L	19.44	PVA/V1
					Lingual Gyrus	R	18.78	PVA/V1
					Calcarine Gyrus	R	14.5	PVA/V1
					Calcarine Gyrus	L	13.59	PVA/V1
					Cuneus	R	8.81	PVA/V1
					Cuneus	L	6.84	PVA/V1
					Superior Occipital Gyrus	R	5.19	PVA/V1
					Superior Occipital Gyrus	L	1.98	PVA/V1
					Fusiform Gyrus	R	4.86	V4

Table 2: Activation areas for the OKR experiment with cluster size, t-values of local maximum, Montreal Neurological Institute (MNI) coordinates, anatomical labels, % of cluster size and functional labels are included. All areas were thresholded at $p < 0.05$ with FDR correction for multiple comparisons and with a minimum cluster size of 10 voxels. (L: left hemisphere, R: right hemisphere; V4: visual area 4, PVA/V1: primary visual areas (V1)) *The unassigned areas for each cluster are not listed in the table.

The analysis of the OKR experiment (figure 3) revealed no significant activation in the frontal, supplementary and parietal eye fields or the motion-sensitive area MT/V5. Cerebellar activation was found unilaterally in the right area VI. Activation was also found unilaterally in the right fusiform gyrus (visual area V4) and bilaterally

in the primary visual areas (PVA/V1: calcarine gyrus, cuneus gyrus, lingual gyrus and the superior occipital gyrus).

The results of the direct comparison between the activation of the smooth pursuit experiment and the OKR experiment are shown in table 3 and figure 4.

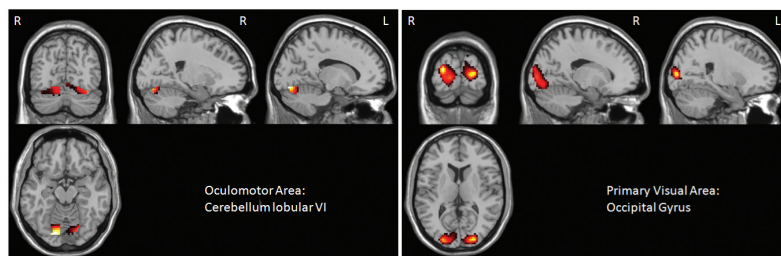
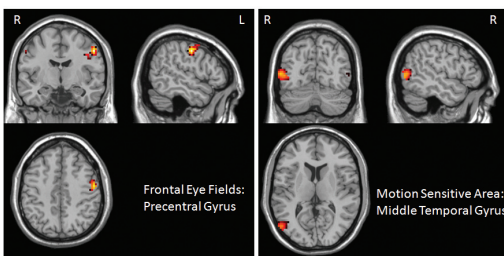


Figure 4: Activated clusters in the smooth pursuit versus OKR experiment. All areas were thresholded at $p < 0.05$ with FDR correction for multiple comparisons and with a minimum cluster size of 10 voxels.

Stronger activation in the smooth pursuit experiment than in the OKR experiment was observed unilaterally in the left precentral gyrus (FEF) and the right middle temporal gyrus (motion-sensitive area, MT/V5), and bilaterally in the cerebellar area VI and Crus I area. Stronger activation was also found bilaterally in the fusiform gyrus (visual area V4), and the primary visual area (PVA/V1: calcarine gyrus, cuneus gyrus, lingual gyrus and the inferior, middle and superior occipital gyri). The

Cluster size	T-value	MNI coordinate (mm)			Anatomic area	side	%*	Functional Area
		x	y	z				
3123	8.7	24	-93	15	Middle Temporal Gyrus	R	1.79	MT/V5
					Cerebellum Crus I	L	3.59	Oculomotor Vermis
					Cerebellum Crus I	R	2.79	Oculomotor Vermis
					Cerebellum VI	R	2.24	Oculomotor Vermis
					Cerebellum VI	L	2.11	Oculomotor Vermis
					Middle Occipital Gyrus	L	12.26	PVA/V1
					Lingual Gyrus	R	9.35	PVA/V1
					Calcarine Gyrus	R	7.59	PVA/V1
					Calcarine Gyrus	L	7.24	PVA/V1
					Superior Occipital Gyrus	L	6.02	PVA/V1
					Lingual Gyrus	L	5.19	PVA/V1
					Superior Occipital Gyrus	R	4.19	PVA/V1
					Middle Occipital Gyrus	R	3.78	PVA/V1
					Cuneus Gyrus	L	3.39	PVA/V1
					Cuneus Gyrus	R	3.04	PVA/V1
					Inferior Occipital Gyrus	L	2.24	PVA/V1
					Inferior Occipital Gyrus	R	2.18	PVA/V1
					Fusiform Gyrus	L	4.67	V4
					Fusiform Gyrus	R	1.89	V4
32	4.34	-54	-9	42	Postcentral Gyrus	L	68.75	FEF
					Precentral Gyrus	L	28.13	FEF
10	4	54	-60	-27	Inferior Temporal Gyrus	R	60	
					Cerebellum Crus I	R	40	

Table 3: Direct comparison between the smooth pursuit and OKR experiments with cluster size, t-values of local maximum, Montreal Neurological Institute (MNI) coordinates, anatomical labels, % of cluster size and functional labels are included. All areas were thresholded at $p < 0.05$ with FDR correction for multiple comparisons and with a minimum cluster size of 10 voxels.

(L: left hemisphere, R: right hemisphere; FEF: frontal eye fields, V4: visual area 4; V5: motion-sensitive area; PVA/V1: primary visual areas (V1)) *The unassigned areas for each cluster are not listed in the table.

	Smooth pursuit	OKR	Smooth pursuit > OKR
FEF	B	-	L
SEF	L	-	-
PEF	B	-	-
MT/V5	R	-	R
Oculomotor (Cerebellum area VI)	B	R	B
PVA/V1	B	B	B

Table 4: A summary of the areas of activation in the functional areas of interest for each of the experiments (smooth pursuit and OKR) separately and for the direct comparison of smooth pursuit > OKR. All areas were thresholded at $p < 0.05$ with FDR correction for multiple comparisons and with a minimum cluster size of 10 voxels. (B: bilateral, L: left hemisphere, R: right hemisphere; -: no significant activation; FEF: frontal eye fields, SEF: supplementary eye fields, PEF: parietal eye fields, MT/V5: motion-sensitive area (MT/V5), PVA/V1: primary visual areas (V1))

direct comparison showed no significant differences in activation in the supplementary and parietal eye fields.

In none of the above-mentioned areas activation was stronger in the OKR experiment than in the smooth pursuit experiment.

A summary of the observed activations is presented in Table 4.

DISCUSSION

In this study, we investigated the possible differences in brain activation between the smooth pursuit and the look OKR eye movements directly. Previous studies used a rotating drum with coloured objects [13] or fixed stripes [14] as a stimulus to evoke OKR eye movements. Such a fixed stimulus could also elicit smooth pursuit eye movements as well as an OKR response. We attempted to eliminate the smooth pursuit component from the OKR response using an OKR stimulus that consisted of a random pattern of dots with a limited lifetime.

The eye movement data showed that both types of stimuli evoked adequate eye movement responses. Subjects produced look nystagmus and did not perceive either circular vection or OKR after nystagmus. The imaging data showed that in accordance with the literature [14, 22], smooth pursuit elicited by a moving single dot yielded activation in the frontal, supplementary and parietal eye fields (FEF, SEF, PEF), in the middle temporal gyrus (MT/V5) and in cerebellar area VI. In our OKR experiment, however, using the limited lifetime dots as the stimulation for the optokinetic system, we did not see any significant activation in the FEF, SEF, PEF or the MT/V5 despite the observed OKR eye movements. The direct comparison of the activation patterns

between the two experiments showed that the FEF, MT/V5 and cerebellar area VI appeared to be more activated during the smooth pursuit than during the OKR experiment.

Although it is likely that the network areas for OKR and smooth pursuit overlap [1, 26], the notion that the two eye movement systems can be disentangled is suggested by the observations from animal and patient studies [6, 8-11, 27].

In our study FEF was found more strongly activated during smooth pursuit eye movement than during OKR. The anatomical location of the FEF activation in our smooth pursuit experiment is in good accordance with previous results [13-15]. Our findings are supported by clinical studies, that have shown that lesions in the precentral gyrus and in the posterior part of the superior and middle frontal gyri induce impairments in smooth pursuit eye movements [28, 29], although lesioning the FEF may also affect OKR [30].

The supplementary eye field (SEF) is located in the medial anterior part of the supplementary motor area (SMA). It is thought to be involved in voluntary movements [31] such as smooth pursuit eye movements [4, 15]. The SEF is likely to play a role in planning this type of eye movement, comparable to the role SMA plays in other movements [4]. The absence of activation in the SEF during OKR stimulation in our study seems to be in contrast with some previous studies in which OKR was elicited by a moving pattern of stripes or objects [13, 14]. However, activation in the SEF area was also not observed in a PET study when OKR was elicited by a moving pattern of full lifetime dots [5].

The parietal eye fields (PEF) are suggested to be involved in visuospatial localization and atten-

tion, and in the initiation and control of visually cued motor actions [4]. Activation in the PEF with fMRI has been observed for smooth pursuit eye movements [15] and for OKR eye movements [13]. For both the SEF and the PEF we did not observe a difference in activation in our direct comparison, which is in accordance with a previous fMRI study that compared smooth pursuit and OKR directly [14].

MST and MT/V5 are separate visual areas. They are anatomically distinct in monkeys and can be separated functionally in humans according to type of motion or retinotopic organization. The role of MT/V5 in smooth pursuit eye movement has been demonstrated in animal experiments [9, 32]. Electrophysiological studies in monkeys suggest that pursuit neurons in the MT/V5 area, processing visual motion information used to guide pursuit [26], responded preferentially to small spot motion; only a few pursuit neurons in MT/V5 responded to the motion of a large pattern [9]. Patients with unilateral cortical lesions in the MT/V5 area exhibit impairments in smooth pursuit behaviour [29]. In accordance with these results, we found that area MT/V5 showed stronger activation during smooth pursuit eye movement than during OKR elicited by limited lifetime dots. This is in contrast with previous studies in which MT/V5 activation was observed during both smooth pursuit and OKR stimulation [5, 13, 14]. Since the fovea is over-represented in MT/V5 as well as in the primary visual areas (PVA/V1), more motion-sensitive receptive fields in these areas could have been targeted in the smooth pursuit experiment than in the OKR experiment. This might explain the increased activation in MT/V5. The right-sided lateralization of activation of MT/V5 might suggest a right hemispheric dominance in oculomotor performance, which may be related to the predominant role of the right hemisphere in spatial visual attention processes [13].

Stronger activation during smooth pursuit than during OKR was also found in the cerebellum. This stronger cerebellar activation can be explained by the fact that the smooth pursuit eye movements are under voluntary control needing constant recalibration and updating of the position of the moving object. As such it has been suggested that smooth pursuit places a high computational demand on the cerebellum [14].

In summary, we observed stronger activation in the FEF, in the MT/V5 area and in the cerebellum during smooth pursuit than during optokinetic stimulation with limited lifetime dots. This suggests that these areas of the brain are less involved in the generation of an eye movement response toward a moving pattern of limited lifetime dots.

The observed differences in activation between smooth pursuit and OKR could be related to the use of limited lifetime dots to elicit optokinetic eye movements. In previous imaging studies, OKR was elicited by a moving pattern of stripes or fixed dots. It can be argued that such a fixed pattern does not only target the optokinetic system due to the peripheral stimulation but also the smooth pursuit system due to foveal stimulation [1], similar to when the eyes have to follow a single moving dot. Indeed, Dieterich and colleagues acknowledged that their OKR stimuli (stripes) could elicit pursuit eye movements as well [13]. Therefore, the previously reported common activation during smooth pursuit and OKR in the FEF, MT/V5, and in the cerebellum, may be related to the confounding influence of smooth pursuit during OKR stimulation with a fixed pattern. In our limited lifetime dot stimulus each dot was repositioned within 50 ms. Furthermore, the OKR stimulus in this study varies from the pursuit condition in luminance (a 50 fold difference over a single dot) and the pre-

sentation is with far more visual transient information (50 dots repositioning themselves every 50ms), these should provide powerful drivers of neural activity. Since smooth pursuit has a latency of more than 100 ms [1], voluntary tracking of individual dots in our OKR stimulus by smooth pursuit eye movements is unlikely to play a role [24]. Therefore, limited lifetime dot stimulation is likely to target the optokinetic system in isolation.

It can be argued that the differences in activation patterns might also be related to the differences in eye movement velocities between the two experiments. It is, for instance, more difficult to track a fast moving stimulus during which an observer will make more tracking errors (reflected by a relatively lower eye velocity compared to the stimulus velocity, i.e., reduced gains (as shown in our eye movements data), and more corrective saccades). Therefore, faster pursuit may require more processing and hence induce more brain activation. To our knowledge, this idea has not been tested using functional imaging so far. It has to be noted that in both of our experiments the velocity of the moving stimuli was well below the threshold for human OKR [1]. Both stimuli would therefore be quite easy to follow. The eye movement behavioural data suggest, however, that tracking of a moving dot seems to be much simpler than tracking the moving pattern of limited lifetime dots, as reflected by the higher eye velocities during smooth pursuit. Therefore, one might also argue that OKR stimulation using limited lifetime dots requires more processing and would induce more brain activity.

CONCLUSION

In the present study we observed that the frontal eye fields (FEF), MT/V5 and area VI of the cerebellum were more activated during smooth pursuit, evoked by a single moving dot, than during OKR evoked by a random pattern of dots with a limited lifetime. We conclude that the smooth pursuit eye movement system and the optokinetic eye movement systems can be differentiated with fMRI using a stimulus that elicits OKR in isolation, without a confounding contribution of the smooth pursuit system.

REFERENCES

1. Leigh, R.J. and D.S. Zee, *The Neurology of Eye Movements*. Third ed. 1999, New York: Oxford University Press.
2. Kandel, E.R., J.H. Schwartz, and T.M. Jessell, *Principles of neural science*. 4th ed. 2000, New York: McGraw-Hill, Health Professions Division. xli, 1414 p.
3. Carpenter, R.H.S., *Movements of the Eyes*. Second ed. 1988, London: Pion Ltd.
4. Krauzlis, R.J., Recasting the smooth pursuit eye movement system. *J Neurophysiol*, 2004. 91(2): p. 591-603.
5. Galati, G., et al., Cortical control of optokinetic nystagmus in humans: a positron emission tomography study. *Exp Brain Res*, 1999. 126(2): p. 149-59.
6. Ilg, U.J. and P. Thier, Visual tracking neurons in primate area MST are activated by smooth-pursuit eye movements of an "imaginary" target. *J Neurophysiol*, 2003. 90(3): p. 1489-502.

7. Bremmer, F., et al., Eye position effects in monkey cortex. I. Visual and pursuit-related activity in extrastriate areas MT and MST. *J Neurophysiol*, 1997. 77(2): p. 944-61.
8. Churchland, A.K. and S.G. Lisberger, Discharge properties of MST neurons that project to the frontal pursuit area in macaque monkeys. *J Neurophysiol*, 2005.
9. Komatsu, H. and R.H. Wurtz, Relation of cortical areas MT and MST to pursuit eye movements. I. Localization and visual properties of neurons. *J Neurophysiol*, 1988. 60(2): p. 580-603.
10. Barratt, H., M.A. Gresty, and N.G. Page, Neurological evidence for dissociation of pursuit and optokinetic systems. *Acta Otolaryngol*, 1985. 100(1-2): p. 89-97.
11. Hutton, S.B., et al., Smooth pursuit eye tracking over a structured background in first-episode schizophrenic patients. *Eur Arch Psychiatry Clin Neurosci*, 2000. 250(5): p. 221-5.
12. Bucher, S.F., et al., Sensorimotor cerebral activation during optokinetic nystagmus. A functional MRI study. *Neurology*, 1997. 49(5): p. 1370-7.
13. Dieterich, M., et al., Horizontal or vertical optokinetic stimulation activates visual motion-sensitive, ocular motor and vestibular cortex areas with right hemispheric dominance. An fMRI study. *Brain*, 1998. 121 (Pt 8): p. 1479-95.
14. Konen, C.S., et al., An fMRI study of optokinetic nystagmus and smooth-pursuit eye movements in humans. *Exp Brain Res*, 2005. 165(2): p. 203-16.
15. Petit, L. and J.V. Haxby, Functional anatomy of pursuit eye movements in humans as revealed by fMRI. *J Neurophysiol*, 1999. 82(1): p. 463-71.
16. Stephan, T., et al., Changes in cerebellar activation pattern during two successive sequences of saccades. *Hum Brain Mapp*, 2002. 16(2): p. 63-70.
17. Dieterich, M., et al., fMRI signal increases and decreases in cortical areas during small-field optokinetic stimulation and central fixation. *Exp Brain Res*, 2003. 148(1): p. 117-27.
18. Dieterich, M., et al., Cerebellar activation during optokinetic stimulation and saccades. *Neurology*, 2000. 54(1): p. 148-55.
19. Rosano, C., et al., Pursuit and saccadic eye movement subregions in human frontal eye field: a high-resolution fMRI investigation. *Cereb Cortex*, 2002. 12(2): p. 107-15.
20. Desmurget, M., et al., Functional anatomy of nonvisual feedback loops during reaching: a positron emission tomography study. *J Neurosci*, 2001. 21(8): p. 2919-28.
21. O'Driscoll, G.A., et al., Differences in cerebral activation during smooth pursuit and saccadic eye movements using positron-emission tomography. *Biol Psychiatry*, 1998. 44(8): p. 685-9.
22. Dieterich, M., Ocular motor system: anatomy and functional magnetic resonance imaging. *Neuroimaging Clin N Am*, 2001. 11(2): p. 251-61, viii-ix.
23. Kelders, W.P., et al., Compensatory increase of the cervico-ocular reflex with age in healthy humans. *J Physiol*, 2003. 553(Pt 1): p. 311-7.
24. Mestre, D.R. and G.S. Masson, Ocular responses to motion parallax stimuli: the role of perceptual and attentional factors. *Vision Res*, 1997. 37(12): p. 1627-41.

25. Tzourio-Mazoyer, N., et al., Automated anatomical labeling of activations in SPM using a macroscopic anatomical parcellation of the MNI MRI single-subject brain. *Neuroimage*, 2002. 15(1): p. 273-89.
26. Dursteler, M.R. and R.H. Wurtz, Pursuit and optokinetic deficits following chemical lesions of cortical areas MT and MST. *J Neurophysiol*, 1988. 60(3): p. 940-65.
27. Bremmer, F., C. Distler, and K.P. Hoffmann, Eye position effects in monkey cortex. II. Pursuit- and fixation-related activity in posterior parietal areas LIP and 7A. *J Neurophysiol*, 1997. 77(2): p. 962-77.
28. Lekwuwa, G.U. and G.R. Barnes, Cerebral control of eye movements. I. The relationship between cerebral lesion sites and smooth pursuit deficits. *Brain*, 1996. 119 (Pt 2): p. 473-90.
29. Heide, W., K. Kurzdin, and D. Kompf, Deficits of smooth pursuit eye movements after frontal and parietal lesions. *Brain*, 1996. 119 (Pt 6): p. 1951-69.
30. Rivaud, S., et al., Eye movement disorders after frontal eye field lesions in humans. *Exp Brain Res*, 1994. 102(1): p. 110-20.
31. Tanji, J., New concepts of the supplementary motor area. *Curr Opin Neurobiol*, 1996. 6(6): p. 782-7.
32. Kawano, K., et al., Neural activity in cortical area MST of alert monkey during ocular following responses. *J Neurophysiol*, 1994. 71(6): p. 2305-24.

CHAPTER 3

FMRI OF OPTOKINETIC EYE MOVEMENTS WITH AND WITHOUT A CONTRIBUTION OF SMOOTH PURSUIT

FMRI OF OPTOKINETIC EYE MOVEMENTS WITH AND WITHOUT A CONTRIBUTION OF SMOOTH PURSUIT

Published by Journal of Neuroimaging, 2008, 18(2):158-167

ABSTRACT

Optokinetic eye movements are elicited when tracking a moving pattern. It can be argued that a moving pattern of stripes invokes both the optokinetic and the smooth pursuit eye movement system, which may confound the observed brain activation patterns using functional magnetic resonance imaging (fMRI). A moving pattern of limited-lifetime-dot stimulation does not target the smooth pursuit eye movement system.

fMRI was used to compare the cortical activity elicited by an optokinetic eye movement response evoked by a moving pattern of stripes and a moving pattern of limited lifetime dots.

The eye movement behavior showed that both types of stimuli evoked an adequate and similar optokinetic eye movement response, but stimulation with stripes evoked more activation in the frontal and parietal eye fields, MT/V5 and in the cerebellar area VI than stimulation with limited-lifetime dots.

These brain areas are implicated in smooth pursuit eye movements. Our results suggest that indeed both the optokinetic and the the smooth pursuit eye movement system are involved in tracking a moving pattern of stripes.

INTRODUCTION

The optokinetic reflex (OKR) is an eye movement that stabilizes the projection of a moving visual environment on the retina. It is elicited by the movement of a large visual stimulus and is driven by peripheral retinal stimulation rather than foveal stimulation [1, 2]. Such a stimulus will generally elicit an eye movement pattern known as nystagmus, which consists of a combination of smooth tracking eye movements (slow phases) and fast resetting saccadic-like eye movements (fast phases) [2, 3]. In the experimental setting, the OKR response is readily evoked by showing a large moving pattern of, for instance, stripes to the observer. Functional magnetic resonance imaging (fMRI) and positron emission tomography (PET) studies have shown that such an OKR stimulus will activate a distinct number of brain areas [1, 4-6], including the frontal (FEF), supplementary (SEF) and parietal eye fields (PEF), as well as the motion-sensitive area (MT/V5).

In these imaging studies, however, the OKR response was elicited by presenting a large moving static visual stimulus that consisted of stripes, randomly positioned dots or colored objects. Such static patterns do not only induce continuous motion stimulation of the retinal periphery (driving the OKR response) but might also induce continuous motion stimulation of the fovea. Foveal stimulation is typically needed to evoke a smooth pursuit response. Smooth pursuit enables an observer to keep a small moving target projected onto the fovea and to ignore

the relative motion of the visual background, e.g., a large moving pattern [2, 7]. However, when the small target is moving congruently with its background, both the OKR system and the smooth pursuit system might contribute to the ocular following of the moving stimulus.

Thus, one can argue that the movement of a large pattern of static elements (e.g. dots or stripes) does not only target the OKR system but the smooth pursuit system as well. This might explain the fact that in previous studies no differences were found in activated brain areas between OKR and smooth pursuit stimulation [5, 6, 8-11], even when the two systems were compared directly [11].

In a previous fMRI pilot study (Schraa-Tam et al., 2004, Functional MRI of optokinetic stimulation with limited and infinite lifetime random dot patterns. Society for Neuroscience 302.8) we evoked an OKR response by using a moving pattern consisting of randomly positioned dots as a stimulus. These dots, however, were not statically positioned within the pattern, but each dot had an individual limited lifetime. In other words, each individual dot in the pattern was randomly relocated to a new position in the pattern after 50 ms. This limited lifetime stimulus has shown to be capable of evoking an OKR eye movement response without a smooth pursuit component [12, 13].

In this study we investigate the possible differences in brain activation during OKR with and without a possibly confounding contribution of the smooth pursuit system. We hypothesized that two different activation patterns might be observed if the cortical pathways of the smooth pursuit system and the OKR system differ.

METHODS & MATERIALS

Subjects

Informed consent was obtained from each participant prior to the study, which was approved by the Institutional Review Board. Fifteen volunteers (9 men, 6 women; average age 29 years, range 24 to 50 years) participated in the study, which consisted of two experiments. None of the subjects had any known neurological or visual defects other than minor refractive anomalies. No subject wore spectacle correction and all subjects reported good visual acuity during the experiment.

Data acquisition

For each subject the functional imaging data were acquired on a 1.5T MRI scanner (Signa CV/i; General Electric, Milwaukee, USA) using a dedicated 8-channel head coil. For the anatomical image, a 3D high resolution FSPGR IR T1 weighted sequence (TR/TE/TI 9.9/2.0/400 ms; ASSET factor 2; matrix 512*512) covering the whole brain was acquired. Acquisition time was 3:10 minutes.

For functional imaging, a single-shot gradient-echo echo-planar imaging (EPI) sequence in transverse orientation was used that is sensitive to blood oxygenation level dependent (BOLD) contrast (TR/TE 3000/40 ms). The imaging volume covered the entire brain including the whole cerebellum (96*96 matrix, 5 mm slice thickness and 1 mm gap, 22 slices). Acquisition time was 5:15 minutes per experiment (including 15 seconds of dummy scans that were discarded).

Stimuli

The experiments were performed in near darkness with all lights turned off except for the video projector. Visual stimuli were shown by means of back projection with a video projector

onto a translucent screen in front of the scanner. Subjects viewed this screen with a mirror system on top of the head coil. The total field-of-view extended 21 degrees horizontally and 17 degrees vertically. Stimuli were presented with a personal computer.

Each subject participated in two experiments performed during one scanning session. In the first experiment (stripes), the OKR stimulation consisted of a pattern of alternating black and white stripes. Each stripe had a width of 0.5 degrees. In the second experiment (dots), the OKR stimulation was a random pattern of 50 white dots (radius 0.4 degrees) distributed across the field-of-view on a black background. Each dot was repositioned every 50 ms to a new random location (random dot "limited-lifetime" stimulation). On average the luminances of both experiments were in the same range (13 cd/m^2 for the stripes experiment and 11 cd/m^2 for the dots experiment). In both experiment the white-black contrast was about 50.

In both experiments the pattern as a whole (dots or stripes) was either not moving (the baseline condition), or was moving toward the left side of the visual field with a velocity of 10 degrees of visual angle per second (motion condition). The path length of an individual dot therefore matched the width of a stripe (0.5 degrees). When a stripe or dot moved out of view on the left edge of the screen it reappeared on the opposite side. Note that in the baseline condition of the dots experiment, each dot was also randomly repositioned every 50 ms. Our pilot study had shown that there is no directional difference between the stimuli moving either to the right or to the left, thus we set out our investigation with one direction only.

Both experiments consisted of a block design with two conditions (baseline and motion). In

each experiment, the two conditions were presented in alternation. Each condition was presented 5 times and each condition lasted 30 seconds during which time 10 imaging volumes were acquired. Subjects were instructed to keep their focus at the center of the screen but not to suppress any eye movement in response to the motion of the stimulus.

Eye movements

Eye movements were recorded outside the scanner in a separate session in all of the same 15 volunteers using the two types of stimulation described. Eye movements were recorded monocular at 250 Hz using video-oculography [14]. Calibration was performed using the built-in nine-point calibration routine of the eye tracking system.

In an off-line analysis, the saccadic eye movements (fast-phases) were detected automatically, using a velocity criterion, and checked manually by the experimenter. Slow phase eye movement velocity was derived from the slope of the position of the eye over time in between the saccadic fast phases. The average and standard deviation of the number of saccades per second as well as the average and standard deviation of the eye movement velocity was calculated for each experiment (stripes and dots) and each condition (baseline and motion) across subjects.

Statistical analysis

The functional imaging data were analyzed using statistical parametric mapping software (SPM 2, distributed by the Wellcome Department of Cognitive Neurology, University College London, UK) implemented in MATLAB (Version 6.5, Mathworks, Sherborn, MA, USA). Motion correction and co-registration were done according to the methodology provided by SPM2 [15]. Brain volumes were normalized to the standard space

defined by the Montreal Neurological Institute (MNI) template (resolution $3 \times 3 \times 3 \text{ mm}^3$). To compensate for inter-subject variability and to attenuate high frequency noise to increase the signal-to-noise ratio, the normalized data were spatially smoothed with a three-dimensional isotropic Gaussian kernel, with a full width half maximum of 6 mm.

Statistical parametric maps were calculated for each subject using the general linear model with hemodynamic convolution with all conditions. Movement parameters resulting from the realignment pre-processing were included as regressors of no interest to further reduce motion artifacts.

The model was estimated without removal of the global effects, with a high pass filter with a cut-off period of 128 s and with a hemodynamic low-pass filter for temporal autocorrelation. For each subject and each experiment, a t-contrast was calculated between the motion and the baseline condition (motion > baseline).

The individual t-contrast maps were used for the second level random effects (group) analyses. An analysis of covariance (ANCOVA) was performed for each of the experiments separately: [motion > baseline]_{stripes} and [motion > baseline]_{dots}. To investigate the differences in brain activations between the two experiments directly we used an ANCOVA in which we compared ([motion > baseline]_{stripes} versus [motion > baseline]_{dots}). In this way we could correct for the possible confounding contribution of the visual differences (e.g., luminance) between the two types of visual stimulation (stripes versus dots). To regress out confounding activation related to differences in saccadic eye movements between the baseline and motion conditions, a regressor of no interest was added to the analyses. This regressor was based on values obtained from

the behavioral eye movement data as measured outside the scanner. For each subject and each experiment we counted the numbers of saccades made in the conditions of the behavioral experiments (N_{baseline} and N_{active}). From these numbers we obtained the ratio $[(N_{\text{active}} - N_{\text{baseline}}) / (N_{\text{active}} + N_{\text{baseline}})]$, which was entered as the regressor value for each experiment.

All activation was thresholded at $p < 0.05$ with false discovery rate (FDR) correction for multiple comparisons and at a minimum cluster size of 5 voxels.

Anatomic labeling of the observed areas of activation in SPM was done by using the macroscopic anatomic parcellation procedure of the Montreal Neurological Institute (MNI) MRI single-subject brain [15].

RESULTS

Eye movements

In two of the 15 subjects inspection of the eye movement responses showed minor abnormalities: latent nystagmus in one subject, amblyopia in another subject. These two subjects were removed from further analysis. The remaining 13 subjects made a clear optokinetic eye movement response when the stimulus pattern was moving and showed a mixture of saccades and fixations during the baseline conditions of both experiments (Figure 1).

In both experiments saccades were made per second in the motion than in the baseline condition (stripes: 2.0 ± 0.5 saccades/s during motion versus 1.0 ± 0.7 saccades/s during baseline, $p < 0.001$; dots: 1.8 ± 0.4 saccades/s during motion versus 1.2 ± 0.6 saccades/s during baseline, $p < 0.001$). No difference in the average number of saccades was observed between the two ex-

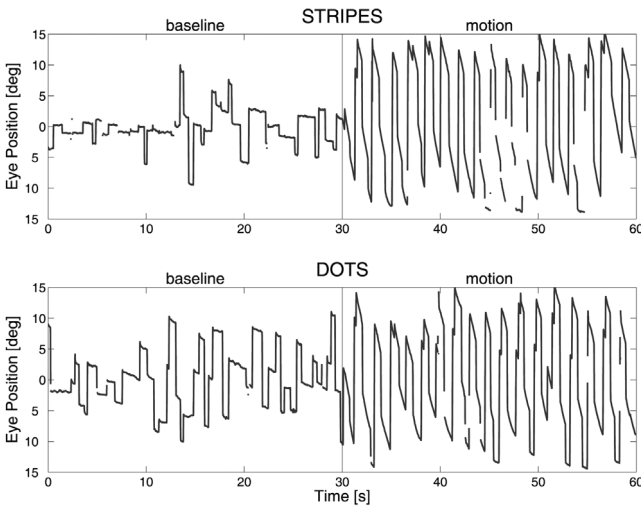


Figure 1: Eye movement traces in the two experiments (stripes and dots) during the baseline and the motion condition (example from one volunteer). Note the nystagmus pattern in both experiments during the motion condition.

periments. The velocity of the eye movements in the slow phases was also higher in the motion condition than in the baseline condition of both experiments (stripes: 8.5 ± 0.6 degrees/s during motion versus 0.0 ± 0.2 degrees/s during baseline, $p < 0.001$; dots: 5.2 ± 1.5 degrees/s during motion versus 0.2 ± 0.5 degrees/s during baseline, $p < 0.001$). The slow phase velocity during the motion condition was higher in the stripes experiment than in the dots experiment ($p < 0.001$).

Stripes

Random effect analysis with ANCOVA of the experiment in which OKR was evoked by a moving pattern of stripes, at $p < 0.05$ with FDR correction for multiple comparisons, yielded bilateral activation in the precentral gyrus (frontal eye fields, FEF) and in the supplementary motor area (supplementary eye fields, SEF). Unilateral activation was found in the left superior parietal gyrus (parietal eye fields, PEF), and in the right middle temporal gyrus (motion-sensitive area, MT/V5). Furthermore, bilateral activation was observed in the cerebellar area VI (oculomotor area) and in the superior occipital, middle occipital, lingual, calcarine and the cuneus gyri (primary visual area V1) (Table 1, Figure 2).

Random effect analysis with cluster-level at $p < 0.05$ corrected for multiple comparisons yielded no additional activation.

Dots

Random effect analysis with ANCOVA of the experiment in which OKR was evoked by a moving pattern of limited lifetime dots, at $p < 0.05$ with FDR correction for multiple comparisons, revealed no significant activation. Random effect

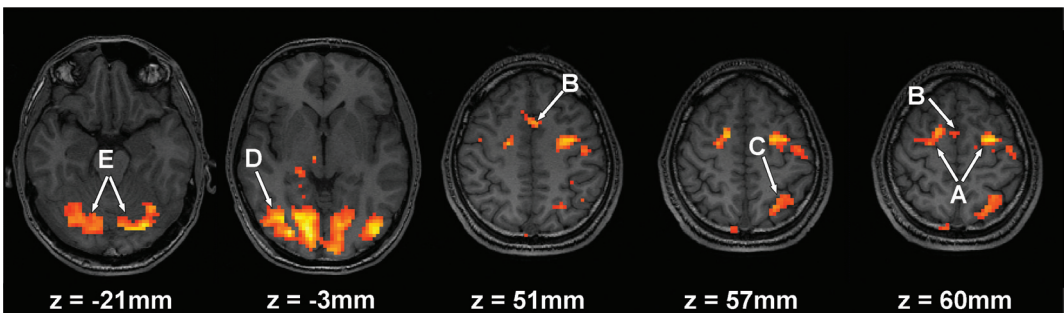


Figure 2: Areas of activation for the stripes experiment with (motion > baseline). All areas were thresholded at $p < 0.05$ with FDR correction for multiple comparisons and with a minimum cluster size of 5 voxels. (Labels: A: FEF, B: SEF, C: PEF, D: MT/V5, E: Cerebellum VI)

Stripes

Cluster size	%*	T-value	MNI co-ordinates			Anatomic area	side	Functional Area
			x	y	z			
3151	9.87	9.33	18	-75	3	Lingual Gyrus	R	PVA/V1
	8.16	7.65	-45	-75	3	Middle Occipital Gyrus	L	PVA/V1
	7.87	9.41	15	-87	3	Calcarine Gyrus	R	PVA/V1
	7.71	10.25	-12	-96	21	Superior Occipital Gyrus	L	PVA/V1
	7.27	7.75	-9	-81	-12	Lingual Gyrus	L	PVA/V1
	6.92	7.83	-12	-81	6	Calcarine Gyrus	L	PVA/V1
	6.76	7.2	18	-90	18	Superior Occipital Gyrus	R	PVA/V1
	5.81	5.58	39	-72	6	Middle Occipital Gyrus	R	PVA/V1
	5.62	9.41	15	-87	24	Cuneus	R	PVA/V1
	4.28	10.25	-12	-96	21	Cuneus	L	PVA/V1
	3.3	6.68	-15	-81	-24	Cerebellum Crus I	L	Oculomotor Area
	3.05	8.59	30	-84	-6	Fusiform Gyrus	R	
	3.01	7.64	-9	-81	-15	Cerebellum VI	L	Oculomotor Area
	2.92	8.81	30	-84	-9	Inferior Occipital Gyrus	R	PVA/V1
	2.89	5.9	12	-81	-15	Cerebellum VI	R	Oculomotor Area
	2.57	7.57	-24	-72	-12	Fusiform Gyrus	L	
	2.22	6.12	42	-69	-3	Middle Temporal Gyrus	R	MT/V5
	2.22	7.6	-42	-81	-3	Inferior Occipital Gyrus	L	PVA/V1
135	37.04	7.2	-30	-3	60	Superior Frontal Gyrus	L	FEF
	31.85	7.2	-30	-3	60	Precentral Gyrus	L	FEF
	22.96	6.11	-30	-3	51	Middle Frontal Gyrus	L	FEF
	1.48	2.94	12	15	60	Supplementary Motor Area	L	
58	58.62	5.42	-42	-9	42	Precentral Gyrus	L	FEF
	36.21	6.89	-42	-12	45	Postcentral Gyrus	L	
125	43.2	6.45	18	0	54	Superior Frontal Gyrus	R	
	42.4	6.34	15	0	54	Supplemental Motor Area	R	
	2.4	4.28	-18	0	53	Supplementary Motor Area	L	
	1.6	4.35	45	39	27	Middle Frontal Gyrus	R	
30	63.33	5.4	0	12	51	Supplementary Motor Area	L	SEF
	26.67	5.14	6	3	66	Supplementary Motor Area	R	SEF
	6.67	**				Superior Medial Frontal Gyrus	L	
	3.33	4.08	-3	15	39	Middle Cingulum Gyrus	L	
35	85.71	5.32	48	-3	45	Precentral Gyrus	R	FEF
	5.71	**				Postcentral Gyrus	R	
	5.71	**				Inferior Opercular Frontal Gyrus	R	
	2.86	4.53	45	39	27	Middle Frontal Gyrus	R	FEF

117	75.21	5.12	-24	-60	57	Superior Parietal Gyrus	L	PEF
	21.37	4.1	-36	-54	57	Inferior Parietal Gyrus	L	PEF
	2.56	**				Precuneus	L	
11	18.18	4.59	18	-30	0	Thalamus	R	
7	85.71	4.88	-39	27	24	Inferior Triangular Frontal Gyrus	L	
	14.29	**				Middle Frontal Gyrus	L	
9	100	4.76	-12	-21	42	Middle Cingulum Gyrus	L	
22	22.73	4.59	18	-30	0	Thalamus	R	
	22.73	4.23	18	-33	0	Hippocampus	R	
12	50	4.41	42	27	30	Inferior Triangular Frontal Gyrus	R	
	41.67	4.35	45	39	27	Middle Frontal Gyrus	R	
	8.33	**				Inferior Opercular Frontal Gyrus	R	
10	60	4.35	-60	-42	36	Inferior Parietal Gyrus	L	
	30	**				SupraMarginal	L	
19	78.95	4.35	45	39	27	Middle Frontal Gyrus	R	
	21.05	4.41	42	27	30	Inferior Triangular Frontal Gyrus	R	
8	62.5	4.3	-30	-39	45	Postcentral Gyrus	L	
	37.5	4.08	-51	-45	45	Inferior Parietal Gyrus	L	
31	96.77	4.3	-57	6	27	Precentral Gyrus	L	
	3.23	**				Postcentral Gyrus	L	
6	100	4.29	-42	45	-6	Middle Orbital Frontal Gyrus	L	
8	37.5	5.26	18	-66	24	Precuneus	R	
5	100	3.85	45	39	-15	Inferior Orbital Frontal Gyrus	R	

Table 1: Areas of activation for the stripes experiment with (motion>baseline) with cluster size, percentage of cluster size, t-values, MNI coordinates, anatomic labels and functional labels. All areas were thresholded at $p < 0.05$ with FDR correction for multiple comparisons and with a minimum cluster size of 5 voxels.

(L: left hemisphere, R: right hemisphere; FEF: frontal eye fields, SEF: supplementary eye fields, PEF: parietal eye fields, MT/V5: motion-sensitive area (MT/V5), PVA/V1: primary visual areas (V1)). *The unassigned areas are not listed in the table. **The anatomical region does not contain a local maximum to obtain a coordinate.

analysis with cluster-level at $p < 0.05$ corrected for multiple comparisons revealed unilateral activation in the right cerebellar area VI and bilateral activation in the cuneus, lingual and the calcarine gyri and unilateral activation in the right superior occipital (primary visual area V1) (Figure 3). This analysis revealed no significant activation in the frontal, supplementary and parietal eye fields, or the motion-sensitive area MT/V5.

Comparison between stripes and dots

The direct comparison between the two OKR experiments corrected for visual stimulation ($[\text{motion} > \text{baseline}]_{\text{stripes}}$ versus $[\text{motion} > \text{baseline}]_{\text{dots}}$) showed differences in activation. When the stripes experiment was compared with the dots experiment ($[\text{motion} > \text{baseline}]_{\text{stripes}} > [\text{motion} > \text{baseline}]_{\text{dots}}$), at $p < 0.05$ with FDR correction for multiple comparisons, the analysis yielded unilateral activation in the left precentral gyrus (FEF), in the left inferior and superior parietal

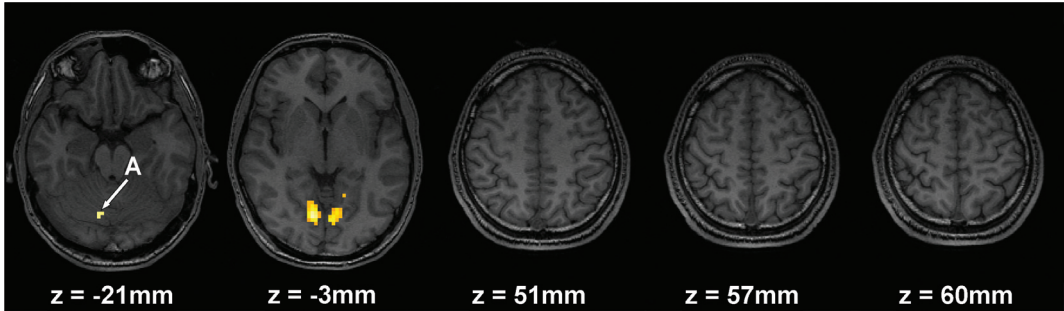


Figure 3: Areas of activation for the dots experiment with (motion > baseline). All areas were thresholded with cluster level at $p < 0.05$ corrected for multiple comparisons and with a minimum cluster size of 5 voxels. (Labels: A: Cerebellum VI)

gyrus (PEF) and in the right middle temporal gyrus (motion-sensitive area, MT/V5). Bilateral activation was found in the cerebellar area VI (oculomotor area) and in the middle occipital, inferior occipital, superior occipital, lingual and unilateral in the left calcarine gyri (primary visual area V1) (Table 2, Figure 4 and 5). Random effect analysis with cluster-level at $p < 0.05$ corrected for

multiple comparisons yielded additional activation in the left supplementary motor area (SEF) and in the left middle temporal gyrus (motion-sensitive area, MT/V5).

When the dots experiment was compared with the stripes experiment ($[\text{motion} > \text{baseline}]_{\text{dots}} > [\text{motion} > \text{baseline}]_{\text{stripes}}$), at $p < 0.05$ with FDR

Stripes vs Dots

Cluster size	%*	T-value	MNI co-ordinates			Anatomic area	side	Functional Area
			x	y	z			
248	54.03	7.01	-48	-81	3	Middle Occipital Gyrus	L	PVA/V1
	18.15	5.47	-35	-81	-9	Inferior Occipital Gyrus	L	PVA/V1
	9.27	5.76	-42	-50	-15	Fusiform Gyrus	L	
	8.87	5.38	-51	-60	-9	Inferior Temporal Gyrus	L	
	4.84	4.77	-42	-50	-24	Cerebellum Crus I	L	Oculomotor Area
	2.82	4.14	-54	-66	-3	Middle Temporal Gyrus	L	
318	23.9	6.33	33	-81	-6	Inferior Occipital Gyrus	R	PVA/V1
	23.58	5.22	45	-72	-5	Inferior Temporal Gyrus	R	
	18.55	4.5	39	-72	6	Middle Occipital Gyrus	R	PVA/V1
	17.92	4.66	48	-63	-3	Middle Temporal Gyrus	R	MT/V5
	4.72	5.5	30	-81	-3	Fusiform Gyrus	R	
	3.77	4.88	30	-45	-21	Cerebellum VI	R	Oculomotor Area
	1.57	4.18	42	-57	-27	Cerebellum Crus I	R	Oculomotor Area
95	41.05	5.32	-9	-81	-18	Cerebellum Crus I	L	Oculomotor Area
	26.32	5.86	-6	-81	-12	Lingual Gyrus	L	PVA/V1
	23.16	5.89	-9	-81	-15	Cerebellum VI	L	Oculomotor Area
	7.37	4.3	-24	-72	-12	Fusiform Gyrus	L	

	1.05	3.95	-9	-81	-27	Cerebellum Crus II	L	
142	68.31	5.43	-12	-93	3	Superior Occipital Gyrus	L	PVA/V1
	12.68	4.62	-12	-95	0	Middle Occipital Gyrus	L	PVA/V1
	12.68	3.51	-12	-87	6	Calcarine Gyrus	L	PVA/V1
	2.82	4.59	-12	-96	21	Cuneus Gyrus	L	
5	100	5.19	18	0	54	Superior Frontal Gyrus	R	
11	54.55	5.5	30	-81	-3	Fusiform Gyrus	R	
	27.27	5.16	30	-42	-21	Cerebellum IV_V	R	
	18.18	4.88	30	-45	-21	Cerebellum VI	R	
38	94.74	5.09	12	-84	-6	Lingual Gyrus	R	PVA/V1
	5.26	4.21	18	-87	6	Calcarine Gyrus	R	
7	57.14	4.92	48	36	18	Middle Frontal Gyrus	R	
	42.86	4.23	48	36	15	Inferior Triangular Frontal Gyrus	R	
18	38.89	4.78	-30	-3	60	Precentral Gyrus	L	FEF
	33.33	4.29	-27	-3	63	Superior Frontal Gyrus	L	FEF
	27.78	4.35	-30	-3	63	Middle Frontal Gyrus	L	
6	33.33	4.1	36	3	27	Inferior Opercular Gyrus	R	
	33.33	3.88	36	3	30	Precentral Gyrus	R	
6	66.67	4.38	-30	-39	48	Postcentral Gyrus	L	
	33.33	4.1	33	-39	48	Inferior Parietal Gyrus	L	
6	66.67	4.07	-33	-48	51	Inferior Parietal Gyrus	L	PEF
	33.33	3.87	-33	-51	57	Superior Parietal Gyrus	L	PEF
5	100	3.79	-48	-48	45	Inferior Parietal Gyrus	L	
8	75	3.71	21	-87	24	Superior Occipital Gyrus	R	

Table 2: Areas of activation for the direct comparison of the two OKR experiments ((motion >baseline) stripes > ((motion >baseline) dots) with cluster size, percentage of cluster size, t-values, MNI coordinates, anatomic labels and functional labels. All areas were thresholded at $p < 0.05$ with FDR correction for multiple comparisons and with a minimum cluster size of 5 voxels. (L: left hemisphere, R: right hemisphere; FEF: frontal eye fields, PEF: parietal eye fields, MT/V5: motion-sensitive area (MT/V5), PVA/V1: primary visual areas (V1)) *The unassigned areas are not listed in the table.

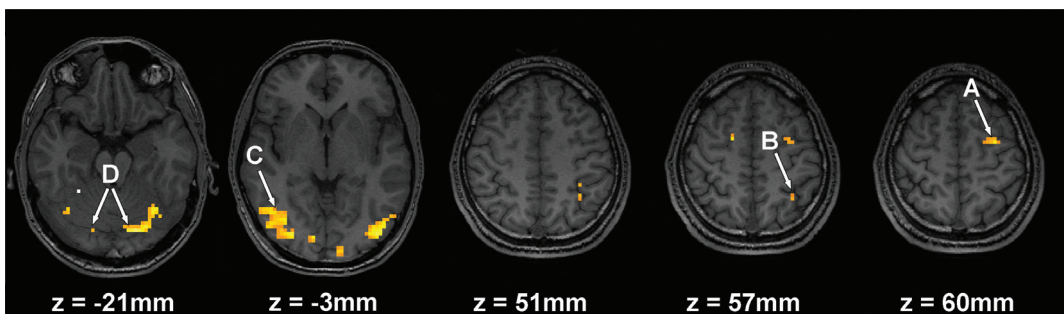


Figure 4: Area of activation for the direct comparison between the two experiments ((motion > baseline) stripes > ((motion > baseline) dots). All areas were thresholded at $p < 0.05$ with FDR correction for multiple comparisons and with a minimum cluster size of 5 voxels. (Labels: A: FEF, B: PEF, C: MT/V5, D: Cerebellum VI)

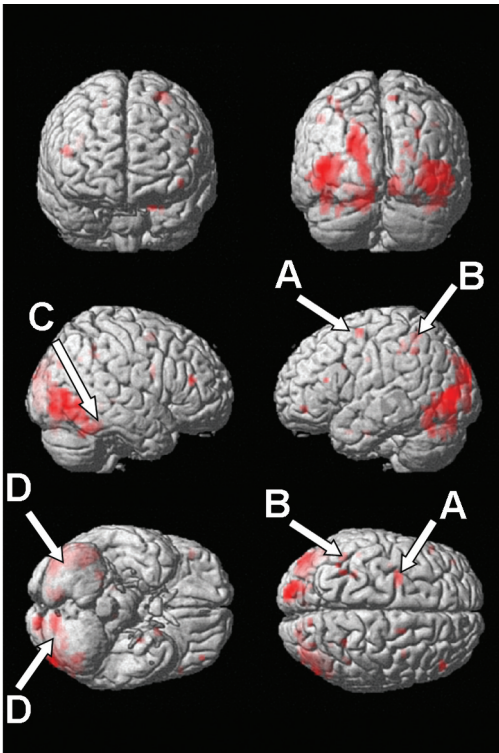


Figure 5: A 3-D view of areas of activation for the direct comparison between the two experiments ([motion > baseline] stripes > ([motion > baseline] dots). All areas were thresholded at $p < 0.05$ with FDR correction for multiple comparisons and with a minimum cluster size of 5 voxels.

(Labels: A: FEF, B: PEF, C: MT/V5, D: Cerebellum VI)

correction for multiple comparisons, no activation of interest was seen. Random effect analysis with cluster-level at $p < 0.05$ corrected for multiple comparisons also revealed no activation.

A summary of the areas of activation in the functional areas of interest is presented in Table 3.

DISCUSSION

The aim of this study was to investigate the confounding contribution of the smooth pursuit system on brain activation during OKR stimulation. Thus, we compared brain activation patterns with fMRI between two types of stimuli that evoke an OKR response: a moving pattern of stripes and a moving pattern of limited lifetime dots. The potential influence of differences in saccadic eye movement activity on brain activations were corrected for in our statistical analysis.

The eye movement behavioral data showed that both types of OKR stimuli evoked an adequate and similar optokinetic eye movement response, namely a mixture of slow and fast phases characteristic of optokinetic nystagmus. However, the fMRI data revealed significant dif-

	Stripes	Dots	Stripes>Dots
FEF	B	X	L
SEF	B	X	X (L)
PEF	L	X	L
MT/V5	R	X	R (B)
Oculomotor (Cerebellum area VI)	B	X (R)	B
PVA/V1	B	X (B)	B

Table 3: Activation in the areas of interest for each of the experiments (stripes and dots) separately and for the direct comparison of stripes > dots. All areas were thresholded at $p < 0.05$ with FDR correction for multiple comparisons and with a minimum cluster size of 5 voxels. Scores between brackets are the results using cluster-level at $p < 0.05$ corrected for multiple comparisons.

(B: bilateral, R: right hemisphere, x: no activation; FEF: frontal eye fields, SEF: supplementary eye fields, PEF: parietal eye fields, MT/V5: motion-sensitive area (MT/V5), PVA/V1: primary visual areas (V1))

ferences in brain activation patterns between the two experiments. In accordance with the literature [11, 16], our first experiment (OKR stimulation with stripes) yielded activation in the frontal eye fields (FEF), supplementary eye fields (SEF), parietal eye fields (PEF), in the middle tem-

poral gyrus (MT/V5) and in the cerebellar area VI. In our second experiment, however, using limited lifetime dots as a novel OKR stimulation, we did not see any significant activation in the FEF, SEF, PEF or MT/V5.

The direct comparison of the activation patterns between the two experiments showed that the FEF, PEF, MT/V5 and cerebellar area VI appear to be more activated when OKR was evoked by stripes than when OKR was evoked by limited lifetime dots. Note that in this direct comparison a possible confounding effect of the differences in visual stimulation in the each of the two experiments (stripes versus dots) is corrected for by first contrasting against baseline, instead of a direct comparison between the motion conditions.

We postulate that these observed differences may be partially explained by the confounding contribution of the smooth pursuit system on the OKR response for a moving pattern of stripes. Although it is likely that the pathways for OKR and smooth pursuit overlap [2, 17], the notion that the two eye movement systems can be distinguished is suggested by the observation that smooth pursuit and OKR can be selectively impaired in patients with specific lesions [18, 19].

Activation in the precentral gyrus (FEF), in the supplementary motor area (SEF), in the superior and inferior parietal gyrus (PEF), and in the middle temporal gyrus (MT/V5) has been observed previously with fMRI during OKR evoked by a moving pattern of stripes or colored objects [9, 11], as well as during smooth pursuit eye movements [11, 20]. Lesion studies suggest that the FEF plays an important role in the control of smooth pursuit and OKR eye movements [21] and that it is involved in visuomotor control, such as the execution of anti-saccades [22, 23].

SEF is thought to be involved in voluntary movements [24] such as smooth pursuit eye movements [20, 25]. The SEF is likely to play a role in planning this type of eye movement, comparable to the role supplementary motor area plays in other movements [25]. The PEF seems to be involved in visuo-spatial localization and attention [23, 26-29], and plays an important role in the initiation and control of visually cued motor actions such as voluntary smooth pursuit and saccadic eye movements [23, 28, 30]. Neurons in MT/V5 encode the direction of a moving object and speed of target motion [31] and it has been suggested that MT/V5 is critically involved in the generation of smooth pursuit eye movements [17, 20, 32, 33]. Indeed, patients with cortical lesions in the MT/V5 area exhibit severe impairments in smooth pursuit [18].

It has been suggested that a moving pattern of stripes or colored objects could elicit both smooth pursuit eye movements and OKR [9]. Indeed, a moving pattern of stripes is not only likely to trigger the OKR system by continuous stimulation in the retinal periphery [2, 7], but also evokes continuous stimulation at the fovea, thereby triggering the smooth pursuit system as well [2, 7]. The notion that a moving pattern of stripes triggers both eye movement systems might explain the previously reported lack of differences in brain activation patterns related to OKR, evoked by stripes, and smooth pursuit eye movements [11]. The results of our stripes experiment revealed activation in the frontal, supplementary and parietal eye fields and in area MT/V5. In our dots experiment, however, no activation was seen in any of the eye fields and the motion-sensitive area MT/V5, even when we lowered the statistical threshold. This suggests that these areas of the brain are less involved in the generation of an eye movement response toward a moving pattern of limited lifetime dots.

Since the smooth pursuit system has a latency of more than 100 ms [2], limited lifetime dots cannot be tracked using smooth pursuit eye movements, as each dot is repositioned within every 50 ms [13]. Activation in the SEF, PEF the motion-sensitive area MT/V5 during smooth pursuit eye movements may additionally be explained by the voluntary and attentional nature of smooth pursuit eye movements [2], e.g. for the selection of a single object or dot that is to be followed [11]. With a moving pattern of dots with a limited lifetime of only 50 ms, voluntary tracking of individual dots by smooth pursuit eye movements is unlikely to play a role [13].

It can be argued that the difference in activation patterns are induced by the differences in eye movement gains (the ratio of eye velocity and target velocity; a gain of 1 indicates the eyes are exactly on target) between the two experiments, as faster pursuit eye movements might involve more processing. It is, for instance, more difficult to track a fast moving stimulus during which an observer will make more tracking errors (relatively lower eye velocity compared to the stimulus velocity, i.e. reduced gains, and more corrective catch-up saccades). Therefore, faster pursuit may induce more brain activation although, to our knowledge, this has not been tested using functional imaging so far. In our experiments the velocity of the moving stimuli was well below the threshold for human OKR [2]. Both stimuli were therefore quite easy to follow, showing high gains and few catch-up saccades. The eye movement behavioral data suggest, however, that the tracking of the stripes seems to be much simpler than tracking the pattern of limited lifetime dots, as reflected by the higher eye velocities. Therefore, one might also argue the other way round that our limited lifetime dot stimulation should involve brain activity.

Furthermore, the amount of visual motion present at each location of the visual field was potentially different between the two experiments, i.e., more motion-sensitive receptive fields in MT/V5 are covered in the stripes experiment than in the dots experiment. This notion might explain the higher activation in MT/V5, but not the increased activation in the cerebellum. In addition, as the fovea is over-represented in MT/V5, the increased activation in this area could also be induced by the increased amount of foveal stimulation in the stripes experiment, similar to smooth pursuit.

Nevertheless, it is well-known that a moving pattern of dots usually evokes activation within the MT/V5 area, even in the absence of eye movements [31]. The lack of activation might than be explained by the activation of MT/V5 in both the active and the baseline condition of the dots experiment. Activation in MT/V5 in the baseline condition could, for instance, be due to apparent motion, which entails the visual illusion of movement of a single dot between two target position when in reality two dots are alternately turned on and off at two spatially separated positions [34]. Apparent motion is found to activate area MT/V5 in humans [35].

We could have compared brain activation patterns between stimulation with limited lifetime dots and stimulation with dots having a fixed lifetime, i.e. a dot has a constant position within the pattern. This might seem a useful comparison. However, there is an inherent problem with a fixed pattern of dots for studying a possible confounding influence of the smooth pursuit system in tracking an OKR stimulus. One cannot prevent an observer to foveate and track a single dot of the fixed dot pattern. Such behavior would transform the fixed dot OKR stimulus into a smooth pursuit stimulus, which would render it an inappropriate stimulus for investigating

the possible confounding contribution of the smooth pursuit system during traditional OKR stimulation.

It would be interesting to employ the two stimulation protocols (stripes and limited lifetime dots) in subjects with and without foveal processing. The absence of central visual function, which might be real (i.e., macular degeneration) or experimentally induced, would effectively eliminate smooth pursuit in both types of stimulation.

The limited field of view in the MR scanner may pose a problem, since OKR stimulation is mainly driven by peripheral stimulation. Other fMRI studies on OKR did not differ with respect to the (limited) field-of-view (25 degrees [11], 20 degrees [5], 20 degrees [9]), and showed comparable outcomes. The field of view is larger than the size of the (para-)fovea (± 8 degrees), which measured peripheral stimulation does occur in our setup. As larger field-of-view stimulation will probably induce better OKR responses, fMRI setups that deliver visual stimulation through goggles may overcome potential problems with the restricted field of view, that is typical of current fMRI studies.

CONCLUSION

Taken together, the present results suggest that the frontal and parietal eye fields, MT/V5 areas and cerebellum are more activated during OKR stimulation with a possible smooth pursuit component (using stripes) than during OKR without any smooth pursuit (using limited lifetime dots), although both types of stimuli elicit similar optokinetic eye movement responses. We conclude that the smooth pursuit system is likely to play a role in tracking an OKR stimulus that consists of a moving pattern of stripes [9].

REFERENCES

1. Galati, G., et al., Cortical control of optokinetic nystagmus in humans: a positron emission tomography study. *Exp Brain Res*, 1999. 126(2): p. 149-59.
2. Leigh, R.J. and D.S. Zee, *The Neurology of Eye Movements*. Third ed. 1999, New York: Oxford University Press.
3. Carpenter, R.H.S., *Movements of the Eyes*. Second ed. 1988, London: Pion Ltd.
4. Konen, C.S., et al., An fMRI study of optokinetic nystagmus and smooth-pursuit eye movements in humans. *Exp Brain Res*, 2005. 165(2): p. 203-16.
5. Brandt, T., et al., Bilateral functional MRI activation of the basal ganglia and middle temporal/medial superior temporal motion-sensitive areas: optokinetic stimulation in homonymous hemianopia. *Arch Neurol*, 1998. 55(8): p. 1126-31.
6. Dieterich, M., et al., fMRI signal increases and decreases in cortical areas during small-field optokinetic stimulation and central fixation. *Exp Brain Res*, 2003. 148(1): p. 117-27.
7. Kandel, E.R., J.H. Schwartz, and T.M. Jessell, in *Principles of Neural Science*. 2000, McGraw-Hill Health Professions Division: New York.
8. Bucher, S.F., et al., Sensorimotor cerebral activation during optokinetic nystagmus. A functional MRI study. *Neurology*, 1997. 49(5): p. 1370-7.
9. Dieterich, M., et al., Horizontal or vertical optokinetic stimulation activates visual motion-sensitive, ocular motor and vestibular cortex areas with right hemispheric dominance. An fMRI study. *Brain*, 1998. 121 (Pt 8): p. 1479-95.

10. Dieterich, M. and T. Brandt, Brain activation studies on visual-vestibular and ocular motor interaction. *Curr Opin Neurol*, 2000. 13(1): p. 13-8.
11. Konen, C.S., et al., An fMRI study of optokinetic nystagmus and smooth-pursuit eye movements in humans. *Exp Brain Res*, 2005.
12. Kelders, W.P., et al., Compensatory increase of the cervico-ocular reflex with age in healthy humans. *J Physiol*, 2003. 553(Pt 1): p. 311-7.
13. Mestre, D.R. and G.S. Masson, Ocular responses to motion parallax stimuli: the role of perceptual and attentional factors. *Vision Res*, 1997. 37(12): p. 1627-41.
14. van der Geest, J.N. and M.A. Frens, Recording eye movements with video-oculography and scleral search coils: a direct comparison of two methods. *J Neurosci Methods*, 2002. 114(2): p. 185-95.
15. Tzourio-Mazoyer, N., et al., Automated anatomical labeling of activations in SPM using a macroscopic anatomical parcellation of the MNI MRI single-subject brain. *Neuroimage*, 2002. 15(1): p. 273-89.
16. Dieterich, M., Ocular motor system: anatomy and functional magnetic resonance imaging. *Neuroimaging Clin N Am*, 2001. 11(2): p. 251-61, viii-ix.
17. Dursteler, M.R. and R.H. Wurtz, Pursuit and optokinetic deficits following chemical lesions of cortical areas MT and MST. *J Neurophysiol*, 1988. 60(3): p. 940-65.
18. Heide, W., K. Kurzydum, and D. Kompf, Deficits of smooth pursuit eye movements after frontal and parietal lesions. *Brain*, 1996. 119 (Pt 6): p. 1951-69.
19. Ilg, U.J., F. Bremmer, and K.P. Hoffmann, Optokinetic and pursuit system: a case report. *Behav Brain Res*, 1993. 57(1): p. 21-9.
20. Petit, L. and J.V. Haxby, Functional anatomy of pursuit eye movements in humans as revealed by fMRI. *J Neurophysiol*, 1999. 82(1): p. 463-71.
21. Rivaud, S., et al., Eye movement disorders after frontal eye field lesions in humans. *Exp Brain Res*, 1994. 102(1): p. 110-20.
22. Paus, T., Location and function of the human frontal eye-field: a selective review. *Neuropsychologia*, 1996. 34(6): p. 475-83.
23. Muri, R.M., et al., Location of the human posterior eye field with functional magnetic resonance imaging. *J Neurol Neurosurg Psychiatry*, 1996. 60(4): p. 445-8.
24. Tanji, J., New concepts of the supplementary motor area. *Curr Opin Neurobiol*, 1996. 6(6): p. 782-7.
25. Krauzlis, R.J., Recasting the smooth pursuit eye movement system. *J Neurophysiol*, 2004. 91(2): p. 591-603.
26. Bisley, J.W. and M.E. Goldberg, The role of the parietal cortex in the neural processing of saccadic eye movements. *Adv Neurol*, 2003. 93: p. 141-57.
27. Bremmer, F., C. Distler, and K.P. Hoffmann, Eye position effects in monkey cortex. II. Pursuit- and fixation-related activity in posterior parietal areas LIP and 7A. *J Neurophysiol*, 1997. 77(2): p. 962-77.
28. Muri, R.M., MRI and fMRI analysis of oculomotor function. *Prog Brain Res*, 2005. 151: p. 503-26.
29. Pierrot-Deseilligny, C., D. Milea, and R.M. Muri, Eye movement control by the cerebral cortex. *Curr Opin Neurol*, 2004. 17(1): p. 17-25.
30. Berman, R.A., et al., Cortical networks subserving pursuit and saccadic eye movements in humans: an FMRI study. *Hum Brain Mapp*, 1999. 8(4): p. 209-25.

31. Churchland, M.M. and S.G. Lisberger, Shifts in the population response in the middle temporal visual area parallel perceptual and motor illusions produced by apparent motion. *J Neurosci*, 2001. 21(23): p. 9387-402.
32. Komatsu, H. and R.H. Wurtz, Relation of cortical areas MT and MST to pursuit eye movements. I. Localization and visual properties of neurons. *J Neurophysiol*, 1988. 60(2): p. 580-603.
33. Thier, P. and R.G. Erickson, Responses of Visual-Tracking Neurons from Cortical Area MST-I to Visual, Eye and Head Motion. *Eur J Neurosci*, 1992. 4(6): p. 539-553.
34. Wertheimer, M., Experimentelle Studien über das Sehen von Bewegung, *Zeitschrift für Psychologie*. 1912. p. 161-265.
35. Goebel, R., et al., The constructive nature of vision: direct evidence from functional magnetic resonance imaging studies of apparent motion and motion imagery. *Eur J Neurosci*, 1998. 10(5): p. 1563-73.

PART 2

SMOOTH PURSUIT AND FIXATION SUPPRESSION



MELBOURNE

墨
爾
本

CHAPTER 4

AN FMRI STUDY ON SMOOTH PURSUIT AND
FIXATION SUPPRESSION OF THE OPTOKINETIC
REFLEX USING SIMILAR VISUAL STIMULATION

AN FMRI STUDY ON SMOOTH PURSUIT AND FIXATION SUPPRESSION OF THE OPTOKINETIC REFLEX USING SIMILAR VISUAL STIMULATION

Published by Experimental Brain Research, 2008, 185(4):535-544

ABSTRACT

This study compares brain activation patterns evoked by smooth pursuit and by fixation suppression of the optokinetic reflex (OKR) using similar retinal stimulation.

Functional magnetic resonance imaging (fMRI) was performed during smooth pursuit stimulation in which a moving target was presented on a stationary pattern of stripes, and during fixation suppression of OKR in which a stationary target was presented on a moving pattern of stripes.

All subjects could effectively ignore the background pattern and were able to keep the target continuously on the fovea with few saccades, in both experiments. Smooth pursuit

evoked activation in the frontal eye fields (FEF), the supplementary eye fields (SEF), the parietal eye fields (PEF), the motion-sensitive area (MT/V5), and in lobules and vermis VI of the cerebellum (oculomotor areas). Fixation suppression of OKR induced activation in the FEF, PEF, and MT/V5. The direct comparison analysis revealed more activation in the right lobule VI of the cerebellum and in the right lingual and calcarine gyri during smooth pursuit than during fixation suppression of OKR.

Using similar retinal stimulation, our results show that smooth pursuit and fixation suppression of the optokinetic reflex appear to activate largely overlapping pathways. The increased activity in the oculomotor areas of the cerebellum during smooth pursuit is probably due to the presence of an active eye movement component.

INTRODUCTION

Both smooth pursuit and fixation are oculomotor behaviors dedicated to keep the image of an object projected onto the fovea so that the object can be visually processed in great detail [1, 2]. Smooth pursuit is commonly evoked by a small moving target whereas fixation is used to foveate a stationary target. For these oculomotor behaviors to be effective, the motion of the visual background relative to the target has to be ignored. A moving background could evoke an optokinetic reflex (OKR) and leads to an eye movement pattern known as optokinetic nystagmus (OKN). The suppression of a moving background during fixation on a stationary target is referred to fixation suppression of the optokinetic reflex (OKR).

Neurophysiological studies in monkeys suggest that smooth pursuit and fixation suppression of OKR are two behavioral phenomena that may be generated by overlapping but distinct pathways. Microstimulation of specific regions in the motion-sensitive temporal areas (MT/V5) [3], the oculomotor vermis of the cerebellum [4] or the dorsolateral pontine nuclei [5], can cause changes in pursuit eye velocity during ongoing pursuit, but is ineffective during fixation on a stationary target. Electrophysiological studies suggest that certain parietal lobe neurons discharge during fixations but not during smooth pursuit [6].

However, the patterns of brain activity observed in humans during functional imaging studies with positron emission tomography (PET) and functional magnetic resonance imaging (fMRI) induced by smooth pursuit of a single target [7-11] are similar to those observed during fixation suppression of OKR [12-14]. Both smooth pursuit and fixation suppression of OKR have been found to elicit activation in the frontal (FEF), sup-

plementary (SEF) and parietal eye fields (PEF), as well as in various visual areas such as the primary visual area (PVA/V1) and the motion-sensitive area MT/V5.

In the above studies, comparison between patterns of brain activity during smooth pursuit and fixation suppression of OKR is, however, hampered by differences in the visual stimulation used. Smooth pursuit eye movements were studied using a single target on a homogeneous (dark) featureless background and this condition was contrasted with fixation on a stationary single target [7-11]. Fixation suppression of OKR, on the other hand, was studied using a single fixation target presented on a moving pattern, and this condition was compared with OKR stimulation using the same moving pattern without a fixation target [12-14]. Thus, the retinal stimulation is different between these studies on either smooth pursuit or fixation suppression of OKR.

The present study compares brain activation evoked by smooth pursuit and fixation suppression of OKR while using a similar retinal stimulation. For smooth pursuit, the stimulus was a single target moving against a stationary background consisting of a pattern of stripes, whereas for fixation suppression of OKR, the stimulus was a stationary single target with a moving background of stripes. Thus, in both cases the same visual background, which is moving relative to the smooth pursuit or to the fixation target, needs to be suppressed. We hypothesize that both smooth pursuit eye movement and fixation suppression of OKR will activate largely overlapping pathways, in line with previous studies. However, direct comparison of smooth pursuit and fixation suppression of OKR might yield differences related to the type of oculomotor behavior that is generated while the retinal stimulation is kept the same.

METHODS & MATERIALS

Subjects

Written informed consent was obtained from each participant prior to the study, which was approved by the Institutional Review Board. Twenty-two healthy volunteers (12 men, 10 women; average age of 27 years, range 22 to 43 years) participated in the study. None of the subjects had any known neurological or visual defects other than minor refractive anomalies. No one wore spectacle correction and all reported good visual acuity during the experiment.

Data acquisition

For each subject the images were acquired on a 1.5T MRI scanner (Signa CV/I; General Electric, Milwaukee, USA) using a dedicated 8-channel head coil. For the anatomical image, a 3D high resolution inversion recovery FSPGR T1 weighted sequence covering the whole brain including the cerebellum was acquired (repetition time (TR)/echo time (TE)/inversion time (TI) /9.99/2/400 ms, flip angle 20 degrees, 320x224 matrix with a rectangular field-of-view of 22 cm, 1.2 mm slice thickness with no gap; ASSET factor 2). Acquisition time was 5 minutes.

For functional imaging, a single-shot gradient-echo echo-planar imaging (EPI) sequence in transverse orientation was used, that is sensitive to blood oxygenation level dependent (BOLD) contrast. The imaging volume covered the entire brain including the whole cerebellum (TR/TE 2500/40 ms, flip angle 60 degrees, 96x96 matrix with a field-of-view of 26 cm, 5.5 mm slice thickness and 1 mm gap, 19 slices; voxel size of 5.5x2.7x2.7 mm³). Acquisition time was 5 minutes 40 seconds per experiment (including 20 seconds of dummy scans that were discarded from further analysis).

Stimuli

Each subject participated in two experiments. The experiments were performed in near darkness. The visual stimuli were binocularly presented by means of a goggle-based system (Silent Vision SV-7021 Fiber Optic Visual System; Avotec Inc., Stuart, Florida, USA). The optical components were mounted on top of the head coil. Screen resolution was 1024x768 pixels and the refresh rate was 60 Hz. In both experiments the visual stimulation consisted of one single red dot (1.0 degrees of visual angle in diameter) presented on a background pattern of black and white stripes (luminance contrast of about 1). Each stripe had a width of 0.9 degrees. The overall luminance of the whole stimulus was 13.9 cd/m². Subjects were instructed to look at the dot continuously in all conditions.

In the first experiment (smooth pursuit), the dot was either positioned in the centre of the field-of-view and was not moving (baseline condition) or it was moving towards the left and right sinusoidally (motion condition). The moving dot in the motion condition stopped exactly at the center of the field-of-view during the change of condition to avoid resetting saccades. In this experiment the background pattern was always stationary. In the second experiment (OKR suppression), the background pattern was either stationary (baseline), or it was moving towards the right and left sinusoidally (motion condition). In this second experiment the dot was always stationary at the center of the field-of-view. The frequency (0.15 Hz) and the sinusoidal amplitude (10 degrees of visual angle) was the same for the moving dot in the smooth pursuit experiment and for the striped pattern in the OKR suppression experiment. So, the retinal stimulation was the same in the two experiments, if the dot was kept onto the fovea.

Both experiments consisted of a block design with two conditions (baseline & motion). In each experiment, the baseline and the motion condition were presented in alternation. The baseline and the motion condition were presented 8 times. Each condition lasted 20 seconds during which time 8 volumes were acquired. The order of the experiments was pseudo-randomly performed across subjects. Eye movements (monocular, left eye) were registered continuously with the Real Eye RE-4601 Imaging System (Avotec Inc., Stuart, Florida, USA) with a 60 Hz sampling rate during each scanning session. Recording and online monitoring of eye movement behavior was done with the iViewX Eye Tracking System (SensoMotoric Instruments, Teltow, Germany). The system was calibrated before each scan session with the built-in 3-by-3 point calibration routine.

ANALYSIS

Behavioral data

The eye movement recordings were analyzed offline. Eye velocity was calculated using a second-order polynome filter. Saccadic eye movements were extracted semi-automatically using an eye velocity criterion of 30 degrees/second and checked manually. The total number of saccades and blinks were counted. For each subject, the average number of saccades and blinks per block, and the gain (i.e., the ratio of eye velocity and target velocity; a gain of 1 indicates the eyes are moving as fast as the stimulus) were calculated for each of the two conditions (baseline and motion) in each of the two experiments (smooth pursuit and OKR suppression). Paired t-tests were used to assess differences in these behavioral parameters.

Functional imaging data

The functional imaging data were analyzed using statistical parametric mapping software (SPM 2, distributed by the Wellcome Department of Cognitive Neurology, University College London, UK) implemented in MATLAB (Version 6.5, Mathworks, Sherborn, MA, USA). For both experiments, motion correction and co-registration were done according to the methodology provided by SPM2 [15]. Brain volumes were normalized to the standard space defined by the Montreal Neurological Institute (MNI) template. The normalized data had a resolution of $3 \times 3 \times 3$ mm³ and were spatially smoothed with a three-dimensional isotropic Gaussian kernel, with a full-width-half-maximum of 10 mm.

Statistical parametric maps were calculated for each subject. Movement parameters resulting from the realignment pre-processing were included as regressors of no interest to further reduce motion artifacts. The model was estimated with a high-pass filter with a cut-off period of 128 seconds. For each subject and for each experiment, a t-contrast map was calculated between the motion condition and the baseline condition (motion > baseline).

The individual t-contrast maps were used for second level random effects (group) analysis. One sample t-tests were performed for both experiments separately: [motion > baseline]_{smooth pursuit} and [motion > baseline]_{OKR suppression}. To investigate the differences in brain activation between smooth pursuit eye movement and OKR suppression conditions corrected for the baseline activation, we used a paired t-test [motion > baseline]_{smooth pursuit} versus [motion > baseline]_{OKR suppression} and vice versa. All tests were thresholded at $p < 0.05$ with false discovery rate (FDR) correction for multiple comparisons and at a minimum cluster size of 10 voxels.

Anatomic labeling of the observed areas of activation in SPM was done using the macroscopic anatomic parcellation procedure of the Montreal Neurological Institute (MNI) MRI single-subject brain [15].

RESULTS

Behavioral data

In 5 of the 22 subjects, inspection of the eye movement responses showed an improper performance during the experiments. One subject

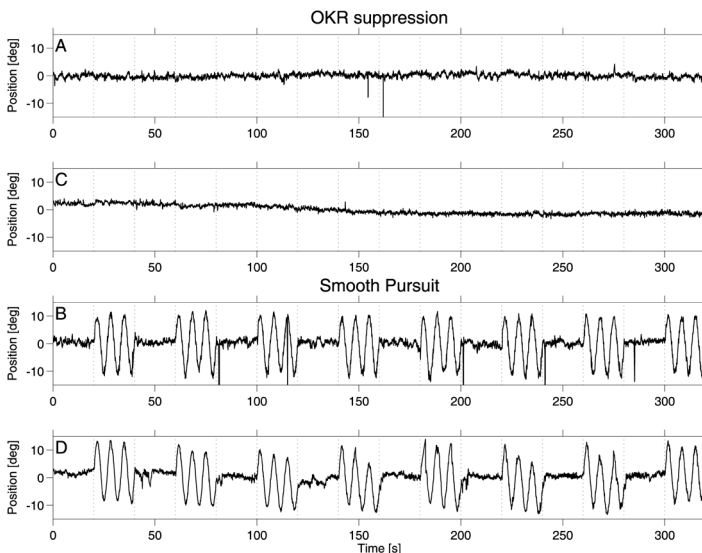


Figure 1: Examples of the 320 seconds recording of the eye movements made by two subjects in the OKR suppression experiment (panel A and B) and in the smooth pursuit experiment (panel C and D). The vertical dotted lines indicate the beginning of each block.

moved her eye position away from the tracker during scanning. One subject failed to complete the OKR suppression experiment. In three subjects, the eye movement recording failed during the smooth pursuit experiment.

All remaining 17 subjects were able to perform the tasks and keep the target on the fovea (fig-

Behavioral parameter	Condition	Smooth Pursuit	OKR suppression
Number of saccades	Baseline	0.24 ± 0.31	0.14 ± 0.26
	Motion	0.48 ± 0.55	0.05 ± 0.10
Eye movement gain	Baseline	0.04 ± 0.03	0.03 ± 0.02
	Motion	0.97 ± 0.13	0.03 ± 0.01
Number of blinks	Baseline	2.28 ± 2.32	3.07 ± 3.52
	Motion	1.18 ± 1.68	1.59 ± 1.94

Table 1: The behavioral eye movement parameters (number of saccades per 20s block, eye movement gain, number of blinks per 20s block) across the 17 subjects measured in the two experiments (Smooth pursuit & OKR suppression) and two conditions (baseline & motion) during the fMRI session.

ure 1). The motion conditions of the smooth pursuit eye experiment evoked typical smooth pursuit eye movements and the moving background was effectively ignored in the motion conditions of the OKR suppression experiment. In all baseline conditions subjects fixated the dot properly.

The statistical analysis of the behavioral data (table 1) showed that the average number of saccades per 20 second block was low, and did not differ between the motion and baseline conditions in both the smooth pursuit experiment ($p=0.09$) and in the OKR suppression experiment ($p=0.12$). There was no difference in the number of saccades between the motion condition

of the smooth pursuit experiment and the motion condition of the OKR suppression experiment. The eye movement gain was about one in the motion condition of the smooth pursuit experiment and about zero in all other conditions. The number of blinks did not differ between the conditions or experiments.

Cluster volume	T-value	MNI coordinate (mm)			Anatomic area	side	%*	Functional Area
		x	y	z				
3700	12.97	42	-72	-3	Superior Parietal Gyrus	R	2.68	PEF
					Inferior Parietal Gyrus	R	1.16	PEF
					Middle Temporal Gyrus	R	2.92	MT/V5
					Inferior Temporal Gyrus	R	1.89	
					Cerebellum VI	R	5.35	Oculomotor area
					Cerebellum VI	L	4.24	Oculomotor area
					Cerebellum Crus I	L	2.19	Oculomotor area
					Vermis VI		1.73	Oculomotor area
					Cerebellum Crus I	R	1.7	Oculomotor area
					Lingual Gyrus	R	8.92	PVA/V1
					Lingual Gyrus	L	7.89	PVA/V1
					Calcarine Gyrus	R	6.05	PVA/V1
					Middle Occipital Gyrus	L	5.84	PVA/V1
					Calcarine Gyrus	L	5.84	PVA/V1
					Middle Occipital Gyrus	R	5.46	PVA/V1
					Superior Occipital Gyrus	R	4.19	PVA/V1
					Inferior Occipital Gyrus	L	3.38	PVA/V1
					Inferior Occipital Gyrus	R	3.22	PVA/V1
					Superior Occipital Gyrus	L	2.14	PVA/V1
				Fusiform Gyrus	L	3.84		
407	7.03	-21	-9	57	Precentral Gyrus	L	47.42	FEF
					Postcentral Gyrus	L	13.76	
					Superior Frontal Gyrus	L	10.32	
					Middle Frontal Gyrus	L	6.63	
					Supplementary Motor Area	L	1.72	SEF
253	5.4	-33	-45	51	Superior Parietal Gyrus	L	49.41	PEF
					Inferior Parietal Gyrus	L	32.02	PEF
					Postcentral Gyrus	L	9.88	
					Precuneus Gyrus	L	1.58	
226	4.84	27	3	57	Superior Frontal Gyrus	R	31.42	
					Middle Frontal Gyrus	R	28.32	
					Precentral Gyrus	R	26.55	FEF

Table 2: Areas of activation for the smooth pursuit eye movement experiment with (smooth pursuit > fixation) with cluster size, t-values of local maximum, MNI coordinates, anatomic labels, percentage of cluster size and functional labels. All areas were thresholded at $p < 0.05$ with FDR correction for multiple comparisons and with a minimum cluster size of 10 voxels.

(L: left hemisphere, R: right hemisphere; FEF: frontal eye fields, SEF: supplemental eye fields, PEF: parietal eye fields, MT/V5: motion-sensitive area (MT/V5), PVA/V1: primary visual areas (V1)). *The unassigned areas for each cluster are not listed in the table.

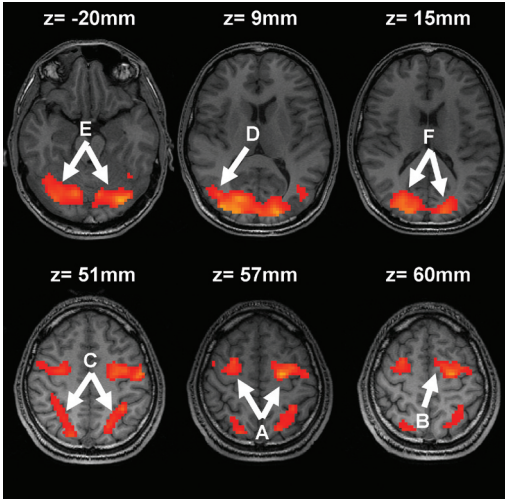


Figure 2: Activated clusters for smooth pursuit experiment. All areas were thresholded at $p < 0.05$ with FDR correction for multiple comparisons and with a minimum cluster size of 10 voxels. (Labels: A: FEF, B: SEF, C: PEF, D: MT/V5, E: Cerebellar lobule VI, F: PVA/V1)

Smooth Pursuit

Random effects group analysis of the smooth pursuit experiment with the contrast [motion > baseline]_{smooth pursuit} revealed bilateral activation in the precentral gyrus (frontal eye fields, FEF), unilateral activation in the left supplementary motor area (supplementary eye fields, SEF) and bilateral activation in the superior and inferior parietal gyrus (parietal eye fields, PEF). Unilateral activation was also found in the right middle temporal gyrus (motion-sensitive area, MT/V5). Bilateral activation was also found in the cerebellar lobule VI and crus I and centrally in vermis VI. Furthermore, bilateral activation was observed in the inferior occipital, middle occipital, superior occipital, lingular, and calcarine gyri (primary

visual area V1) as well as in the fusiform gyrus (visual area V4) (table 2, figure 2).

OKR suppression

Random effects group analysis of the OKR suppression experiment with the contrast [motion > baseline]_{OKR suppression} revealed bilateral activation in the precentral gyrus (FEF), in the superior and inferior parietal gyrus (PEF), and in the middle temporal gyrus (MT/V5). Furthermore, bilateral activation was observed in the inferior occipital, middle occipital, superior occipital, lingular gyri and unilateral activation in the right calcarine gyrus (primary visual area V1). Bilateral activation was found in the fusiform gyrus (visual area V4). There was no significant activation in the supplementary motor area (SEF) and in the oculomotor areas of the cerebellum (table 3, figure 3).

Comparison between smooth pursuit and OKR suppression

When the activation in the smooth pursuit eye movement experiment was compared with the OKR suppression experiment ([motion > baseline]_{smooth pursuit} versus [motion > baseline]_{OKR suppression}), at $p < 0.05$ with FDR correction no activation

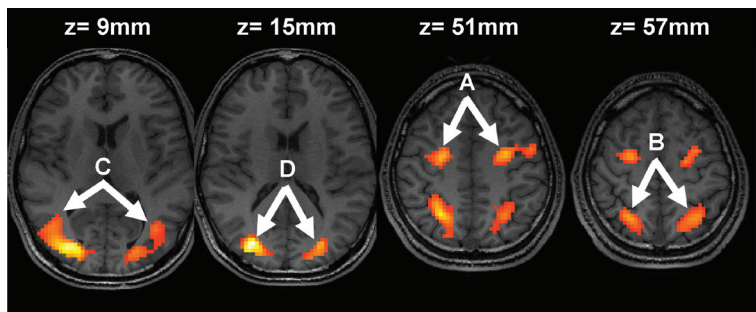


Figure 3: Activated clusters for OKR suppression experiment. All areas were thresholded at $p < 0.05$ with FDR correction for multiple comparisons and with a minimum cluster size of 10 voxels. (Labels: A: FEF, B: PEF, C: MT/V5, D: PVA/V1)

of interest was seen. Random effects analysis with a threshold at $p < 0.05$ corrected for multi-

Cluster volume	T-value	MNI coordinate (mm)			Anatomic area	side	%*	Functional Area
		x	y	z				
937	10.37	33	-78	12	Middle Temporal Gyrus	R	15.58	MT/V5
					Inferior Temporal Gyrus	R	10.03	
					Middle Occipital Gyrus	R	21.24	PVA/V1
					Inferior Occipital Gyrus	R	11.95	PVA/V1
					Superior Occipital Gyrus	R	6.94	PVA/V1
					Calcarine Gyrus	R	4.8	PVA/V1
					Lingual Gyrus	R	4.38	PVA/V1
					Lingual Gyrus	L	1.07	PVA/V1
					Fusiform Gyrus	R	8.11	
315	7.82	27	-54	51	Superior Parietal Gyrus	R	42.86	PEF
					Inferior Parietal Gyrus	R	13.97	PEF
					Postcentral Gyrus	R	8.25	
					SupraMarginal Gyrus	R	3.49	
					Superior Occipital Gyrus	R	2.86	
					Angular Gyrus	R	1.9	
					Precuneus	R	1.27	
568	7.62	-27	-78	21	Middle Temporal Gyrus	L	7.04	MT/V5
					Middle Occipital Gyrus	L	41.2	PVA/V1
					Inferior Occipital Gyrus	L	16.2	PVA/V1
					Superior Occipital Gyrus	L	10.92	PVA/V1
					Fusiform Gyrus	L	9.86	
175	5.91	-27	-3	51	Precentral Gyrus	L	54.86	FEF
					Middle Frontal Gyrus	L	16	
					Superior Frontal Gyrus	L	12	
112	5.79	27	-6	51	Superior Frontal Gyrus	R	30.36	
					Precentral Gyrus	R	21.43	FEF
					Middle Frontal Gyrus	R	16.96	
215	5.16	-27	-57	57	Superior Parietal Gyrus	L	57.21	PEF
					Inferior Parietal Gyrus	L	29.77	PEF
					Precuneus Gyrus	L	3.72	
18	4.05	-12	-21	45	Middle Cingulum Gyrus	L	50	
15	3.9	-54	-39	33	SupraMarginal Gyrus	L	80	
					Inferior Parietal Gyrus	L	20	

Table 3: Areas of activation for the fixation suppression of OKR (OKR suppression > fixation) with cluster size, t-values of local maximum, MNI coordinates, anatomic labels, percentage of cluster size and functional area. All areas were thresholded at $p < 0.05$ with FDR correction for multiple comparisons and with a minimum cluster size of 10 voxels.

(L: left hemisphere, R: right hemisphere; FEF: frontal eye fields, PEF: parietal eye fields, MT/V5: motion-sensitive area (MT/V5), PVA/V1: primary visual areas (V1)). *The unassigned areas for each cluster are not listed in the table.

Cluster volume	T-value	MNI coordinate (mm)			Anatomic area	side	%*	Functional Area
		x	y	z				
175	5.64	21	-75	9	Cerebellum VI	R	6.86	Oculomotor Area
					Calcarine Gyrus	R	60.57	PVA/V1
					Lingual Gyrus	R	28.57	PVA/V1

Table 4: Areas of activation for the direct comparison of the two experiments (smooth pursuit > OKR suppression) with cluster size, t-values of local maximum, MNI coordinates, anatomic labels, percentage of cluster size and functional area. All areas were thresholded at $p < 0.05$ corrected for multiple comparisons at cluster level and with a minimum cluster size of 10 voxels. (R: right hemisphere; PVA/V1: primary visual areas (V1)) *The unassigned areas for each cluster are not listed in the table.

ple comparisons at cluster level and a minimum cluster size of 10 voxels revealed activation in the right cerebellar lobule VI. Furthermore, unilateral activation was found in the right lingual and calcarine gyrus (table 4, figure 4).

When the activation in the OKR suppression experiment was compared with the activation in the smooth pursuit eye movement experiment ($[\text{motion} > \text{baseline}]_{\text{OKR suppression}}$ versus $[\text{motion} >$

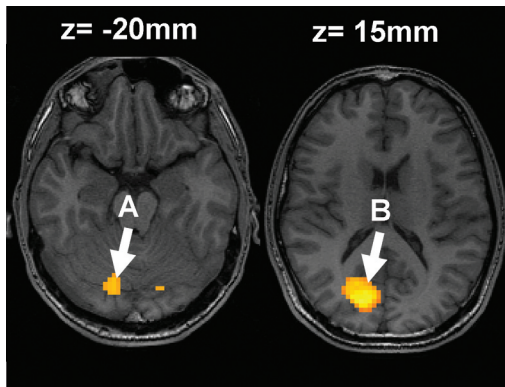


Figure 4 Activated clusters for the direct comparison (smooth pursuit vs OKR suppression). All areas were thresholded at $p < 0.05$ with correction for multiple comparisons at cluster level and with a minimum cluster size of 10 voxels. (Labels: A: Cerebellar lobule VI, B: PVA/V1)

baseline] $_{\text{smooth pursuit}}$), at $p < 0.05$ with FDR correction, no activation of interest was seen. Random effects analysis thresholded at $p < 0.05$ corrected for multiple comparisons at cluster level also revealed no activation of interest.

A summary of the results is presented in Table 5.

DISCUSSION

The aim of this study was to investigate possible differences in brain activation patterns evoked by smooth pursuit eye movements and fixation suppression of the OKR. Both oculomotor behaviors were evoked by the same retinal stimulation, in which a background pattern of stripes and a target were moving relative to each other. In both experiments the (relative) motion of the background needed to be ignored, while the target was to be kept on the fovea. The eye movement recordings which were acquired during the fMRI scans showed that all subjects were able to perform the tasks accurately, and could keep the target on the fovea continuously. Therefore, the alleged differences in brain activation between the two types of oculomotor behaviors are likely to be related to the differences between smooth pursuit eye movements and fixation suppression of OKR, rather than to differences in retinal stimulation, or to the number of saccades or blinks.

The fMRI data revealed differences in brain activation patterns between the two oculomotor behaviors. Smooth pursuit eye movements induced activation in the FEF, the SEF, the PEF, the MT/V5, and lobule VI and vermis VI of the cer-

Functional Area	Anatomic Location	Smooth Pursuit	OKR Suppression	Smooth Pursuit vs OKR Suppression	OKR Suppression vs Smooth Pursuit
Frontal Eye Fields (FEF)	Precentral Gyrus	B	B	-	-
Supplementary Eye Fields (SEF)	Supplementary Motor Areas	L	-	-	-
Parietal Eye Fields (PEF)	Inferior and Superior Parietal Gyrus	B	B	-	-
Visual Area 5 (MT/V5)	Middle Temporal Gyrus	R	B	-	-
Oculomotor Vermis	Cerebellum VI	B	-	-(R)	-

Table 5: Activation in the areas of interest for each of the experiment (smooth pursuit and fixation suppression of OKR) separately and for the direct comparison between the two experiments.

All areas were thresholded at $p < 0.05$ with FDR correction for multiple comparisons and with a minimum cluster size of 10 voxels. Scores between brackets are the results thresholded at $p < 0.05$ corrected for multiple comparisons at cluster level. (B: bilateral; R: right hemisphere; L: left hemisphere; - indicates no significant activation.)

ebellum. Fixation suppression of the OKR also induced activation in the FEF, the PEF, MT/V5, but not in the SEF or the cerebellum.

Smooth pursuit

During smooth pursuit the eyes follow a slowly moving target by matching its velocity (motion condition), whereas during fixation, gaze is maintained at a stationary target (baseline condition). The observed activation in our first experiment is likely to be evoked by the motion of the dot and the associated smooth pursuit response. Previous fMRI studies on smooth pursuit eye movements all used homogeneous backgrounds without any features [7, 8, 10, 11], whereas in the present study smooth pursuit was induced by a moving small target on a background with features, similar to natural smooth pursuit during daily life. Although the use of a cluttered background during smooth pursuit stimulation could have influenced our results, the activated areas in the present smooth pursuit experiment (FEF, SEF, PEF, MT/V5 and cerebellum) are in good accordance with previous fMRI studies [7, 8, 10, 11]. All these areas are known to be involved in pursuit oculomotor behavior. For instance, the

FEF and PEF contain neurons that are responsive to foveated tracking [16, 17]. Lesions of the FEF impair predictive and visually-guided smooth pursuit [2, 18-20]. The SEF are likely to play a role in planning and timing of voluntary movements, such as smooth pursuit [2]. Neurons in the middle temporal gyrus (MT/V5) encode visual motion [2, 21-23], which information can be used to guide pursuit of a small moving target [24, 25]. Patients with unilateral cortical lesions in the MT/V5 area exhibit impairments in smooth pursuit behavior, showing reduced eye movement gains and an increase in the number of catch-up saccades [20].

Fixation suppression of OKR

The main difference between the two conditions (motion and baseline) in the fixation suppression of OKR experiment was the motion of the background. Since the subjects were making no eye movements as they continuously fixated on the stationary dot, the induced brain activation is likely due to the suppression of the moving pattern of stripes, rather than to eye movements. The observed activation (FEF, PEF, MT/V5) is congruent with the observations of

previous fMRI studies, which studied small-field optokinetic stimulation with and without fixation [13, 14]. These studies reported that fixation suppression of the optokinetic response induced FEF, SEF, and PEF activation, albeit weaker than with optokinetic stimulation without suppression that induced optokinetic nystagmus. The activation of MT/V5 observed in the present study was previously reported in a PET study comparing OKR suppression with baseline [26]. As mentioned above, neurons in MT/V5 are sensitive to the presence of visual motion.

Smooth pursuit eye movement versus fixation suppression of OKR

When we directly compared the two experiments, the only difference in activation was observed in one cluster of activation spanning the cerebellum and primary visual areas when the smooth pursuit experiment was compared to the fixation suppression of OKR experiment. But this activation was present only with a more lenient statistical threshold at cluster level. This outcome suggests that smooth pursuit eye movement and fixation suppression of OKR activate overlapping cortical pathways. The difference in cerebellar activation is likely to be induced the presence of an active eye movement component in the smooth pursuit experiment. The differences in activation in the right lingual and calcarine gyri do suggest differences in the visual input and subsequent visual processing of the stimuli between the two experiments. Although the in-scanner recordings did not reveal significant differences in eye movement behavior, it should be noted that small eye movements (such as micro-saccades and small drifts) cannot be detected with the present equipment. Such small differences in eye movement behavior could nonetheless lead to small differences in visual input and processing.

Note that in the present study, using sinusoidal stimulation, no differences in saccadic activity was observed. This could explain the absence of differential activity between the two experiments in saccadic related areas like the frontal eye fields. Furthermore, there was no difference in activation of area MT/V5 between the two experiments. Cells in MT/V5 are sensitive to visual motion [2, 21-23, 27]. The comparable activation of MT/V5 in the two experiments supports the notion that the visual motion stimulation between the two experiments was indeed very similar.

The majority of activation was found to appear bilaterally, but activation was found to be unilateral in the right MT/V5 area in the smooth pursuit experiment. This right-sided lateralization of activation suggests a right hemispheric dominance in oculomotor performance, which may be related to the predominant role of the right hemisphere in spatial visual attention processes [14].

CONCLUSION

In conclusion, our imaging results suggest that under similar retinal stimulation conditions smooth pursuit eye movement and fixation suppression of the optokinetic response activate overlapping pathways. The increased activity in the oculomotor areas of the cerebellum during active smooth pursuit is probably due to the presence of an active eye movement component.

REFERENCES

1. Carpenter, R.H.S., *Movements of the Eyes*. Second ed. 1988, London: Pion Ltd.
2. Kandel, E.R., J.H. Schwartz, and T.M. Jessell, *Principles of neural science*. 4th ed. 2000, New York: McGraw-Hill, Health Professions Division. xli, 1414 p.
3. Komatsu, H. and R.H. Wurtz, Relation of cortical areas MT and MST to pursuit eye movements. I. Localization and visual properties of neurons. *J Neurophysiol*, 1988. 60(2): p. 580-603.
4. Krauzlis, R.J. and F.A. Miles, Role of the oculomotor vermis in generating pursuit and saccades: effects of microstimulation. *J Neurophysiol*, 1998. 80(4): p. 2046-62.
5. May JG, K.E., Crandall J, Changes in eye velocity during smooth pursuit tracking induced by microstimulation in the dorsolateral pontine nucleus of the macaque. *Soc Neurosci Abstr*, 1985. 11(79).
6. Lynch, J.C. and J.W. McLaren, Deficits of visual attention and saccadic eye movements after lesions of parietooccipital cortex in monkeys. *J Neurophysiol*, 1989. 61(1): p. 74-90.
7. Berman, R.A., et al., Cortical networks subserving pursuit and saccadic eye movements in humans: an fMRI study. *Hum Brain Mapp*, 1999. 8(4): p. 209-25.
8. Konen, C.S., et al., An fMRI study of optokinetic nystagmus and smooth-pursuit eye movements in humans. *Exp Brain Res*, 2005. 165(2): p. 203-16.
9. O'Driscoll, G.A., et al., Functional neuroanatomy of smooth pursuit and predictive saccades. *Neuroreport*, 2000. 11(6): p. 1335-40.
10. Petit, L. and J.V. Haxby, Functional anatomy of pursuit eye movements in humans as revealed by fMRI. *J Neurophysiol*, 1999. 82(1): p. 463-71.
11. Tanabe, J., et al., Brain activation during smooth-pursuit eye movements. *Neuroimage*, 2002. 17(3): p. 1315-24.
12. Bense, S., et al., Direction-dependent visual cortex activation during horizontal optokinetic stimulation (fMRI study). *Hum Brain Mapp*, 2005.
13. Bucher, S.F., et al., Sensorimotor cerebral activation during optokinetic nystagmus. A functional MRI study. *Neurology*, 1997. 49(5): p. 1370-7.
14. Dieterich, M., et al., Horizontal or vertical optokinetic stimulation activates visual motion-sensitive, ocular motor and vestibular cortex areas with right hemispheric dominance. An fMRI study. *Brain*, 1998. 121 (Pt 8): p. 1479-95.
15. Tzourio-Mazoyer, N., et al., Automated anatomical labeling of activations in SPM using a macroscopic anatomical parcellation of the MNI MRI single-subject brain. *Neuroimage*, 2002. 15(1): p. 273-89.
16. Fukushima, J., et al., The vestibular-related frontal cortex and its role in smooth-pursuit eye movements and vestibular-pursuit interactions. *J Vestib Res*, 2006. 16(1-2): p. 1-22.
17. Fukushima, J., et al., Pursuit-related neurons in the supplementary eye fields: discharge during pursuit and passive whole body rotation. *J Neurophysiol*, 2004. 91(6): p. 2809-25.
18. Keating, E.G., Frontal eye field lesions impair predictive and visually-guided pursuit eye movements. *Exp Brain Res*, 1991. 86(2): p. 311-23.

19. Keating, E.G., Lesions of the frontal eye field impair pursuit eye movements, but preserve the predictions driving them. *Behav Brain Res*, 1993. 53(1-2): p. 91-104.
20. Leigh, R.J. and D.S. Zee, *The Neurology of Eye Movements*. Third ed. 1999, New York: Oxford University Press.
21. Albright, T.D., Direction and orientation selectivity of neurons in visual area MT of the macaque. *J Neurophysiol*, 1984. 52(6): p. 1106-30.
22. Duffy, C.J. and R.H. Wurtz, Sensitivity of MST neurons to optic flow stimuli. II. Mechanisms of response selectivity revealed by small-field stimuli. *J Neurophysiol*, 1991. 65(6): p. 1346-59.
23. Muri, R.M., et al., Hemispheric asymmetry in cortical control of memory-guided saccades. A transcranial magnetic stimulation study. *Neuropsychologia*, 2000. 38(8): p. 1105-11.
24. Dursteler, M.R. and R.H. Wurtz, Pursuit and optokinetic deficits following chemical lesions of cortical areas MT and MST. *J Neurophysiol*, 1988. 60(3): p. 940-65.
25. Newsome, W.T., R.H. Wurtz, and H. Komatsu, Relation of cortical areas MT and MST to pursuit eye movements. II. Differentiation of retinal from extraretinal inputs. *J Neurophysiol*, 1988. 60(2): p. 604-20.
26. Bense, S., et al., Multisensory cortical signal increases and decreases during vestibular galvanic stimulation (fMRI). *J Neurophysiol*, 2001. 85(2): p. 886-99.
27. Bremmer, F., et al., Eye position effects in monkey cortex. I. Visual and pursuit-related activity in extrastriate areas MT and MST. *J Neurophysiol*, 1997. 77(2): p. 944-61.

PART 3

SACCADIC EYE MOVEMENT



EDMONTON

愛民頓

CHAPTER 5
CORTICAL AND CEREBELLAR
ACTIVATION INDUCED BY REFLEXIVE
AND VOLUNTARY SACCADDES

CORTICAL AND CEREBELLAR ACTIVATION INDUCED BY REFLEXIVE AND VOLUNTARY SACCADDES

Published by Experimental Brain Research, 2008, DOI: 10.1007/s00221-008-1569-4

ABSTRACT

Reflexive saccades are driven by visual stimulation whereas voluntary saccades require volitional control. Behavioral and lesional studies suggest that there are two separate mechanisms involved in the generation of these two types of saccades. This study investigated differences in cerebral and cerebellar activation between reflexive and self-paced voluntary saccadic eye movements using functional magnetic resonance imaging. In two experiments (whole brain and cerebellum) using the same paradigm, differences in brain activations induced by reflexive and self-paced voluntary saccades were assessed. Direct comparison of the activation patterns showed that the frontal eye fields, parietal eye field, the motion-sensitive area (MT/V5), the precuneus (V6), and the angular and the cingulate gyri were more activated in reflexive saccades than in voluntary saccades. No significant difference in activation was found in the cerebellum. Our results suggest that the alleged separate mechanisms for saccadic control of reflexive and self-paced voluntary are mainly observed in cerebral rather than cerebellar areas.

INTRODUCTION

Saccades are fast rotatory eye movements that serve to move the eyes as quickly as possible, so that an object of interest is projected onto the fovea where it can be visually processed in detail [1-4]. Saccades can be classified into two broad categories: reflexive and higher-order saccades. Reflexive saccades are saccades toward suddenly appearing targets and are described as reflexive or targeting saccades. Higher-order saccades have a more volitional nature and include voluntary, memory-guided and delayed saccades. Voluntary saccades are made with a cognitive judgment in order to determine when and where to move gaze [5-7].

The neurophysiological circuit that drives saccadic eye movements includes several distinct regions of the brain [5]. The mesencephalic and the pontine reticular formations of the brainstem encode the motor signals that drive the eye muscles. The superior colliculus encodes the direction and amplitude of the saccadic eye movements [5]. Several cortical brain areas, such as the frontal eye fields (FEF), the supplementary eye fields (SEF), the parietal eye fields (PEF), and the motion sensitive area (MT/V5), are also known to be involved in saccadic generation. Furthermore, the cerebellum is involved in maintaining saccadic accuracy [5]. Specific areas of the human cerebellum, such as lobule VI and VII and the fastigial nucleus, have been implicated in maintaining saccadic accuracy [6, 8]. Patients with cerebellar lesions often show inac-

curate saccades (known as saccadic dysmetria) that do not resolve over time [6].

Several functional magnetic resonance imaging (fMRI) and positron emission tomography (PET) imaging studies have shown activation in the human cerebellum during saccadic eye movements [2, 9-11]. For instance, Hayakawa et al. observed activity in the posterior vermis and the bilateral hemispheres of the cerebellum when subjects made saccades between two stationary targets [2].

It has been suggested that there are two separate and largely independent mechanisms involved in the generation of reflexive saccades and voluntary saccades [12]. Mort et al. aimed to compare the cortical activation patterns induced by these two types of saccades with fMRI [13]. In their paradigm, reflexive saccades were evoked by flashing a peripheral spot to the left or the right of the fixation spot. Voluntary saccades were evoked by means of an arrow cue as an indicator to the observer to change their point of gaze to a dot pointed at by the arrow. Their results suggested that FEF and PEF were more activated during voluntary saccades and that the angular gyrus and the precuneus were more activated during reflexive saccades [13]. Furthermore, behavioral studies showed that modification of the amplitudes of reflexive saccades in a saccade adaptation paradigm [14] does not influence the amplitudes of voluntary saccades, and vice versa [15-17]. The cerebellum is an important brain structure in saccadic gain control [6, 9, 18-20]. Desmurget et al. [21] demonstrated that the oculomotor vermis of the cerebellum is activated in a saccade adaptation paradigm. The results of the behavioral studies suggest that the cerebellum might also be involved in a different way in maintaining the accuracy of reflexive and voluntary saccades. In the present study fMRI was used to investi-

gate putative differences in cerebral and cerebellar activation patterns between reflexive and self-paced voluntary saccadic eye movements. We performed two experiments using the same experimental paradigm. The first experiment aimed to assess cerebral activations of saccadic eye movements and to compare the results with data from existing literature. The second experiment focused on the cerebellum, specifically obtaining more detailed activation within this brain structure. We hypothesized that the differences between reflexive and self-paced voluntary saccadic eye movements might be reflected by differences in cerebral as well as in cerebellar activation patterns.

MATERIALS AND METHODS

Subjects

Written informed consent was obtained from each participant prior to the study, which was approved by the Institutional Review Board. Subjects could participate in either one or both of the two experiments that were performed: whole brain and cerebellum. A total of 26 healthy volunteers (13 men, 13 women; average age 26.7 years, range 22 to 37 years) participated in the whole brain experiment, and 26 healthy volunteers (15 men, 11 women; average age 26.7 years, range 22 to 37 years) participated in the cerebellum experiment. Ten of these subjects participated in both experiments. None of the subjects had any known neurological or visual defects other than minor refractive anomalies. None of the subjects wore spectacle correction during the experiments, as minor refractive anomalies could be adjusted for by the goggle system that was used to display the stimuli. All subjects reported good visual acuity during the experiment.

Data acquisition

For each subject the images were acquired on a 1.5T MRI scanner (Signa CV/I; General Electric, Milwaukee, USA) using a dedicated 8-channel head coil. For the anatomical image, a 3D high-resolution inversion recovery FSPGR T1-weighted sequence covering the entire brain was acquired (repetition time (TR)/echo time (TE)/inversion time (TI) /9.99/2/400 ms, flip angle 20 degrees, 320x224 matrix with a rectangular field-of-view of 22 cm, 1.2 mm slice thickness with no gap; parallel imaging factor of 2). Acquisition time was 5 minutes.

Functional Imaging

For functional imaging, a single-shot gradient-echo echo-planar imaging (EPI) sequence in transverse orientation was used in each study that is sensitive to blood oxygenation level dependent (BOLD) contrast. For the whole brain experiment, the imaging volume covered the entire brain (TR/TE 4500/50 ms, 64x64 matrix with a rectangular field-of-view of 22 cm, 2.5 mm slice thickness, 48 contiguous slices; voxel size of 2.5x3.5x3.5 mm³). Acquisition time was 10:03 minutes per scanning session (including 18 seconds of dummy scans that were discarded). For the cerebellum experiment, the imaging volume only covered the whole cerebellum with higher spatial and temporal resolution (TR/TE 3000/50 ms, 96x96 matrix with a rectangular field-of-view of 24 cm, 2.5 mm slice thickness, 18 contiguous slices; voxel size of 2.5x2.5x2.5 mm³). Acquisition time was 10:00 minutes per scanning session (including 12 seconds of dummy scans that were discarded).

Eye tracking

Eye movements (monocular, left eye) were registered continuously with the Real Eye RE-4601 Imaging System (Avotec Inc., Stuart, Florida, USA) with a 60 Hz sampling rate. Online monitoring of eye movements and recording was done with

the iViewX Eye Tracking System (SensoMotoric Instruments, Teltow, Germany). The system was calibrated before each scan session with the built-in 3-by-3 point calibration routine.

Stimulus paradigm

The experiments were performed in near darkness. The visual stimuli were binocularly presented by means of a goggle-based system (Silent Vision SV-7021 Fiber Optic Visual System; Avotec Inc., Stuart, Florida, USA). The optical components were mounted on top of the head coil. Screen resolution was 1024x768 pixels and the refresh rate was 60 Hz.

The visual stimulation was exactly the same for both experiments (whole brain and cerebellum), and consisted of three different visual displays, corresponding to three experimental conditions. In all three displays, three horizontally aligned dots (0.9 degrees of visual angle in diameter) were presented on a dark background. The horizontal separation between the dots was 9 degrees, and the central dot was centered in the subject's visual field-of-view. The overall luminance was 0.43 cd/m².

In the fixation condition (baseline), the central dot was yellow, and the two peripheral dots were gray. Subjects were instructed to look at the yellow dot continuously. In the first active condition (reflexive saccades), the central dot and one of the peripheral dots were gray, and the other one was yellow. The two peripheral dots were intermittently yellow with a random interval between 1 and 2 seconds. In this condition saccade pace was therefore imposed by the other peripheral dot turning yellow.

In the second active condition (voluntary saccades), the central dot was gray, and both peripheral dots were yellow. Subjects were instructed to change their point of gaze between the two

dots about every second, thus performing self-paced voluntary saccadic eye movements.

Task Design

An experiment consisted of a block design in which the baseline condition [fixation (F)] and one of the two active conditions [reflexive (R) saccades and voluntary (V) saccades] were presented in alternation. The sequence of conditions started and ended with the baseline condition. The order of the two active conditions was switched halfway through the experiment [F-R-F-V ... F-R-F-V-F-(switch)-V-F-R ... F-V-F-R-F].

In the whole brain experiment, an active condition lasted for 31.5 seconds during which 7 volumes were acquired. The baseline (fixation) condition lasted either 13.5 seconds (6 times) or 18 seconds (7 times) during which 3 or 4 volumes, respectively, were acquired. Each of the two active conditions was presented 6 times and the baseline condition was presented 13 times in total. In the cerebellum experiment, each active condition lasted for 24 seconds during which time 8 volumes were acquired. The baseline condition lasted for 12 seconds during which 4 volumes were acquired. Each of the two active conditions was presented 8 times and the baseline condition was presented 17 times.

ANALYSIS

Eye movements

The eye movement recordings were analyzed offline. Saccadic eye movements were extracted semi-automatically using an eye velocity criterion of 30 degrees/second and checked manually. The total number of saccades was counted, and the average number of saccades per second was calculated for each subject, for each of the three conditions and for each of the two experi-

ments. Paired t-tests were used to assess differences between the conditions for significance. Subjects were excluded from the analyses if they showed inadequate eye movement behavior, such as not looking at the yellow dot continuously or making more than one saccade per second in the voluntary condition. Subjects, in whom eye tracking failed due to technical problems, were also excluded.

Functional imaging data

The functional imaging data were analyzed using statistical parametric mapping software (SPM 2, distributed by the Wellcome Department of Cognitive Neurology, University College London, UK) implemented in MATLAB (Version 6.5, Mathworks, Sherborn, MA, USA). For both studies, motion correction and co-registration were done according to the methodology provided by SPM2 [22]. The time-series of images were realigned using a least square approach and a 6 parameter spatial transformation. The central image in the time-series was the reference to which all subsequent images were realigned [23]. Motion parameters were checked for each subject to ascertain that no excessive motion (>3 mm translation or >1.5° rotation) has occurred. None of the scan sessions had to be discarded due to excessive motion.

Brain volumes were normalized to the standard space defined by the Montreal Neurological Institute (MNI) template. The normalized data had a resolution of $2 \times 2 \times 2 \text{ mm}^3$ and were spatially smoothed with a three-dimensional isotropic Gaussian kernel, with a full width half maximum of 8 mm for the whole brain experiment and 6 mm for the cerebellum experiment.

Statistical parametric maps were calculated for each subject. Movement parameters resulting from the realignment pre-processing were included as regressors of no interest to further re-

duce motion artifacts. The model was estimated with a high-pass filter with a cut-off period of 128 seconds. For each subject and for each experiment, t-contrast maps were calculated between each of the two active condition and the baseline condition ($[\text{active}_{\text{reflexive}} > \text{baseline}]$ and $[\text{active}_{\text{voluntary}} > \text{baseline}]$) and between the two active conditions.

The individual t-contrast maps were used for second level random effects (group) analysis. One sample t-tests were performed for each of the conditions and each of the experiments separately: $[\text{active}_{\text{reflexive}} > \text{baseline}]$ and $[\text{active}_{\text{voluntary}} > \text{baseline}]$. To investigate the differences in brain activation between the reflexive and the voluntary saccade conditions directly we used an analysis of covariance (ANCOVA) in which we compared $\text{active}_{\text{reflexive}}$ versus $\text{active}_{\text{voluntary}}$ and vice versa. In order to ensure that the differences in brain activation between these two active conditions are not caused by differences in the number of saccades made during the active condition, for each subject we counted the numbers of saccades made in the active conditions of the behavioral experiments ($N_{\text{reflexive}}$ and $N_{\text{voluntary}}$). From these numbers we obtained the ratio $[(N_{\text{reflexive}} - N_{\text{voluntary}})/(N_{\text{reflexive}} + N_{\text{voluntary}})]$ for each active condition, which was entered as a regressor of no interest. All tests were thresholded at $p < 0.05$ with false discovery rate (FDR) correction for multiple comparisons and at a minimum cluster size of 10 voxels.

Reporting of activation is focused on the brain areas that are involved in saccadic eye movements, namely the FEF, SEF, PEF, MT/V5, precuneus (V6), cingular and angular gyri, PVA/V1 and the cerebellum. In the whole brain experiment we focused on cerebral activations, whereas the cerebellum study allowed for a more detailed assessment of cerebellar activation.

RESULTS

Eye movements

Inspection of the eye movement behavioral data showed that eye tracking failed in 4 subjects and that 12 subjects did not perform properly during the experiments (7 subjects in the whole brain experiment, and 5 subjects in the cerebellum experiment): 4 subjects made too many saccades in the voluntary conditions and 8 subjects did not look at the yellow dot continuously. These 16 subjects were excluded from further analyses leaving 18 subjects for each of the two experiments; 9 of these subjects participated in both experiments.

For the whole brain experiment, the average (\pm standard deviation) number of saccades per second was 0.11 ± 0.04 for the fixation condition, 0.71 ± 0.05 for the reflexive condition and 0.81 ± 0.15 for the voluntary condition. For the cerebellum experiment, the average (\pm standard deviation) number of saccades per second was 0.09 ± 0.05 for the fixation condition, 0.70 ± 0.07 for the reflexive condition and 0.72 ± 0.09 for the voluntary condition.

As expected, the number of saccades per second was significantly higher in each of the active conditions than in the baseline condition for both the whole brain experiment and the cerebellum experiment. For the whole brain experiment, the number of saccades per second made in the voluntary condition was higher than in the reflexive condition ($p = 0.012$). In the cerebellum experiment subjects made an equal number of saccades in both active conditions ($p = 0.55$). In both experiments, the average number of saccades per second made in the reflexive condition matched the number of target onsets (0.7 per second). None of the subjects made saccades toward the target before it turned yellow in the reflexive condition.

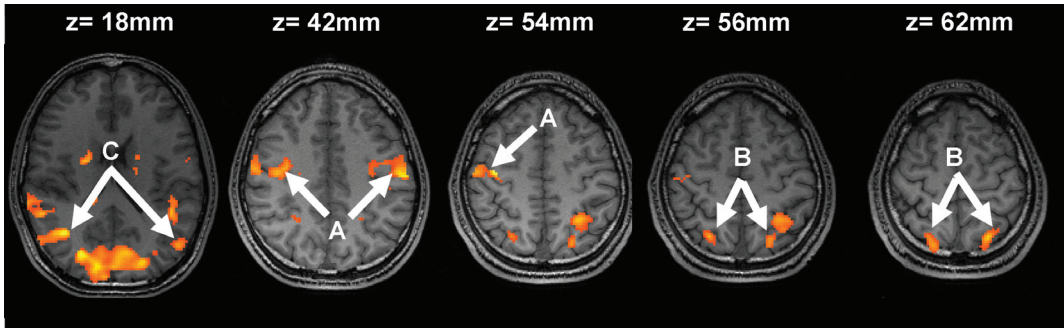


Figure 1: Reflexive saccade eye movement: Activation clusters in the whole brain study for reflexive saccades versus fixation. All areas were thresholded at $p < 0.05$ with FDR correction for multiple comparisons and with a minimum cluster size of 10 voxels. (Labels: A: FEF, B: PEF C: MT/V5)



Figure 2: Reflexive saccade eye movement: Activation clusters in the cerebellum study. All areas were thresholded at $p < 0.05$ with correction for multiple comparisons at cluster level and with a minimum cluster size of 10 voxels. (label A: cerebellum lobule VI; B: vermis VI and VII)

fMRI activation

The results of the random effects group analysis for the whole brain experiment and for the cerebellum experiment are shown in Tables 1 and 2. In the cerebellum experiment no significant activation was found at a threshold of $p < 0.05$ with FDR correction. Therefore, we used a more lenient statistical threshold of $p < 0.05$ corrected for multiple comparisons at cluster level and with a minimum cluster size of 10 voxels.

Reflexive saccades

Analysis of the reflexive saccade condition for the whole brain experiment revealed bilateral activation in the precentral gyrus (frontal eye fields, FEF), in the superior parietal gyrus (parietal eye fields, PEF) and in the middle temporal gyrus (MT/V5) (Fig. 1). Unilateral activation was found in the left angular gyrus.

The cerebellum experiment revealed bilateral activation in lobule VI and unilaterally in crus I on the left (Fig. 2). Activity was also found in vermis VI and VII.

Table 1: Areas of activation (reflexive saccades > fixation) with cluster size, maximum t-value within the cluster, MNI coordinates of the maximum t value, anatomic labels, percentage of cluster size and functional area.

Whole Brain Study: Reflexive								
Cluster size	T-value	MNI coordinate (mm)			Anatomic area	side	%*	Functional Area
		x	y	z				
14877	7.78	46	-74	-2	Middle Temporal Gyrus	R	4.89	MT/V5
					Middle Temporal Gyrus	L	3.6	MT/V5
					Lingual and Calcarine gyri			
					Middle, Inferior and Superior Occipital Gyri, Cuneus	L	31.33	PVA/V1
					Lingual and Calcarine gyri			
					Middle, Inferior and Superior Occipital Gyri, Cuneus	R	26.56	PVA/V1
					Fusiform Gyrus	R	4.38	
					Fusiform Gyrus	L	2.65	
					Angular Gyrus	L	1.18	Angular Gyrus
					Superior Temporal Gyrus	L	1.01	
1124	6022	40	-10	54	Precentral Gyrus	R	51.6	FEF
					Postcentral Gyrus	R	30.78	
					Middle Frontal Gyrus	R	3.2	
454	5.78	-60	-14	42	Postcentral Gyrus	L	68.72	
					Precentral Gyrus	L	26.87	FEF
394	4.64	-24	-62	62	Superior and Inferior Parietal Gyrus	L	91.11	PEF
					Postcentral Gyrus	L	2.54	
99	4.51	24	-48	40	Superior and Inferior Parietal Gyrus	R	33.33	PEF
146	4.28	26	-62	56	Superior Parietal Gyrus	R	98.63	PEF
Cerebellum Study: Reflexive								
Cluster size	T-value	MNI coordinate (mm)			Anatomic area	side	%*	Functional Area
		x	y	z				
409	7.02	-4	-76	-14	Cerebellum VI	L	38.39	Oculomotor Area
					Cerebellum VI	R	20.29	
					Vermis VI		18.09	
					Vermis VII		4.16	
					Cerebellum Crus 1	L	2.44	

All areas were thresholded at $p < 0.05$ with FDR (whole brain study) or at cluster level ($p < 0.05$) corrected for multiple comparisons (cerebellum study) and with a minimum cluster size of 10 voxels.

(L: left hemisphere, R: right hemisphere; FEF: frontal eye fields, PEF: parietal eye fields, MT/V5: motion-sensitive area (MT/V5), PVA/V1: primary visual areas (V1)). *The unassigned areas for each cluster are not listed in the table.

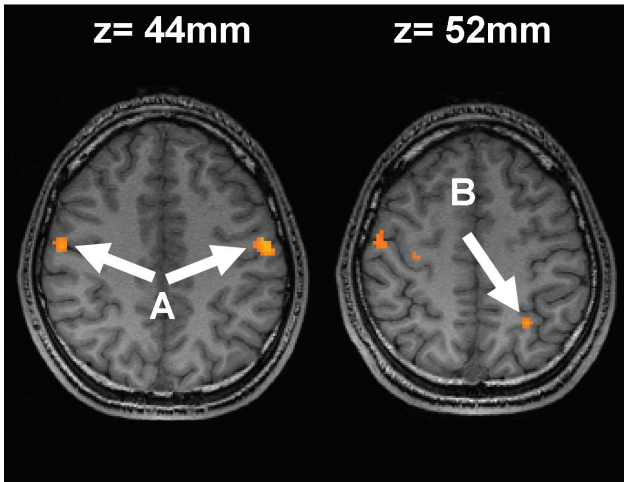


Figure 3: Voluntary saccade eye movement: Activation clusters in the whole brain study for voluntary saccades versus fixation. All areas were thresholded at $p < 0.05$ with FDR correction for multiple comparisons and with a minimum cluster size of 10 voxels. (Labels: A: FEF, B: PEF)

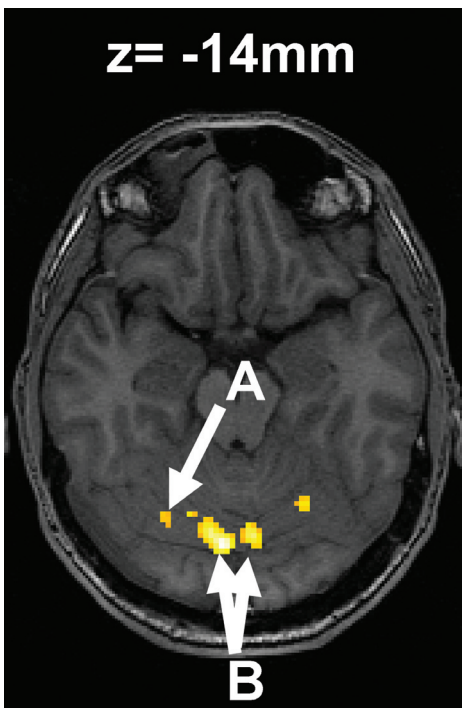


Figure 4: Voluntary saccades eye movement: Activation clusters in the cerebellum study. All areas were thresholded at $p < 0.05$ with correction for multiple comparisons at cluster level and with a minimum cluster size of 10 voxels. (label A: cerebellum lobule VI; B: vermis VI and VII)

Voluntary saccades

Analysis of the voluntary saccade condition for the whole brain experiment revealed bilateral activation in the precentral gyrus (FEF) and unilateral activation in the left inferior parietal gyrus (PEF) (Fig. 3).

The cerebellum experiment (figure 4) only revealed unilateral activation in the right lobule VI. Activity was also found in vermis VI and VII.

Direct comparison between reflexive and voluntary saccades

Results of the direct comparison between the two active (saccade)

conditions are given in Table 3, and visualized in Figure 5. When the reflexive saccade condition was compared with the voluntary saccade condition ($\text{active}_{\text{reflexive}} > \text{active}_{\text{voluntary}}$) for the whole brain experiment, the analysis yielded bilateral activation in the precentral gyrus (FEF), in the inferior and superior parietal gyrus (PEF), in the middle temporal gyrus (MT/V5), the precuneus (V6), and the angular and the anterior cingulate gyrus, and unilateral right activation in the posterior cingulate gyrus.

When the reflexive saccade condition was compared with the voluntary saccade condition ($[\text{active}_{\text{reflexive}} > \text{active}_{\text{voluntary}}]$) in the cerebellum experiment, the analysis yielded unilateral activation in the left lobule VI. This area of activation, however, was part of the large activation cluster in the fusiform gyrus, similar to that observed in the whole brain experiment. The actual part of this larger cluster being located in the left cerebellar lobule VI was less than 10 voxels.

For both the whole brain and the cerebellum experiment, no significant activation was found

Table 2: Areas of activation (voluntary saccades > fixation) with cluster size, maximum t-value within the cluster, MNI coordinates of the maximum t value, anatomic labels, percentage of cluster size and functional area.

Whole Brain Study: Voluntary								
Cluster size	T-value	MNI coordinate (mm)			Anatomic area	side	%*	Functional Area
		x	y	z				
323	8.35	-62	2	20	Postcentral Gyrus	L	44.89	FEF
					Precentral Gyrus	L	19.81	
					Rolandic Opercular Gyrus	L	16.72	
					Inferior Frontal Opercular Gyrus	L	14.24	
2848	7.62	-16	-78	6	Lingual and Calcarine gyri	R	40.81	PVA/V1
					Middle, Inferior and Superior Occipital Gyri, Cuneus			
					Lingual and Calcarine gyri	L	49.31	
					Middle, Inferior and Superior Occipital Gyri, Cuneus			
					Fusiform Gyrus	R	1.19	
31	5.1	-34	-74	-6	Inferior and Middle Occipital Gyri	L	61.92	PVA/V1
36	4.94	28	-84	24	Middle and Superior Occipital Gyri	R	100	PVA/V1
14	4.37	-28	-50	52	Inferior Parietal Gyrus	L	100	PEF
137	4.32	56	-8	44	Precentral Gyrus	R	57.66	FEF
					Postcentral Gyrus	R	33.58	
					Middle Frontal Gyrus	R	8.76	
Cerebellum Study: Voluntary								
Cluster size	T-value	MNI coordinate (mm)			Anatomic area	side	%*	Functional Area
		x	y	z				
48	4.65	6	-76	-20	Cerebellum VI	R	70.83	Oculomotor Area
					Vermis VI		20.83	
					Vermis VII		8.33	

All areas were thresholded at $p < 0.05$ with FDR (whole brain study) or at cluster level ($p < 0.05$) corrected for multiple comparisons (cerebellum study) and with a minimum cluster size of 10 voxels.

(L: left hemisphere, R: right hemisphere; FEF: frontal eye fields, PEF: parietal eye fields, MT/V5: motion-sensitive area (MT/V5), PVA/V1: primary visual areas (V1)). *The unassigned areas for each cluster are not listed in the table.

when the voluntary saccade condition was compared with the reflexive saccade condition.

A summary of the results is presented in Table 4.

					Inferior Temporal Gyrus ParaHippocampal Gyrus	L	5.15	
					Posterior Cingulate Gyrus	R	1.54	Posterior Cingulate Gyrus
					Middle Cingulate Gyrus	L	1.3	
					Lingual Gyrus	R	1.04	
139	4.96	30	-46	64	Superior and Inferior Parietal Gyrus	R	71.95	PEF
					PostCentral Gyrus	R	28.06	
277	4.76	32	0	44	Middle Frontal Gyrus	R	28.16	FEF
					Precentral Gyrus	R	25.99	
					Inferior Opercular Frontal Gyrus	R	19.86	
918	4.5	-2	44	20	Superior Middle Frontal Gyrus	L	40.41	
					Superior Middle Frontal Gyrus	R	14.81	
					Anterior Cingulate Gyrus	L	12.53	Anterior Cingulate Gyrus
					Middle Orbital Frontal Gyrus	R	10.24	
					Middle Orbital Frontal Gyrus	L	10.02	
					Anterior Cingulate Gyrus	R	7.19	Anterior Cingulate Gyrus
25	3.94	-52	-62	52	Angular Gyrus	L	16	Angular Gyrus
					Inferior Parietal Gyrus	L	16	
77	3.73	-24	-78	54	Superior and Inferior Parietal Gyrus	L	63.63	PEF
26	3.6	2	-36	60	Precuneus	L	46.15	V6
					Paracentral Lobule	R	30.77	
					Paracentral Lobule	L	3.85	
					Precuneus	R	3.85	V6
15	3.56	-6	28	14	Anterior Cingulate Gyrus	L	33.33	Anterior Cingulate Gyrus
14	3.24	-46	16	38	Middle Frontal Gyrus	L	92.86	FEF
					Precentral Gyrus	L	7.14	

Cerebellum Study: reflexive saccade > voluntary saccade

Cluster size	T-value	MNI coordinate (mm)			Anatomic area	side	%	Functional Area
		x	y	z				
103	7.07	-44	-44	-22	Cerebellum VI	L	6.8	Oculomotor Area

All areas were thresholded at $p < 0.05$ with FDR (whole brain study) or at cluster level ($p < 0.05$) corrected for multiple comparisons (cerebellum study) and with a minimum cluster size of 10 voxels.

(L: left hemisphere, R: right hemisphere; FEF: frontal eye fields, PEF: parietal eye fields, MT/V5: motion-sensitive area (MT/V5), V6: Precuneus, PVA/V1: primary visual areas (V1)). *The unassigned areas for each cluster are not listed in the table.

Table 4: A summary of areas of activation in the functional areas of interest for the whole brain and the cerebellum experiments.

Areas	Reflexive saccade	Voluntary saccade	Reflexive > Voluntary	Voluntary > Reflexive
Whole brain study				
FEF	B	B	B	-
SEF	-	-	-	-
PEF	B	L	B	-
MT/V5	B	-	B	-
Precuneus /V6	-	-	B	-
Angular Gyrus	L	-	B	-
Cingulate Gyrus	-	-	B	-
Cerebellum study				
Lobule VI	B	R	-	-
Crus I	L	-	-	-
Vermis VI	+	+	-	-
Vermis VII	+	+	-	-

All areas were thresholded at $p < 0.05$ with FDR (whole brain study) or at cluster level ($p < 0.05$) corrected for multiple comparisons (cerebellum study) and with a minimum cluster size of 10 voxels.

(B: bilateral, L: left hemisphere, R: right hemisphere; +: with significant activation, -: no significant activation; FEF: frontal eye fields, SEF: supplementary eye fields, PEF: parietal eye fields, MT/V5: motion-sensitive area (MT/V5), PVA/V1: primary visual areas (V1))

wards suddenly appearing peripheral targets. In our study, we also found that reflexive saccades yielded activation in the FEF, PEF, MT/V5 and in the angular gyrus, as well as in the cerebellum, more specifically in the cerebellar lobule VI, crus I and in the vermis VI and VII.

For voluntary saccades, PET studies have shown activation in FEF [31-33], SEF [31-33], PEF [33], PVA/V1 [31], the anterior cingulate cortex [34], the precuneus [33], the midbrain and the cerebellar vermis [32, 33]. fMRI studies have also shown activation in FEF [35, 36], SEF [36], PEF, PVA/V1, and the posterior vermis of the cerebellum [35], as well as in V4. In general, subjects in these studies were asked to execute self-paced voluntary horizontal saccades. In our study, self-paced voluntary saccades yielded activation in the FEF and PEF only, while activation was also found in the cerebellar lobules VI and in the vermis VI and VII.

Taken together, the previous imaging studies suggest a considerable overlap in brain activation during both types of saccadic eye movements. However, direct comparison studies of the brain activation patterns induced by reflexive and voluntary saccades are scarce. So far, only one fMRI study has investigated differences in activation patterns between both types of saccades [13]. In the latter study, voluntary saccades were evoked by the sudden onset of a central cue indicating the direction of the saccade that was to be made. Using more lenient statistical thresholds than used in our study, the authors reported that, relative to voluntary saccades, the precuneus and the angular gyri were more strongly activated during reflexive saccades and that, relative to reflexive saccades, FEF and PEF were more strongly activated during voluntary saccades [13]. In our study it was found that, relative to self-paced voluntary saccades, the MT/V5, the precuneus, and angular and cingulate gyri were more strongly activated during

reflexive saccades. Relative to reflexive saccades, we found no area of interest which was more activated during self-paced voluntary saccades. In the cerebellum we found no significant differences in activation patterns between reflexive and voluntary saccadic eye movements.

Frontal, supplemental and parietal eye fields (FEF, SEF, PEF)

Studies on FEF and SEF lesions in human patients and non-human primates suggest that both areas are either not dominantly involved in the generation of reflexive saccades or that damage can be compensated for on a behavioral level by other areas, such as the brainstem [37-42]. However, lesions of the PEF in non-human primates [43] and humans [44] considerably delay the onset of reflexive saccades, suggesting that the PEF might be more essential than the FEF or SEF for the adequate performance of reflexive saccades [45].

On the contrary, the contribution of FEF and PEF to voluntary saccades has not been extensively evaluated by lesion studies. Until now, the most studied form of voluntary saccades is the memory-guided saccades [42, 44, 46]. These studies suggest that unilateral FEF lesions in humans slow down the onset of contralesional memory-guided saccades. Similarly, comparable data on the contribution of PEF to voluntary saccades are scarce as well.

We found that PEF was more activated in reflexive than voluntary saccades, which is in accordance with the lesion studies [43, 45, 47]. The PEF is thought to be involved in saccades in terms of visuospatial localization, attention and integration [44, 48]. These cognitive processes are likely to be involved in a reflexive saccade condition. At each target onset, the brain needs to attend to it, localize the peripheral target and encode the appropriate spatial directions for the sac-

cadic eye movement towards it (i.e. integration) [49]. In the voluntary condition these processes may have a less prominent role, which might relate to the increased activation in PEF in the reflexive saccade condition.

We also found that the FEF was more activated during the generation of reflexive rather than voluntary saccades, which seems to be at odds with the physiological and functional studies mentioned above. However, it has been proposed that the FEF, which is related to the preparatory stage of saccadic responses, sends out intention and readiness signals to the superior colliculus [50]. Since in our paradigm subjects were aware that they were about to make reflexive saccades, the activation in the FEF could reflect such intention and readiness signals.

The increased activation in the FEF and PEF during the generation of reflexive compared to voluntary saccades is in contrast to an earlier study which found that FEF and PEF were more activated during voluntary saccades [13]. In the latter study eye movement was not recorded during scanning and the number of saccades may not have matched the number of stimuli. In the present study we recorded the in-scanner behavior and found that the number of saccades in the different active conditions was different. However, adding the number of saccades as a regressor in the fMRI analysis did not change the differences in the activation between reflexive and voluntary saccades. We did not observe any significant activation in the SEF during saccadic eye movements. Activation in the SEF related to reflexive or voluntary saccade eye movements has been reported by some [26-29, 31-33, 36], but not by others [13, 25].

Motion-sensitive area (MT/V5)

Neurons in the MT area of monkeys are specifically responsive to visual motion, selectively for

both direction and speed, and have receptive field sizes of up to 25 degrees in visual angle [51-56]. Functional imaging studies in humans have shown that the human homologue, area MT/V5, is also highly responsive to visual motion stimuli [57-59]. We found that MT/V5 was bilaterally more activated in the reflexive than in the voluntary saccade condition, although no real visual motion was present in either condition. This activation could be explained by a phenomenon known as apparent motion [60]. When two stimuli at two different locations are turned on and off in alternation (as was the case in our reflexive condition), subjects often perceive this as one single stimulus moving between two locations, rather than two stimuli flashing in alternation at the two locations. This percept is absent when the two stimuli are presented simultaneously, as in our voluntary saccade condition. Such a stimulus, in which the apparent motion phenomenon occurs, evokes activation in the human MT/V5 region [61] and in area MT of monkeys [62, 63], just like a true visual motion stimulus.

Precuneus, Cingulate Gyrus and Angular Gyrus

The present study demonstrated that the precuneus, the posterior and anterior cingulate and the angular gyri showed more activation during reflexive and voluntary saccades.

Studies in non-human primates suggest that the precuneus belongs to part of the neural network specialized for the processing of spatially-guided behavior [64]. Functional imaging studies have shown that the precuneus is involved in reflexive saccadic eye movements [27] and is associated with shifts of spatial attention [65]. The anterior cingulate gyrus is involved in target detection [66] and is activated during self-paced saccades [24, 33, 34] and during reflexive saccades [13, 27]. Neurons in the posterior cingulate

cortex of primates fire instantly to assign the spatial coordinates after a saccade in which the eye position signals are provided and to permit monitoring of either eye or self motion. [67]. Functional studies have shown that the posterior cingulate cortex is involved in confirming the new target position during reflexive saccades [13]. Lesion studies show that the main area facilitating the triggering of reflexive visually-guided saccades, but not voluntary saccades [65], is located in the posterior parietal cortex, in or near the superior part of the angular gyrus [44, 47].

Cerebellar Activation

The cerebellum plays an important role in the control rather than in the generation of saccadic eye movements. The vermis (VI and VII) are involved in controlling the accuracy and timing of saccades [68, 69].

Microstimulation of vermis VI and VII in the alert monkey induce and influence saccadic eye movements [18]. The Purkinje cells of vermis VI and VII project to the caudal part of the fastigial nucleus, which projects to the vestibular nuclei and saccade-related brainstem nuclei [69]. Electrophysiological experiments and clinical studies suggest that the vermis VI and VII are involved in the direction-selective control of saccade metrics and in saccadic adaptation [70-72]. Disrupting the posterior vermis, especially area VI, VII and paravermis, in humans using transcranial magnetic stimulation also suggest that these areas are related to the execution of visually-guided saccades [73]. Lesioning the oculomotor vermis in monkeys leads to a clear shortening of saccades (saccadic hypometria), an increase in saccadic amplitude variability and loss of adaptive capability of saccadic amplitudes [19, 74]. Although hypometria dissolves within a year, saccadic amplitudes remain highly variable [19]. Saccadic behavior of patients with lesions of the

vermis VI and VII suggest that there is a dissociation between the extent of saccadic variability and the lack of adaptive capability [20]. Indeed, an increased variability in saccadic accuracy does not generally lead to diminished saccadic adaptation [75]. Lesions of the vermis VI and VII and the posterior hemispheres do not only affect saccadic accuracy, but may also delay the covert orientation of visuospatial attention [76].

Several fMRI studies have reported activation of the cerebellum during saccadic eye movements. The cerebellar hemispheres were bilaterally activated during both voluntary [11] and reflexive saccades [2]. Activation in vermis VI and VII was observed in reflexive saccades [2, 10]. Dieterich et al. proposed that vermis IX and lobule IV and V, as well as a small portion of vermis VIII, might be involved in oculomotor performance and the activation of the cerebellar hemispheres could possibly reflect visuospatial attention processes [11]. Nitschke et al. suggested that the vermis VI and VII of the cerebellum play a predominant role in the control of visually-triggered saccadic eye movements, and are involved in processing visuospatial working memory and attention [10].

In accordance with these previous studies, we also found activation in cerebellar lobule VI and vermis VI and VII, for both types of saccades. However, when we compared the two types of saccades directly, no significant difference in activation was found. So, although the cerebellum is thought to be critically involved in saccade amplitude modifications in humans [9, 20], the lack of transfer between the adaptation of reflexive and voluntary saccades as observed in behavioral studies [15-17] is not reflected by differences in cerebellar activation between the two types of saccades. There are two possible, and not mutually exclusive, explanations for the lack of differential activation. It is possible

that the modification of amplitudes of the two types of saccades is processed by different sets of neurons within the same cerebellar regions. Alternatively or additionally, the lack of transfer between voluntary and reflexive saccade adaptation arises on a cerebral level.

In the present experiments, voluntary saccades were self-paced saccades made between two targets. The present paradigm was chosen to mimic the saccadic adaptation experiments in which voluntary and reflexive saccades were dissociated with respect to their amplitude modifications. However, compared to other voluntary eye movement tasks (such as antisaccades and memory-guided saccades), the present task does not engage cognitive processes of inhibitory control and working memory which would recruit frontal areas. Hence, the lack of findings in these regions is not entirely unexpected. Moreover, subjects are able to actively suppress a reflexive saccade using cognitive processes of inhibition. It can be argued that the presently observed differences in circuitry between voluntary and reflexive saccades are mainly related to a self-paced mechanism which is, in our view, still volitional in nature.

CONCLUSION

The execution of reflexive saccades induced stronger activation in several cerebral areas, but not in the cerebellum, than the execution of self-paced voluntary saccades. This could indicate that functional difference in maintaining the accuracy of the two types of saccades is mediated on a cerebral level, or that it involves overlapping cerebellar regions with possible functional differences.

ACKNOWLEDGMENTS

The authors thank Dr. Tom Ruigrok for his assistance in anatomical localization of cerebellar fMRI activation.

REFERENCES

1. Schall, J.D., Neural basis of saccade target selection. *Rev Neurosci*, 1995. 6(1): p. 63-85.
2. Hayakawa, Y., et al., Human cerebellar activation in relation to saccadic eye movements: a functional magnetic resonance imaging study. *Ophthalmologica*, 2002. 216(6): p. 399-405.
3. Schiller, P.H. and E.J. Tehovnik, Neural mechanisms underlying target selection with saccadic eye movements. *Prog Brain Res*, 2005. 149: p. 157-71.
4. Amlot, R. and R. Walker, Are somatosensory saccades voluntary or reflexive? *Exp Brain Res*, 2006. 168(4): p. 557-65.
5. Leigh, R.J. and D.S. Zee, *The Neurology of Eye Movements*. Third ed. 1999, New York: Oxford University Press.
6. Straube, A. and H. Deubel, Rapid gain adaptation affects the dynamics of saccadic eye movements in humans. *Vision Res*, 1995. 35(23-24): p. 3451-8.
7. Walker, R., et al., Control of voluntary and reflexive saccades. *Exp Brain Res*, 2000. 130(4): p. 540-4.
8. Zee, D.S., et al., Slow saccades in spinocerebellar degeneration. *Arch Neurol*, 1976. 33(4): p. 243-51.
9. Desmurget, M., et al., Functional anatomy of saccadic adaptation in humans. *Nat Neurosci*, 1998. 1(6): p. 524-8.
10. Nitschke, M.F., et al., Activation of cerebellar hemispheres in spatial memorization of saccadic eye movements: an fMRI study. *Hum Brain Mapp*, 2004. 22(2): p. 155-64.
11. Dieterich, M., et al., Cerebellar activation during optokinetic stimulation and saccades. *Neurology*, 2000. 54(1): p. 148-55.
12. Deubel, H., Separate adaptive mechanisms for the control of reactive and volitional saccadic eye movements. *Vision Res*, 1995. 35(23-24): p. 3529-40.
13. Mort, D.J., et al., Differential cortical activation during voluntary and reflexive saccades in man. *Neuroimage*, 2003. 18(2): p. 231-46.
14. McLaughlin, S.C., Parametric adjustment in saccadic eye movements. *Percept Psychophys*, 1967. 2: p. 359-362.
15. Erkelens, C.J. and J. Hulleman, Selective adaptation of internally triggered saccades made to visual targets. *Exp Brain Res*, 1993. 93(1): p. 157-64.
16. Gaveau, V., et al., Self-generated saccades do not modify the gain of adapted reactive saccades. *Exp Brain Res*, 2005. 162(4): p. 526-31.
17. Alahyane, N., et al., Oculomotor plasticity: are mechanisms of adaptation for reactive and voluntary saccades separate? *Brain Res*, 2007. 1135(1): p. 107-21.
8. Ron, S. and D.A. Robinson, Eye movements evoked by cerebellar stimulation in the alert monkey. *J Neurophysiol*, 1973. 36(6): p. 1004-22.
19. Barash, S., et al., Saccadic dysmetria and adaptation after lesions of the cerebellar cortex. *J Neurosci*, 1999. 19(24): p. 10931-9.

20. Straube, A., et al., Cerebellar lesions impair rapid saccade amplitude adaptation. *Neurology*, 2001. 57(11): p. 2105-8.
21. Desmurget, M., et al., Functional adaptation of reactive saccades in humans: a PET study. *Exp Brain Res*, 2000. 132(2): p. 243-59.
22. Tzourio-Mazoyer, N., et al., Automated anatomical labeling of activations in SPM using a macroscopic anatomical parcellation of the MNI MRI single-subject brain. *Neuroimage*, 2002. 15(1): p. 273-89.
23. Friston, K.J., et al., Characterizing dynamic brain responses with fMRI: a multivariate approach. *Neuroimage*, 1995. 2(2): p. 166-72.
24. Sweeney, J.A., et al., Positron emission tomography study of voluntary saccadic eye movements and spatial working memory. *J Neurophysiol*, 1996. 75(1): p. 454-68.
25. Anderson, T.J., et al., Cortical control of saccades and fixation in man. A PET study. *Brain*, 1994. 117 (Pt 5): p. 1073-84.
26. Muri, R.M., et al., Functional organisation of saccades and antisaccades in the frontal lobe in humans: a study with echo planar functional magnetic resonance imaging. *J Neurol Neurosurg Psychiatry*, 1998. 65(3): p. 374-7.
27. Berman, R.A., et al., Cortical networks subserving pursuit and saccadic eye movements in humans: an FMRI study. *Hum Brain Mapp*, 1999. 8(4): p. 209-25.
28. Nobre, A.C., et al., Covert visual spatial orienting and saccades: overlapping neural systems. *Neuroimage*, 2000. 11(3): p. 210-6.
29. Luna, B., et al., Dorsal cortical regions subserving visually guided saccades in humans: an fMRI study. *Cereb Cortex*, 1998. 8(1): p. 40-7.
30. Petit, L., et al., Dissociation of saccade-related and pursuit-related activation in human frontal eye fields as revealed by fMRI. *J Neurophysiol*, 1997. 77(6): p. 3386-90.
31. Fox, P.T., et al., The role of cerebral cortex in the generation of voluntary saccades: a positron emission tomographic study. *J Neurophysiol*, 1985. 54(2): p. 348-69.
32. Law, I., et al., Parieto-occipital cortex activation during self-generated eye movements in the dark. *Brain*, 1998. 121 (Pt 11): p. 2189-200.
33. Petit, L., et al., Functional anatomy of a prelearned sequence of horizontal saccades in humans. *J Neurosci*, 1996. 16(11): p. 3714-26.
34. Paus, T., et al., Role of the human anterior cingulate cortex in the control of oculomotor, manual, and speech responses: a positron emission tomography study. *J Neurophysiol*, 1993. 70(2): p. 453-69.
35. Corbetta, M., et al., A common network of functional areas for attention and eye movements. *Neuron*, 1998. 21(4): p. 761-73.
36. Darby, D.G., et al., Cortical activation in the human brain during lateral saccades using EPISTAR functional magnetic resonance imaging. *Neuroimage*, 1996. 3(1): p. 53-62.
37. Dias, E.C. and M.A. Segraves, Muscimol-induced inactivation of monkey frontal eye field: effects on visually and memory-guided saccades. *J Neurophysiol*, 1999. 81(5): p. 2191-214.
38. Lee, K. and E.J. Tehovnik, Topographic distribution of fixation-related units in the dorsomedial frontal cortex of the rhesus monkey. *Eur J Neurosci*, 1995. 7(5): p. 1005-11.

39. Schiller, P.H. and I.H. Chou, The effects of frontal eye field and dorsomedial frontal cortex lesions on visually guided eye movements. *Nat Neurosci*, 1998. 1(3): p. 248-53.
40. Schiller, P.H., S.D. True, and J.L. Conway, Deficits in eye movements following frontal eye-field and superior colliculus ablations. *J Neurophysiol*, 1980. 44(6): p. 1175-89.
41. van der Steen, J., I.S. Russell, and G.O. James, Effects of unilateral frontal eye-field lesions on eye-head coordination in monkey. *J Neurophysiol*, 1986. 55(4): p. 696-714.
42. Sommer, M.A. and E.J. Tehovnik, Reversible inactivation of macaque frontal eye field. *Exp Brain Res*, 1997. 116(2): p. 229-49.
43. Lynch, J.C. and J.W. McLaren, Deficits of visual attention and saccadic eye movements after lesions of parietooccipital cortex in monkeys. *J Neurophysiol*, 1989. 61(1): p. 74-90.
44. Pierrot-Deseilligny, C., Cortical control of saccades in man. *Acta Neurol Belg*, 1991. 91(2): p. 63-79.
45. Gaymard, B., et al., Cortical control of saccades. *Exp Brain Res*, 1998. 123(1-2): p. 159-63.
46. Rivaud, S., et al., Eye movement disorders after frontal eye field lesions in humans. *Exp Brain Res*, 1994. 102(1): p. 110-20.
47. Pierrot-Deseilligny, C., et al., Cortical control of reflexive visually-guided saccades. *Brain*, 1991. 114 (Pt 3): p. 1473-85.
48. Muri, R.M., MRI and fMRI analysis of oculomotor function. *Prog Brain Res*, 2005. 151: p. 503-26.
49. Matsuda, T., et al., Functional MRI mapping of brain activation during visually guided saccades and antisaccades: cortical and subcortical networks. *Psychiatry Res*, 2004. 131(2): p. 147-55.
50. Connolly, J.D., et al., Human fMRI evidence for the neural correlates of preparatory set. *Nat Neurosci*, 2002. 5(12): p. 1345-52.
51. Churchland, M.M. and S.G. Lisberger, Shifts in the population response in the middle temporal visual area parallel perceptual and motor illusions produced by apparent motion. *J Neurosci*, 2001. 21(23): p. 9387-402.
52. Maunsell, J.H. and D.C. Van Essen, Functional properties of neurons in middle temporal visual area of the macaque monkey. I. Selectivity for stimulus direction, speed, and orientation. *J Neurophysiol*, 1983. 49(5): p. 1127-47.
53. Zeki, S.M., Functional organization of a visual area in the posterior bank of the superior temporal sulcus of the rhesus monkey. *J Physiol*, 1974. 236(3): p. 549-73.
54. Van Essen, D.C., J.H. Maunsell, and J.L. Bixby, The middle temporal visual area in the macaque: myeloarchitecture, connections, functional properties and topographic organization. *J Comp Neurol*, 1981. 199(3): p. 293-326.
55. Baker, J.F., et al., Visual response properties of neurons in four extrastriate visual areas of the owl monkey (*Aotus trivirgatus*): a quantitative comparison of medial, dorsomedial, dorsolateral, and middle temporal areas. *J Neurophysiol*, 1981. 45(3): p. 397-416.
56. Felleman, D.J. and J.H. Kaas, Receptive-field properties of neurons in middle temporal visual area (MT) of owl monkeys. *J Neurophysiol*, 1984. 52(3): p. 488-513.

57. Tootell, R.B., et al., Functional analysis of human MT and related visual cortical areas using magnetic resonance imaging. *J Neurosci*, 1995. 15(4): p. 3215-30.
58. Watson, J.D., et al., Area V5 of the human brain: evidence from a combined study using positron emission tomography and magnetic resonance imaging. *Cereb Cortex*, 1993. 3(2): p. 79-94.
59. Zeki, S., et al., A direct demonstration of functional specialization in human visual cortex. *J Neurosci*, 1991. 11(3): p. 641-9.
60. Wertheimer, M., Experimentelle Studien über das Sehen von Bewegung. *Zeitschrift für Psychologie*, 1912. 61: p. 161-265.
61. Goebel, R., et al., The constructive nature of vision: direct evidence from functional magnetic resonance imaging studies of apparent motion and motion imagery. *Eur J Neurosci*, 1998. 10(5): p. 1563-73.
62. Mikami, A., Direction selective neurons respond to short-range and long-range apparent motion stimuli in macaque visual area MT. *Int J Neurosci*, 1991. 61(1-2): p. 101-12.
63. Albright, T.D., Cortical processing of visual motion. *Rev Oculomot Res*, 1993. 5: p. 177-201.
64. Selemon, L.D. and P.S. Goldman-Rakic, Common cortical and subcortical targets of the dorsolateral prefrontal and posterior parietal cortices in the rhesus monkey: evidence for a distributed neural network subserving spatially guided behavior. *J Neurosci*, 1988. 8(11): p. 4049-68.
65. Cavanna, A.E. and M.R. Trimble, The precuneus: a review of its functional anatomy and behavioural correlates. *Brain*, 2006. 129(Pt 3): p. 564-83.
66. Posner, M.I. and S.E. Petersen, The attention system of the human brain. *Annu Rev Neurosci*, 1990. 13: p. 25-42.
67. Olson, C.R., S.Y. Musil, and M.E. Goldberg, Single neurons in posterior cingulate cortex of behaving macaque: eye movement signals. *J Neurophysiol*, 1996. 76(5): p. 3285-300.
68. Voogd, J. and N.H. Barmack, Oculomotor cerebellum. *Prog Brain Res*, 2005. 151: p. 231-68.
69. Noda, H., S. Sugita, and Y. Ikeda, Afferent and efferent connections of the oculomotor region of the fastigial nucleus in the macaque monkey. *J Comp Neurol*, 1990. 302(2): p. 330-48.
70. Suzuki, D.A. and E.L. Keller, The role of the posterior vermis of monkey cerebellum in smooth-pursuit eye movement control. II. Target velocity-related Purkinje cell activity. *J Neurophysiol*, 1988. 59(1): p. 19-40.
71. Kase, M., D.C. Miller, and H. Noda, Discharges of Purkinje cells and mossy fibres in the cerebellar vermis of the monkey during saccadic eye movements and fixation. *J Physiol*, 1980. 300: p. 539-55.
72. Fuchs, A.F., F.R. Robinson, and A. Straube, Role of the caudal fastigial nucleus in saccade generation. I. Neuronal discharge pattern. *J Neurophysiol*, 1993. 70(5): p. 1723-40.
73. Hashimoto, M. and K. Ohtsuka, Transcranial magnetic stimulation over the posterior cerebellum during visually guided saccades in man. *Brain*, 1995. 118 (Pt 5): p. 1185-93.
74. Takagi, M., D.S. Zee, and R.J. Tamargo, Effects of lesions of the oculomotor vermis on eye movements in primate: saccades. *J Neurophysiol*, 1998. 80(4): p. 1911-31.

-
75. van der Geest, J.N., G.C. Haselen, and M.A. Frens, Saccade adaptation in Williams-Beuren Syndrome. *Invest Ophthalmol Vis Sci*, 2006. 47(4): p. 1464-8.
 76. Townsend, J., et al., Spatial attention deficits in patients with acquired or developmental cerebellar abnormality. *J Neurosci*, 1999. 19(13): p. 5632-43.

CHAPTER 6

CEREBELLAR CONTRIBUTIONS TO THE PROCESSING OF SACCADIC ERROR

Cerebellar Contributions to the Processing of Saccadic Errors

Submitted

ABSTRACT

Saccades are fast eye movements that direct the point of regard to a target in the visual field. Repeated post-saccadic visual errors can induce modifications of the amplitude of these saccades, a process known as saccadic adaptation. Two experiments using the same paradigm were performed to study the involvement of the cerebrum and the cerebellum in the processing of post-saccadic errors, using functional magnetic resonance imaging (fMRI) and in-scanner eye movement recordings.

In the first active condition, saccadic adaptation was prevented by using a condition in which the saccadic target was shifted to a variable position during the saccade towards it. This condition induced random post-saccadic errors as opposed to the second active condition in which the saccadic target was not shifted. In the baseline condition subjects looked at a stationary dot.

Both active conditions compared with baseline evoked activation in the expected saccade-related regions (the frontal and parietal eye fields, primary visual area, MT/V5, and the precuneus (V6) in the cerebrum; vermis VI-VII and lobule VI in the cerebellum, known as the oculomotor vermis). In the direct comparison between the two active conditions, significantly more cerebellar activation (vermis VIII, lobules VIII-X, left lobule VIIb) was observed with random post-saccadic visual error.

These results suggest a possible role for areas outside the oculomotor vermis of the cerebellum in the processing of post-saccadic errors. Future studies of these areas with e.g. electrophysiological recordings may reveal the nature of the error signals that drive the amplitude modification of saccadic eye movements.

INTRODUCTION

Saccades are fast and accurate eye movements that are encoded within several distinct brain regions, such as the frontal, supplementary and parietal eye fields (FEF, SEF and PEF) [1, 2]. The cerebellum is involved in maintaining saccadic accuracy [3] and saccade-related activation in the human cerebellum has been shown previously using Positron Emission Tomography (PET) [4, 5] and functional magnetic resonance imaging (fMRI) [6, 7].

Saccadic accuracy can be artificially reduced in the laboratory using a so-called saccade adaptation paradigm (McLaughlin, 1967), in which the onset of a saccade triggers an intra-saccadic shift of the target to a new position. Post-saccadic visual errors, induced by consistent intra-saccadic target steps, drive the gradual modification of subsequent saccadic amplitudes over a series of trials in order to retain saccadic accuracy [1, 8, 9]. i.e. to minimize saccadic errors

In a classical saccadic adaptation paradigm, systematic saccadic visual errors induce a gradual change of saccadic amplitudes in order to minimize the saccadic errors [8, 9]. In this paradigm, the processing of saccadic errors and the actual modification of saccadic amplitudes are confounded, because changes in saccadic amplitude are invariably accompanied by changes in post-saccadic errors.

In order to separate the processing of post-saccadic errors from the actual modification of saccadic amplitudes, Desmurget and colleagues implemented a paradigm in which the intra-saccadic target step was variable [10]. They showed that variable intra-saccadic target steps did induce saccadic errors and corrective eye movements, but this so-called random paradigm did not lead to a gradual modification of saccadic

amplitudes over a series of trials. Behavioral studies showed that such a single but random saccadic error has an effect on the amplitude of the subsequent saccade. This suggests that the brain is quite efficient in processing saccadic errors, for which the cerebellum is a likely candidate. However, in the only study comparing variable intra-saccadic target steps to a condition without intra-saccadic target steps, using PET imaging, no cerebral or cerebellar activation was observed [10]. It is possible, however, that the neuronal activity related to the saccadic visual error processing is simply too small to detect with PET.

In the present study the activation in the cerebrum and the cerebellum related to the processing of saccadic errors was investigated using fMRI, which provides a better spatial and temporal resolution than PET [11]. In order to induce saccadic errors without sustained amplitude changes saccadic adaptation, we used variable forward and backward intra-saccadic target steps, similar to the random paradigm of Desmurget et al. [10].

In two separate experiments we first looked at activation in the cerebral cortex, and in the second experiment we focused on activation in the cerebellum so that we could obtain more detailed information about this structure, using the same behavioral paradigm. We hypothesized that specific cerebellar regions are involved in the processing of post-saccadic errors.

MATERIALS AND METHODS

Subjects

Written informed consent was obtained from each participant prior to this study, that adhered to the tenets of the Declaration of Helsinki, and was approved by the Institutional Review Board.

Subjects could participate in either one or both of the two experiments (whole brain and cerebellum) that were performed. Seventeen subjects (10 male, 7 female; on average 27 years of age, range 19 to 60 years) participated in the whole brain experiment, and 23 subjects (15 male, 8 female; on average 28 years of age, range 19 to 60 years) participated in the cerebellum experiment. Six of these subjects participated in both experiments. None of the subjects had any known neurological or visual deficits other than minor refractive anomalies. None of the subjects wore spectacle correction during the experiments, as minor refractive anomalies could be adjusted for by the goggle system that was used for displaying the stimuli. All subjects reported good visual acuity during the experiment.

Data acquisition

Data were acquired on a 1.5T MRI scanner (Signa CV/i; General Electric, Milwaukee, USA) using a dedicated 8-channel head coil. An anatomical image covering the whole brain was acquired (3D high-resolution inversion recovery fast spoiled gradient-echo T1 weighted sequence; repetition time (TR)/echo time (TE)/inversion time (TI) 9.99/2/400 ms; flip angle 20 degrees, 320x224 matrix with a rectangular field-of-view of 22 cm, 1.2 mm slice thickness with no gap; array spatial sensitivity encoding technique (ASSET) factor 2; acquisition time 5 minutes).

In both the whole brain and the cerebellum experiment, functional imaging was performed with single-shot gradient-echo echo-planar imaging (EPI) sequences in transverse orientation that is sensitive to blood oxygenation level dependent (BOLD) contrast. For the whole brain experiment, the imaging volume covered the whole brain (TR/TE 4500/50 ms; 64x64 matrix with a field-of-view of 22 cm, 2.5 mm slice thickness, 48 contiguous slices, voxel size of 2.5x3.4x3.4 mm³; 10:03 minutes acquisition

time, including 18 seconds of dummy scans that were discarded). For the cerebellum experiment, the imaging volume only covered the whole cerebellum with higher spatial and temporal resolution (TR/TE 3000/30 ms; 96x96 matrix with a rectangular field-of-view of 24 cm, 2.5 mm slice thickness, 18 contiguous slices, voxel size of 2.5x2.5x2.5 mm³; 10:00 minutes acquisition time, including 12 seconds of dummy scans that were discarded).

Eye-tracking

Eye movements (monocular, left eye) were monitored with the Real Eye RE-4601 Imaging System (Avotec Inc., Stuart, Florida, USA) recorded with a 60 Hz sampling rate with the iViewX Eye Tracking System (SensoMotoric Instruments, Teltow, Germany). The system was calibrated before each scanning session with the built-in 3-by-3 point calibration routine. Online eye position was sent to the stimulation computer, where it was used for on-line updating of the visual display.

Experimental Design

Both experiments consisted of a blocked design in which the baseline and active conditions were presented in alternation (baseline – active – baseline – active – etc.). The sequence of conditions started and ended with the baseline condition. The order of the two active conditions (“no-step” and “random-step”) was switched halfway the experiment (e.g., baseline – no-step – baseline – random-step ... baseline – no-step – baseline – random-step – (switch) – baseline – random-step – baseline – no-step ... baseline – random-step – baseline – no-step – baseline). In the whole brain experiment, each of the two active conditions was presented 6 times and the baseline condition was presented 13 times. An active condition lasted for 31.5 seconds, during which 7 volumes were acquired, and baseline-conditions lasted randomly either for 13.5 or

18 seconds during which 3 or 4 volumes were acquired, respectively. In total, 42 volumes per active condition and 46 volumes of the baseline condition were acquired.

In the cerebellum experiment, each of the two active conditions was presented 8 times and the baseline condition was presented 17 times. An active condition lasted for 24 seconds during which 8 imaging volumes were acquired, and the baseline-condition lasted for 12 seconds during which 4 imaging volumes were acquired. In total, 64 volumes per active condition and 68 volumes of the baseline condition were acquired.

Stimulus paradigm

The experiments were performed in near darkness. The visual stimuli were binocularly presented by means of a goggle-based system (Silent Vision SV-7021 Fiber Optic Visual System; Avotec Inc., Stuart, Florida, USA). The optical components were mounted on top of the head coil. Screen resolution was 1024x768 pixels and the refresh rate 60 Hz. The visual stimulus was a single yellow dot (0.9 degrees in diameter) presented against a black background. Overall luminance of the whole display was 0.43cd/m². Subjects were instructed to continuously look at that dot. In the baseline condition, the yellow dot was positioned in the center of the screen for the duration of the block.

Both active conditions consisted of a series of several trials per block, during which the dot jumped repeatedly between the left and right side of the screen. At the beginning of each trial the dot was shown at 9.0 degrees on the left. After a random interval of 1 to 2 seconds the dot disappeared from the left side and then flashed once at 9.0 degrees on the right for a period of 100 ms. The flashed dot evoked a reflexive saccadic eye movement towards it.

The onset of this primary saccade was estimated on-line using a position threshold with respect to the initial fixation position on the left. The saccade triggered the dot to re-appear on the right side of the screen, on a position dependent of the specific active condition (no-step or random-step). After 1 to 2 seconds, the dot on the right disappeared and the next trial was initiated by the appearance of the dot on the left side. This procedure was repeated for the duration of the active block (31.5s in the whole brain experiment or 24s in the cerebellum experiment), yielding about 8 to 10 trials per block.

The only difference between the two active conditions was the position where the dot re-appeared when triggered by the saccade to the right. In the no-step condition the position where the dot re-appeared was the same as the flashed position, i.e., 9.0 degrees on the right. In the random-step condition the position where the dot re-appeared varied randomly between one out of seven possible positions (5.1, 6.4, 7.7, 9.0, 10.3, 11.6 and 12.9 degrees on the right).

In contrast to existing literature on saccade adaptation where sustained targets are commonly used [1], the initial saccade to the right was evoked by a flashed target. Usually the intra-saccadic target step and the concurrent removal of the initial saccadic target are triggered by the onset or the peak velocity of the saccade. This point in time can be estimated very reliably in setups with higher eye movement recording frequencies. However, the recording frequency of the in-scanner eye tracking device is limited to 60 Hz, and therefore this moment of saccadic onset or maximum eye velocity could easily have been missed. In the present stimulation protocol, the dot had already disappeared at the onset of the saccade, preventing subjects from perceiving the actual displacement of the target. In a pilot experiment outside the scanner, we

performed a saccadic adaptation experiment using flashed targets and a consistent intra-saccadic target step, and observed that subjects did normally adapt the amplitudes of their saccades toward these flashed targets. None of the subjects in the present study reported that they saw differences between the two active conditions.

Statistical analysis

Eye Movements

Eye movement recordings were analyzed offline using Matlab (Version 6.5, The MathWorks, Inc., Natick, MA, USA). Data points in which the vertical eye position deviated from zero by more than 2 degrees were marked as missing data and discarded from analysis. These data include both blinks and tracking failures. Horizontal eye position data was subsequently smoothed using a Savitsky-Golay polynomial filter.

Saccades were marked automatically using a velocity criterion of 50 degrees per second. Saccadic onsets were defined as the moments of minimum eye velocity in the 50 ms periods before eye velocity exceeded this criterion. Likewise, saccadic offsets were defined as the moments of minimum eye velocity in the 50 ms periods after eye velocity dropped below the criterion. By definition, the automatically detected saccades needed to have a minimum amplitude of 3 degrees and a minimum duration criterion of 40 milliseconds. Subsequently, the eye movement recordings were checked manually to ensure proper automatic detection and to manually include small correction saccades.

For each subject and each condition the numbers of all saccades were counted and the average amplitude gain of the primary saccades toward the flashed target on the right was calculated for the two active conditions. The gain was defined as the ratio between the amplitude

of the primary saccade and the distance to the target (18 degrees). A gain of 1 indicates that a saccade lands perfectly on target. Paired t-tests were used to assess significant differences in number of saccades and in saccade amplitude gains between the conditions in each of the experiments.

Functional Imaging Data

The functional imaging data were analyzed using statistical parametric mapping software (SPM 2, distributed by the Wellcome Department of Cognitive Neurology, University College London, UK) implemented in MATLAB (Version 6.5, Mathworks, Sherborn, MA, USA). For both studies, motion correction and co-registration were performed according to the methodology provided in SPM2. Brain volumes were normalized to the standard space defined by the Montreal Neurological Institute (MNI) template. The normalized data had a resolution of $2 \times 2 \times 2$ mm³ and were spatially smoothed with a three-dimensional isotropic Gaussian kernel, with a full width half maximum of 8 mm in the whole brain experiment and 6 mm in the cerebellum experiment.

Statistical parametric maps were calculated for each subject. Movement parameters resulting from the realignment pre-processing were included as regressors of no interest to further reduce motion artifacts. The model was estimated with a high pass filter with a cut-off period of 128 seconds. For each subject and for each experiment, a t-contrast map was calculated for each of the two active conditions between the active condition and the baseline condition (active > baseline).

The individual t-contrast maps were used for second level random effect group analysis. One sample t-tests were performed to assess main effects ([active_{no-step} > baseline] and [active_{random}

$>$ baseline]) in both experiments separately. To investigate the differences in activation between the two active conditions corrected for baseline activation (direct comparisons), we used a paired t-test ([active_{no-step} $>$ baseline] versus [active_{random-step} $>$ baseline] and vice versa). All tests were thresholded at $p < 0.05$ with false discovery rate (FDR) correction for multiple

RESULTS

Eye Movements

Qualitative inspection showed that the eye movement data were insufficient in two subjects in the whole brain experiment and in five subjects in the cerebellum experiment. This included tracking failures, problems in keep-

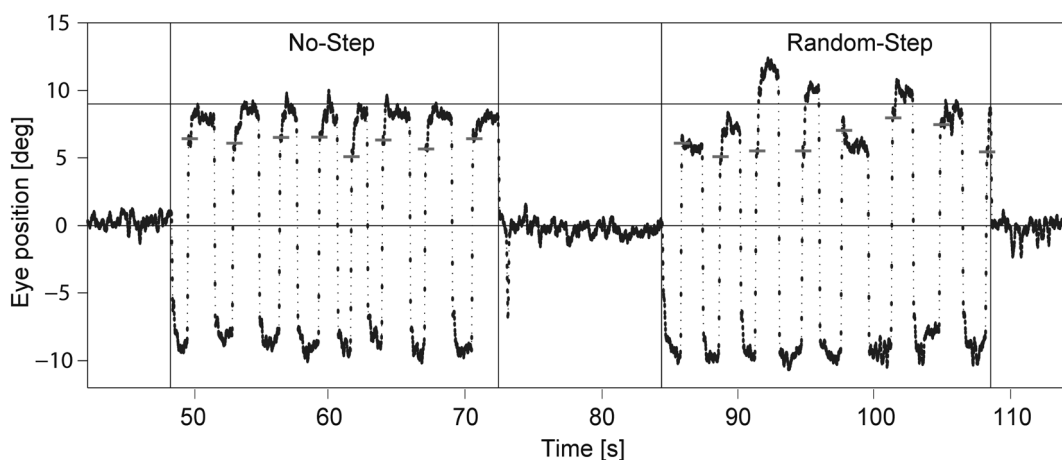


Figure 1 – Eye Movements: An example of the eye movement behavior of one subject in the cerebellum study. Shown are a no-step condition (between 48s and 72s) and a random-step condition (between 84s and 108s) interspersed with the baseline condition (fixation) during which no saccades were made. In the no-step condition, the initial saccade and the post-saccadic correction movement brings the eye to the fixed target position of 9 degrees to the right. In the random-step condition, the final target position is variable, explaining the varying fixation positions after the primary saccade and the corrective movements if needed. Note that in both conditions the end points of the primary saccades, indicated by the small horizontal lines that intersect the eye movement traces, are at about 7 degrees to the right, as opposed to 9 degrees, indicating hypometric gain.

comparisons and at a minimum cluster size of 10 voxels. When no voxels were found to survive the threshold using FDR correction, a more lenient correction for multiple comparisons at cluster level.

Anatomic labeling of the observed areas of activation in SPM was done using the macroscopic anatomic parcellation procedure of the Montreal Neurological Institute (MNI) MRI single-subject brain [12]. Reporting of activation is focused on the brain areas that are involved in eye movements, namely the FEF, SEF, PEF, primary visual area, MT/V5, V6 and the cerebellum.

ing fixation during the baseline condition, and a lack of saccadic eye movements in the active conditions. These 7 subjects were discarded from further analysis, leaving 15 subjects in the whole brain experiment and 18 subjects in the cerebellum experiment. The eye movement behavior of these subjects consisted of stable fixations in the baseline condition and saccadic eye movements toward the targets in the active conditions (see figure 1).

Experiment	Parameter	Baseline	No-step	Random-step
Whole brain	N saccades / block	1.0 ± 0.2	24.5 ± 4.6	25.9 ± 3.6
	Saccadic Gain		0.93 ± 0.11	0.94 ± 0.12
Cerebellum	N saccades / block	1.0 ± 0.3	17.9 ± 2.5	19.5 ± 2.3
	Saccadic Gain		0.89 ± 0.13	0.89 ± 0.12

Table 1 - Eye Movements The number of saccades per block (N saccades / block) and the gain of the primary saccades (saccadic gain) for each of the three conditions (baseline, no-step and random-step) for each of the experiments (whole brain and cerebellum) across subjects (mean ± standard deviation). Note that in the baseline condition no primary saccades were made and that the block duration of the two active conditions was different between the two experiments (31.5 seconds in the whole brain experiment and 24 seconds in the cerebellum experiment).

Number of saccades and saccadic amplitudes

In both experiments (whole brain and cerebellum) the saccadic eye movement behavior was similar in the two active conditions (no-step and random-step) with respect to the number of saccades and saccadic gains (table 1). Subjects made more saccades per block in either active condition than in the baseline condition ($p < 0.001$). The number of saccades was slightly but not significantly increased in the random-step condition of the cerebellum experiment when compared to the no-step condition ($p = 0.05$). In all conditions, the primary saccades towards the flashed target on the right were slightly hypometric with a gain below 1 (table 1). No differences in these gains were observed between the random-step and no-step conditions in both experiments ($p > 0.8$). In the no-step condition, these hypometric primary saccades were followed by a small rightward correction saccade, whereas in the random-step condition, the direction and amplitude of the correction saccade following the primary saccades depended on the position of the target after the intra-saccadic step.

Functional imaging data

The results of the random effects group analyses in both experiments are shown in table 2 for the no-step condition and in table 3 for the random-step condition.

No-Step condition

Comparison of the no-step condition with the baseline condition in the whole brain experiment revealed bilateral activation in the precentral gyrus (FEF) and in the superior parietal gyrus and unilateral activation in the right inferior parietal gyrus (PEF). Bilateral activation was also found in the middle temporal gyrus (MT/V5) and the precuneus (V6). No significant activation was found in the supplementary motor area (SEF).

Comparison of the no-step condition with the baseline condition in the cerebellum experiment revealed activation in the vermis VI and VII, and bilateral activation in lobule VI of the cerebellar hemispheres.

Random-step condition

Comparison of the random-step condition with the baseline condition in the whole brain experiment revealed bilateral activation in the precentral gyrus (FEF), in the superior parietal gyrus and unilateral in the right inferior parietal gyrus (PEF). Bilateral activation was also found in the middle temporal gyrus (MT/V5) and the precuneus (V6). No significant activation was found in the supplementary motor area (SEF).

Comparison of the random-step condition with the baseline condition in the cerebellum experi-

Whole Brain Experiment

Cluster size	T-value	MNI coordinates			Anatomical area	Side	%(*)	Functional area
		x	y	z				
5734	8.92	-14	-76	-2	Lingual Gyrus	L	14.4	PVA/V1
					Lingual Gyrus	R	11.8	PVA/V1
					Calcarine Gyrus	R	11.1	PVA/V1
					Calcarine Gyrus	L	10.8	PVA/V1
					Middle Temporal Gyrus	L	8.2	MT/V5
					Cuneus	L	6.5	PVA/V1
					Middle Occipital Gyrus	L	5.6	PVA/V1
					Fusiform Gyrus	R	3.4	
					Supramarginal Gyrus	L	3.1	
					Cuneus	R	2.6	PVA/V1
					Angular Gyrus	L	2.2	
					Superior Temporal Gyrus	L	1.9	
					Inferior Occipital Gyrus	L	1.5	PVA/V1
Superior Occipital Gyrus	L	1.1	PVA/V1					
45	6.98	-42	36	-14	Inferior Frontal Gyrus	L	100.0	
380	6.59	-48	-10	42	Postcentral Gyrus	L	60.5	
					Precentral Gyrus	L	37.4	FEF
294	6.31	52	-6	38	Precentral Gyrus	R	59.9	FEF
					Postcentral Gyrus	R	38.8	
133	5.84	20	4	4	Globus Pallidus	R	45.1	
					Putamen	R	39.9	
386	5.63	42	-64	10	Middle Temporal Gyrus	R	74.6	MT/V5
					Middle Occipital Gyrus	R	8.8	
104	5.63	58	-50	38	Inferior Parietal Gyrus	R	48.1	
					Angular Gyrus	R	36.5	
					Supramarginal Gyrus	R	11.5	
177	5.59	32	-64	56	Superior Parietal Gyrus	R	78.5	PEF
					Inferior Parietal Gyrus	R	10.7	PEF
					Angular Gyrus	R	7.3	
75	5.33	-20	16	4	Putamen	L	82.7	
					Caudate	L	5.3	
229	5.3	-26	-6	8	Putamen	L	52.0	
					Globus Pallidus	L	28.4	
					Thalamus	L	2.2	
134	5.12	50	40	-14	Inferior Orbital Frontal Gyrus	R	82.8	
					Middle Frontal Gyrus	R	17.2	
243	5.02	62	-42	10	Superior Temporal Gyrus	R	60.9	

					Middle Temporal Gyrus	R	38.3	
26	5.00	40	-10	48	Precentral Gyrus	R	100.0	FEF
19	4.4	18	-44	0	Lingual Gyrus	R	68.4	
					Precuneus	R	31.6	V6
49	4.36	-34	-58	60	Superior Parietal Gyrus	L	98.0	PEF
					Precuneus	L	2.0	V6
19	4.29	12	-16	0	Thalamus	R	42.1	
23	4.26	-24	-74	24	Superior Occipital Gyrus	L	69.6	PVA/V1
					Middle Occipital Gyrus	L	30.4	PVA/V1
14	4.01	22	-84	52	Superior Parietal Gyrus	R	57.1	
17	4.01	46	-36	34	Supramarginal Gyrus	R	76.5	
14	3.87	-56	-8	-28	Inferior Temporal Gyrus	L	64.3	
					Middle Temporal Gyrus	L	35.7	
11	3.64	-50	4	-2	Superior Temporal Gyrus	L	45.5	
					Rolandic Operculum	L	36.4	
					Temporal Pole	L	9.1	
					Inferior Opercular Frontal Gyrus	L	9.1	
10	3.58	32	-80	10	Middle Occipital Gyrus	R	60.0	

Cerebellum Experiment

Cluster size	T-value	MNI coordinates			Anatomical area	Side	%(*)	Functional area
		x	y	z				
88	6.33	8	-72	-14	Cerebellum VI	R	81.82	Oculomotor
					Vermis VII		14.77	
					Vermis VI		3.41	
36	6.09	-30	-66	-24	Cerebellum VI	L	100	Oculomotor
70	5.48	40	-60	-26	Cerebellum VI	R	100	Oculomotor
32	5.17	-8	-76	-12	Cerebellum VI	L	100	Oculomotor

Table 2 – No-Step condition: Areas of activation (no-step > baseline) in the whole brain and the cerebellum experiments with cluster size (number of significantly activated voxels), T-values of the local maximum, Montreal Neurological Institute (MNI) coordinates, the anatomical areas, the percentage (%) of the cluster size for each anatomical area and the corresponding functional area. All areas were thresholded at $p < 0.05$ with FDR correction for multiple comparisons. (L: left hemisphere, R: right hemisphere; FEF: frontal eye fields, PEF: parietal eye fields, MT/V5: motion-sensitive area, V6: precuneus and PVA/V1: primary visual areas/V1). (*) The anatomically unassigned areas for each cluster are not listed in the table.

ment revealed activation in the vermis VI and VII, and bilateral activation in lobule VI of the cerebellar hemispheres.

Direct comparison

Direct comparison of the two active conditions (no-step vs. random-step and vice versa) yielded no significant activation in either experiment using FDR correction at voxel level. The correction for multiple comparisons was therefore relaxed to correction at cluster level.

Whole Brain Experiment

Cluster size	T-value	MNI coordinates			Anatomical area	Side	%(*)	Functional area
		x	y	z				
8677	11.91	10	-78	-12	Lingual Gyrus	L	12.9	PVA/V1
					Lingual Gyrus	R	12.08	PVA/V1
					Calcarine Gyrus	L	8.98	PVA/V1
					Calcarine Gyrus	R	8.38	PVA/V1
					Middle Occipital Gyrus	L	6.49	
					Middle Temporal Gyrus	R	4.64	MT/V5
					Fusiform Gyrus	R	4.53	
					Cuneus	L	3.81	PVA/V1
					Fusiform Gyrus	L	3.68	
					Superior Occipital Gyrus	L	3.24	PVA/V1
					Cuneus	R	3.16	PVA/V1
					Middle Temporal Gyrus	L	3.02	MT/V5
					Inferior Occipital Gyrus	L	2.96	PVA/V1
					Superior Occipital Gyrus	R	2.37	PVA/V1
					Middle Occipital Gyrus	R	1.99	PVA/V1
Supramarginal Gyrus	L	1.29						
410	7.30	-20	-64	60	Superior Parietal Gyrus	L	70.24	PEF
					Precuneus	L	23.17	V6
181	7.20	68	-36	14	Superior Temporal Gyrus	R	85.08	
					Middle Temporal Gyrus	R	11.05	
					Supramarginal Gyrus	R	2.21	
534	6.15	28	-62	54	Superior Parietal Gyrus	R	69.48	PEF
					Inferior Parietal Gyrus	R	11.24	PEF
					Angular Gyrus	R	7.49	
					Precuneus	R	2.81	V6
248	5.59	-48	-2	40	Precentral Gyrus	L	63.71	FEF
					Postcentral Gyrus	L	35.89	
61	5.07	26	6	6	Putamen	R	88.52	
					Globus Pallidus	R	3.28	
					Insula	R	3.28	
27	4.96	56	-54	42	Inferior Parietal Gyrus	R	62.96	
					Supramarginal Gyrus	R	33.33	
					Angular Gyrus	R	3.7	
32	4.70	-64	-34	0	Middle Temporal Gyrus	L	100	
179	4.68	60	-6	46	Precentral Gyrus	R	92.74	FEF
					Inferior Opercular Frontal Gyrus	R	6.7	
20	4.51	-30	-4	42	Precentral Gyrus	L	40	

21	4.35	48	-42	30	Supramarginal Gyrus	R	95.24	
13	4.31	20	-28	-4	Hippocampus	R	38.46	
					Thalamus	R	7.69	
10	4.12	36	-6	-14	Hippocampus	R	20	
45	3.88	50	12	2	Inferior Opercular Frontal Gyrus	R	55.56	
					Inferior Triangular Frontal Gyrus	R	42.22	
					Inferior Orbital Frontal Gyrus	R	2.22	
19	3.88	-14	4	12	Caudate	L	52.63	
					Putamen	L	10.53	
20	3.81	-60	-32	-10	Middle Temporal Gyrus	L	100	
20	3.74	50	2	16	Rolandic Operculum	R	70	
					Precentral Gyrus	R	15	
					Inferior Opercular Frontal Gyrus	R	10	
18	3.55	-24	-2	6	Putamen	L	72.22	
					Globus Pallidus	L	27.78	

Cerebellum Experiment

Cluster size	T-value	MNI coordinates			Anatomical area	Side	%(*)	Functional area
		x	y	z				
136	6.69	8	-74	-14	Cerebellum VI	R	77.21	Oculomotor
					Vermis VII		16.18	
					Vermis VI		6.62	
78	5.84	-34	-64	-20	Cerebellum VI	L	100	Oculomotor
66	5.78	-8	-76	-12	Cerebellum VI	L	100	Oculomotor
100	5.19	36	-64	-22	Cerebellum VI	R	100	Oculomotor

Table 3 - Random-Step condition: Areas of activation (random-step > baseline) in the whole brain and the cerebellum experiments with cluster size (number of significantly activated voxels), T-values of the local maximum, Montreal Neurological Institute (MNI) coordinates, the anatomical areas within a cluster, the percentage (%) of the cluster size for each anatomical area and the corresponding functional area. All areas were thresholded at $p < 0.05$ with FDR correction for multiple comparisons. (L: left hemisphere, R: right hemisphere; FEF: frontal eye fields, PEF: parietal eye fields, MT/V5: motion-sensitive area, V6: precuneus and PVA/V1: primary visual areas/V1). (*) The anatomically unsigned areas for each cluster are not listed in the table.

The direct comparison of the no-step condition with the random-step condition ($[\text{active}_{\text{no-step}} > \text{baseline}]$ versus $[\text{active}_{\text{random-step}} > \text{baseline}]$) revealed activation in the right middle temporal gyrus (MT/V5). For the cerebellum experiment, this comparison revealed no significant activation.

The comparison of the random-step condition with the no-step condition ($[\text{active}_{\text{random-step}} > \text{baseline}]$ versus $[\text{active}_{\text{no-step}} > \text{baseline}]$) revealed activation in the left middle temporal gyrus (MT/V5). For the cerebellum experiment, the analysis yielded activation in vermis VIII and bilateral activation in the lobules VIII, IX and X, and unilateral activation in the left lobule VIIIb of the cerebellar hemisphere. (table 4)

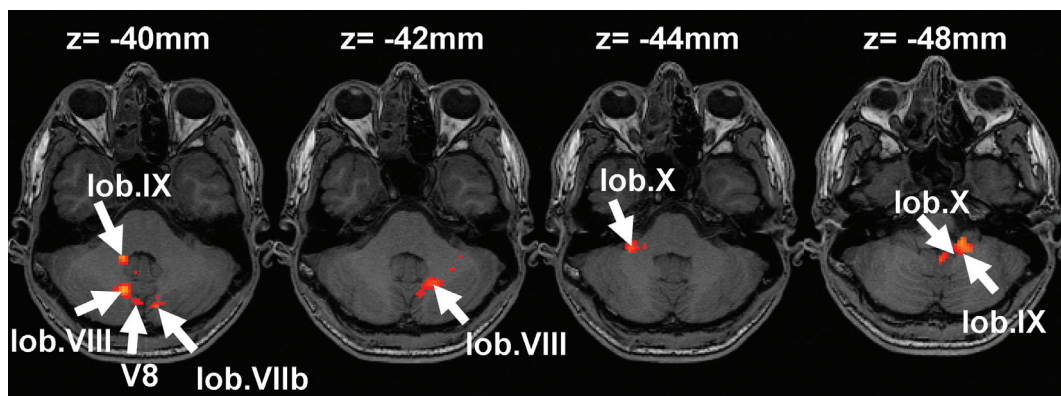


Figure 2 – Direct Comparison: Four axial slices showing areas of activation of the direct comparison ($[\text{random-step} > \text{baseline}] > [\text{no-step} > \text{baseline}]$, group analysis) in the cerebellum experiment (lob. = lobule; V8 = vermis VIII). All areas were thresholded at $p < 0.05$ corrected for multiple comparisons at cluster level and a minimum cluster size of 10 voxels.

Cerebellum Experiment

Cluster size	T-value	MNI coordinates			Anatomical area	Side	%(*)	Functional area
		x	y	z				
1099	5.08	12	-44	-40	Cerebellum IX	R	13.92	Oculomotor
		12	-66	-40	Cerebellum VIII	R	11.19	Oculomotor
		-16	-38	-48	Cerebellum IX	L	9.19	Oculomotor
		-18	-60	-42	Cerebellum VIII	L	8.28	Oculomotor
		28	-38	-44	Cerebellum X	R	4.73	Oculomotor
		-10	-76	-40	Cerebellum VIIb	L	2.46	Oculomotor
		-16	-36	-48	Cerebellum X	L	1.91	Oculomotor
		4	-74	-40	Vermis VIII		1.18	

Table 4 - Random-Step vs. No-Step: Areas of activation ($[\text{random-step} > \text{baseline}] > [\text{no-step} > \text{baseline}]$) in the cerebellum experiment with cluster size, T-values of the local maximum, Montreal Neurological Institute (MNI) coordinates, the anatomical areas within a cluster, the percentage of the cluster size and the functional area. All areas were thresholded at $p < 0.05$ corrected for multiple comparisons at cluster level and a minimum cluster size of 10 voxels. (L: left hemisphere, R: right hemisphere). (*) The anatomically unassigned areas for each cluster are not listed in the table.

DISCUSSION

The principal aim of this study was to evaluate the involvement of the cerebrum and the cerebellum in the processing of saccadic errors. We used a modification of the classical saccade adaptation paradigm, in which the random intra-saccadic target steps do lead to an increase in saccadic error. Although these increased errors might induce transient changes in saccade amplitude, the random distribution of the saccadic

errors prevent the sustained adaptation of saccades as would have been observed in a classical saccade adaptation paradigm with a fixed intrasaccadic target step. We performed two fMRI experiments: one on the whole brain and one in which we focussed on the cerebellum, using different scan parameters to increase the sensitivity for cerebellar activation.

Our main observation was an increase in cerebellar activity with random post-saccadic er-

rors compared to saccades without induced error. This activity was located in vermis VIII, in the hemispheric lobules VIII, IX and X bilaterally, and in the left lobule VIIb. In a previous study with a similar experimental paradigm using PET, this cerebellar activation was not observed [5, 10], which is possibly due to the low spatial resolution achieved with PET imaging. When we looked at the main effects of each condition separately, activation related to saccadic eye movements was observed in the expected cerebral and cerebellar regions.

Cerebral activation

In the whole brain experiment, cerebral activation was located in known visual areas (primary visual area (PVA/V1), MT/V5 and the precuneus (V6)) as well as in eye movement related areas (frontal (FEF) and parietal (PEF) eye fields) in both conditions (saccades without errors and saccades with random saccadic errors). PVA/V1, MT/V5 and V6 process visual information, which is used to guide saccadic eye movements. The FEF and PEF are involved in the planning and generation of saccadic eye movements [1, 2] Activation in these areas is consistent with the results from previous functional imaging studies on saccadic eye movements [4, 13, 14].

The direct comparisons of the conditions without target steps and with random intra saccadic target steps. In the whole brain experiment only revealed activation in MT/V5, which is an area specifically involved in the processing of real and apparent visual motion [15]. Although subjects did not see the target step consciously, it is possible that the use of a flashed target and the re-appearance of the target after the saccade may have induced differences in low-level processing of apparent motion between the two conditions. Apparent motion can induce fMRI activation of MT/V5 [16], although it does not explain the observed laterality of the activation,

dependent on the direction of the comparison, in the present study.

Cerebellar activation

In the cerebellum experiment, activation was found in the vermis VI and VII (known as the oculomotor vermis) and in the cerebellar hemispheric lobule VI bilaterally in both conditions. These findings are consistent with previous studies in humans imaging on saccade eye movements using fMRI [6, 7, 17, 18].

Several human and non-human primate studies suggest that the oculomotor vermis is critically involved in the accurate performance of saccadic eye movements. Electrophysiological recordings in vermis VI and VII of the cerebellum yield neuronal activity during saccade generation [19, 20] and microstimulation in these areas evokes saccadic eye movements [21, 22]. Lesions in vermal areas V-VIII, which includes the oculomotor vermis, impaired the initiation, accuracy and dynamics of saccades in monkeys [23, 24]. Similarly, studies in human patients with cerebellar degeneration, cerebellar infarcts or congenital malformations showed an increase in saccadic variability [25, 26].

With respect to saccadic adaptation, electrophysiological recordings in monkeys showed that neurons in vermis VI and VII are active in a saccade adaptation task [27, 28]. Microstimulation of the vermis VI and VII in monkeys changes the amplitude of saccadic eye movements [29]. Finally, lesions of vermis V-VIII impair the gradual modification of saccadic amplitudes in a saccade adaptation task [23, 24]. Similarly, patients with cerebellar lesions [26], cerebellar atrophy [30] or paraneoplastic cerebellar ataxia [31] showed impairments in or complete lack of saccadic adaptation capacities. In a functional imaging study using PET cerebellar involvement during saccadic adaptation was confirmed [5, 10].

The direct comparisons of the two saccadic conditions in our cerebellum experiment revealed an increase in activation in vermis VIII and in the hemispheric lobules VIII, IX, X bilaterally and in left lobule VIIb with random intra-saccadic target steps compared to the condition without target steps. It could be argued that this increase in activation may – in part – be related to a difference in motor activity. However, due to differences in the number, direction and size of saccades between the no target step we did not observe any difference in the number of primary and correction saccades between the two conditions in either experiment. Furthermore, despite the obvious differences in the corrective saccade metrics, their amplitudes are still small in both conditions. Neurophysiological recordings suggest that saccade size and direction of small saccades do not have an effect on the neuronal activity of cerebellar Purkinje cells. Therefore, we postulate that the increase in activation is related to the increase in post-saccadic errors.

To the best of our knowledge, the involvement of these areas has not been reported previously in the literature on electrophysiological and micro-stimulation studies in monkeys related to saccadic eye movements, except for lobule VIIb, nor was activation observed using PET imaging [10].

The lack of activity in the saccade-related regions of the cerebellum might relate to the results of electrophysiological studies in monkeys, which suggests that the complex spike activity of cerebellar Purkinje cells does not signal saccadic errors, but changed saccadic amplitudes, although another study suggested that spiking activity might be related to the direction of errors. However, the relationship between Purkinje cell activity and the BOLD response remains to be elucidated.

Lobule VIIb of the cerebellum is known to be involved in the generation of saccades [3]. Furthermore, left- and rightward saccades are under the control of the ipsilateral cerebellar hemisphere. Although the total number of saccades was not different between the two conditions, it can be argued that the increase in activity of the left lobule VIIb in the random-step condition is related to a relative increase in leftward saccades. This is not unlikely given the physiological undershoot of normal saccadic behavior. Saccades tend to fall short of the target, so that, in general, correction saccades will be directed to the right in the no-step condition. In the random-step condition, the target is sometimes shifted backwards. Correction saccades in the random-step condition can thus also be directed to the left, as well as to the right.

Vermis VIII (pyramis) is not part of the oculomotor vermis, but has been reported to be involved in the performance of hand movements [32]. A previous fMRI study on saccades and hand movements suggested that this area may be related to the execution of a sequence of saccades [18].

Lobules VIII, IX and X have been reported to be involved in eye movements other than saccades, namely in smooth pursuit and in the adaptation of the vestibulo-ocular reflex (VOR) [33, 34]. These areas receive mossy fiber input from the dorsolateral region of the pontine nuclei, relaying information from cerebral visual areas [35]. They also receive input from the inferior olivary nuclei

[36, 37]. The nature of olivary input to the cerebellum in oculomotor learning processes has been subject of extensive research and is generally thought to serve as an error signal [38, 39].

In all types of eye movements, it is thought that error signals provide the input for the oculomotor system by which means it can maintain its high spatial accuracy. For saccades it has been shown that the visual post-saccadic errors (i.e. the difference between saccade endpoint position and final target position) are indeed potent stimuli to modify saccadic behaviour [8, 9, 40].

Furthermore, the accuracy of smooth pursuit and VOR eye movements depends on the processing of visual errors [41]. The nature of the error signals, however, may vary. The visual error after a discrete saccadic eye movement is static, and consists of the perceived distance between the fovea and a stationary target. This error is then used to execute a corrective eye movement. In contrast, the visual error in smooth pursuit and the vestibulo-ocular reflex is regarded as dynamic. For instance, the visual error during smooth pursuit is the perceived distance of the fovea to a moving target in the visual field. Adequate smooth pursuit therefore requires a dynamic adjustment of eye velocity and proper anticipation of the future position of the target to keep it projected on the fovea [42].

Activity in the cerebellar lobules VIII-X related to saccadic errors may therefore represent the visual error signals used for the maintenance of saccadic accuracy. Future studies, using electrophysiological recordings of these areas might provide more insight into the nature of the cerebellar activity in the processing of static and dynamic visual errors.

For the assessment of fMRI activation in the direct comparison of the two active conditions we used a more lenient multiple comparison correction, as at the most stringent correction for multiple comparisons no voxels were seen to survive the threshold for significance. This lack of statistical power may be due to two things:

first, in the direct comparison only small differences in activation are likely to be measured, as the two conditions are very similar. Second, it has become clear from neurophysiological studies that the activation related to the processing of visual errors and saccade adaptation depends on small electrophysiological changes and not all cells in an involved area are committed to the same task. For example, subgroups of cells may be dedicated to a specific direction of movement. Furthermore, the changes in activity are not always dependent on in- or decrease of neuronal firing rate, but can also depend on changes in the timing of neuronal firing [27, 28, 43]. These factors increase variation and noise, thus reducing statistical power. It should be noted, on the other hand, that the more lenient multiple comparisons correction did not reveal any significant activation in the whole brain experiment. Neurophysiological recording and stimulation studies will be needed to corroborate the present findings, which are the first to suggest activity in areas outside the oculomotor vermis in relation to errors in saccadic motor performance.

If areas outside the oculomotor areas indeed participate in saccadic error processing, it is conceivable that these areas are also involved in the modification of saccadic amplitudes, such as in the normal saccadic adaptation paradigm. In the classical saccade adaptation paradigm subjects are presented with consistent errors rather than the random errors such as those used in the present study. In a functional MRI study using a classical saccade adaptation paradigm, it may however be too difficult to detect the contribution of these areas to saccadic error processing for various reasons. First, consistent saccadic errors induce sustained changes in saccadic amplitudes during the course of the experiment (adaptation). These motor changes may lead to confounding changes in motor signals in the

cerebrum and cerebellum. Second, the saccadic adaptation process during the course of the experiment will reduce the magnitude of the saccadic errors, which, in turn, results in a concurrent reduction of the brain activation related to saccadic errors. Finally, subjects vary greatly with respect to the speed at which they adapt their saccadic amplitudes over a series of trials: some subjects need a few trials of post-saccadic errors, whereas others need tens of trials or do not adapt systematically at all. The present paradigm of using random step post-saccadic errors minimizes these confounding factors associated with consistent errors.

CONCLUSION

Using fMRI, we found an increase in cerebellar activity, but not in cerebral activity, related to random post-saccadic errors. These results suggest a possible role for areas outside the oculomotor vermis in the processing of visual post-saccadic errors. Future studies with e.g. electrophysiological recordings in monkeys may be directed specifically towards these areas to corroborate our findings and to investigate the precise nature of the error signals that drive the modification of saccadic eye movements.

REFERENCES

1. Hopp, J.J. and A.F. Fuchs, The characteristics and neuronal substrate of saccadic eye movement plasticity. *Prog Neurobiol*, 2004. 72(1): p. 27-53.
2. Moschovakis, A.K., C.A. Scudder, and S.M. Highstein, The microscopic anatomy and physiology of the mammalian saccadic system. *Prog Neurobiol*, 1996. 50(2-3): p. 133-254.
3. Leigh, R.J. and D.S. Zee, *The Neurology of Eye Movements*. Third ed. 1999, New York: Oxford University Press.
4. Anderson, T.J., et al., Cortical control of saccades and fixation in man. A PET study. *Brain*, 1994. 117 (Pt 5): p. 1073-84.
5. Desmurget, M., et al., Functional anatomy of saccadic adaptation in humans. *Nat Neurosci*, 1998. 1(6): p. 524-8.
6. Dieterich, M. and T. Brandt, Brain activation studies on visual-vestibular and ocular motor interaction. *Curr Opin Neurol*, 2000. 13(1): p. 13-8.
7. Hayakawa, Y., et al., Human cerebellar activation in relation to saccadic eye movements: a functional magnetic resonance imaging study. *Ophthalmologica*, 2002. 216(6): p. 399-405.
8. Robinson, F.R., C.T. Noto, and S.E. Bevans, Effect of visual error size on saccade adaptation in monkey. *J Neurophysiol*, 2003. 90(2): p. 1235-44.
9. Wallman, J. and A.F. Fuchs, Saccadic gain modification: visual error drives motor adaptation. *J Neurophysiol*, 1998. 80(5): p. 2405-16.
10. Desmurget, M., et al., Functional adaptation of reactive saccades in humans: a PET study. *Exp Brain Res*, 2000. 132(2): p. 243-59.
11. Le Bihan, D., et al., Functional magnetic resonance imaging of the brain. *Ann Intern Med*, 1995. 122(4): p. 296-303.
12. Tzourio-Mazoyer, N., et al., Automated anatomical labeling of activations in SPM using a macroscopic anatomical parcellation of the MNI MRI single-subject brain. *Neuroimage*, 2002. 15(1): p. 273-89.

13. Matsuda, T., et al., Functional MRI mapping of brain activation during visually guided saccades and antisaccades: cortical and subcortical networks. *Psychiatry Res*, 2004. 131(2): p. 147-55.
14. Mort, D.J., et al., Differential cortical activation during voluntary and reflexive saccades in man. *Neuroimage*, 2003. 18(2): p. 231-46.
15. Born, R. and D. Bradley, Structure and function of visual area MT. *Annu Rev Neurosci*, 2005. 28:157-189.
16. Goebel, R., et al., The constructive nature of vision: direct evidence from functional magnetic resonance imaging studies of apparent motion and motion imagery. *Eur J Neurosci*, 1998. 10(5): p. 1563-73.
17. DeJardin, S., et al., PET study of human voluntary saccadic eye movements in darkness: effect of task repetition on the activation pattern. *Eur J Neurosci*, 1998. 10(7): p. 2328-36.
18. Nitschke, M.F., et al., Activation of cerebellar hemispheres in spatial memorization of saccadic eye movements: an fMRI study. *Hum Brain Mapp*, 2004. 22(2): p. 155-64.
19. Kase, M., D.C. Miller, and H. Noda, Discharges of Purkinje cells and mossy fibres in the cerebellar vermis of the monkey during saccadic eye movements and fixation. *J Physiol*, 1980. 300: p. 539-55.
20. Ohtsuka, K. and H. Noda, Discharge properties of Purkinje cells in the oculomotor vermis during visually guided saccades in the macaque monkey. *J Neurophysiol*, 1995. 74(5): p. 1828-40.
21. Krauzlis, R.J. and F.A. Miles, Role of the oculomotor vermis in generating pursuit and saccades: effects of microstimulation. *J Neurophysiol*, 1998. 80(4): p. 2046-62.
22. Noda, H., S. Sugita, and Y. Ikeda, Afferent and efferent connections of the oculomotor region of the fastigial nucleus in the macaque monkey. *J Comp Neurol*, 1990. 302(2): p. 330-48.
23. Barash, S., et al., Saccadic dysmetria and adaptation after lesions of the cerebellar cortex. *J Neurosci*, 1999. 19(24): p. 10931-9.
24. Takagi, M., D.S. Zee, and R.J. Tamargo, Effects of lesions of the oculomotor vermis on eye movements in primate: saccades. *J Neurophysiol*, 1998. 80(4): p. 1911-31.
25. Botzel, K., K. Rottach, and U. Buttner, Normal and pathological saccadic dysmetria. *Brain*, 1993. 116 (Pt 2): p. 337-53.
26. Straube, A., et al., Cerebellar lesions impair rapid saccade amplitude adaptation. *Neurology*, 2001. 57(11): p. 2105-8.
27. Catz, N., P.W. Dicke, and P. Thier, Cerebellar complex spike firing is suitable to induce as well as to stabilize motor learning. *Curr Biol*, 2005. 15(24): p. 2179-89.
28. Soetedjo, R. and A.F. Fuchs, Complex spike activity of purkinje cells in the oculomotor vermis during behavioral adaptation of monkey saccades. *J Neurosci*, 2006. 26(29): p. 7741-55.
29. Keller, E.L. and S.J. Heinen, Generation of smooth-pursuit eye movements: neuronal mechanisms and pathways. *Neurosci Res*, 1991. 11(2): p. 79-107.
30. Waespe, W. and R. Baumgartner, Enduring dysmetria and impaired gain adaptivity of saccadic eye movements in Wallenberg's lateral medullary syndrome. *Brain*, 1992. 115 (Pt 4): p. 1123-46.
31. Coesmans, M., et al., Mechanisms underlying cerebellar motor deficits due to mGluR1-autoantibodies. *Ann Neurol*, 2003. 53(3): p. 325-36.

32. Nitschke, M.F., et al., The cerebellum in the cerebro-cerebellar network for the control of eye and hand movements--an fMRI study. *Prog Brain Res*, 2005. 148: p. 151-64.
33. Rambold, H., et al., Partial ablations of the flocculus and ventral paraflocculus in monkeys cause linked deficits in smooth pursuit eye movements and adaptive modification of the VOR. *J Neurophysiol*, 2002. 87(2): p. 912-24.
34. Thier, P. and U.J. Ilg, The neural basis of smooth-pursuit eye movements. *Curr Opin Neurobiol*, 2005. 15(6): p. 645-52.
35. Glickstein, M., Functional localisation in the cerebral cortex and cerebellum: lessons from the past. *Eur J Morphol*, 2000. 38(5): p. 291-300.
36. Brodal, P. and A. Brodal, Further observations on the olivocerebellar projection in the monkey. *Exp Brain Res*, 1982. 45(1-2): p. 71-83.
37. Noda, H. and A. Mikami, Discharges of neurons in the dorsal paraflocculus of monkeys during eye movements and visual stimulation. *J Neurophysiol*, 1986. 56(4): p. 1129-46.
38. Ito, M., Mechanisms of motor learning in the cerebellum. *Brain Res*, 2000. 886(1-2): p. 237-245.
39. Winkelman, B. and M. Frens, Motor coding in floccular climbing fibers. *J Neurophysiol*, 2006. 95(4): p. 2342-51.
40. McLaughlin, S.C., Parametric adjustment in saccadic eye movements. *Percept Psychophys*, 1967. 2: p. 359-362.
41. Raymond, J.L. and S.G. Lisberger, Error signals in horizontal gaze velocity Purkinje cells under stimulus conditions that cause learning in the VOR. *Ann N Y Acad Sci*, 1996. 781: p. 686-9.
42. Barnes, G.R. and P.T. Asselman, The assessment of predictive effects in smooth eye movement control. *Acta Otolaryngol Suppl*, 1991. 481: p. 343-7.
43. Takeichi, N., C.R. Kaneko, and A.F. Fuchs, Discharge of monkey nucleus reticularis tegmenti pontis neurons changes during saccade adaptation. *J Neurophysiol*, 2005. 94(3): p. 1938-51.

PART 4

SUMMARY



ROTTERDAM

鹿
特
丹

CHAPTER 7

SUMMARY

SUMMARY

In this thesis, we explored the neuronal basis of several types of eye movements. Functional magnetic resonance imaging (fMRI) was used to investigate and compare the brain activations evoked by smooth pursuit eye movements, the optokinetic reflex (OKR) and saccadic eye movements. We looked at activations in both cerebral as well as cerebellar areas.

PART 1 – SMOOTH PURSUIT AND OKR

In **Chapter 2** we compared the brain activation related to smooth pursuit and OKR eye movements. A single moving dot was used as stimulus for smooth pursuit eye movement. The OKR stimulus consisted of a random pattern of dots with a limited lifetime. Brain activation related to smooth pursuit was found in the cortical eye movement areas (FEF, SEF, PEF), area MT/V5, and the cerebellum. Stronger activation was observed in the FEF, in the MT/V5 area and in the cerebellum during smooth pursuit than during OKR eye movement. We concluded that the smooth pursuit eye movement system and the optokinetic eye movement systems can be differentiated with fMRI.

In previous studies no difference in activation between smooth pursuit and OKR eye movement was observed. In those studies OKR was elicited by a standard stimulus which consisted of a moving pattern of stripes or fixed dots [1-6]. We hypothesized that such a fixed pattern targets not only the optokinetic system due to the peripheral stimulation, but also the smooth pursuit system due to concurrent foveal stimulation, similar to when the eyes have to follow a single moving dot.

In **Chapter 3** we studied the contribution of the smooth pursuit system to the brain activations evoked by a standard OKR stimulus. We investigated to what extent brain activations evoked by smooth pursuit and OKR eye movements can be isolated by eliminating the smooth pursuit component from the OKR response. For this, we used the OKR stimulus described in Chapter 2. In this limited lifetime dot stimulus each dot was repositioned within 50 ms. Since smooth pursuit has a latency of more than 100 ms, voluntary tracking of individual dots in this OKR stimulus by smooth pursuit eye movements is unlikely to play a role [1, 7]. Therefore, limited lifetime dot stimulation is likely to target the optokinetic system in isolation.

We compared the brain activations that were associated with eye movements in response to a standard OKR stimulus consisting of a fixed pattern of stripes and an OKR stimulus consisting of limited lifetime dots. These results suggest that these areas of the brain are predominantly involved in tracking a moving stimulus using smooth pursuit. We observed stronger activation in the FEF and PEF, the MT/V5 area and in the cerebellum, when the standard OKRT stimulus was used (Table 1). These areas are predominantly involved in the voluntary tracking of a moving stimulus with the smooth pursuit eye movement system.

We concluded that the smooth pursuit eye movement and the optokinetic eye movement systems can be differentiated with fMRI using a stimulus that elicits OKR in isolation, without a confounding contribution of the smooth pursuit system.

PART 2 – SMOOTH PURSUIT AND FIXATION SUPPRESSION OF THE OKR

In **Chapter 4**, we investigated the possible differences in brain activation patterns evoked by smooth pursuit eye movements and fixation suppression of the OKR. In this study, both oculomotor behaviors were evoked by a target moving relative to the background. In the smooth pursuit experiment the target moved, whereas in the fixation suppression of the OKR experiment the background moved. Subjects had to look at the target. In other words, in both experiments the (relative) motion of the background needed to be ignored and the target was to be kept on the fovea. Thus the retinal stimulation was similar in both experiments.

Similar to the experiments in Chapters 2 and 3, smooth pursuit eye movements induced activation in the FEF, SEF, PEF, the MT/V5, and lobule VI and vermis VI of the cerebellum. Fixation suppression of the OKR also induced activation in the FEF, PEF and MT/V5, but not in the SEF or the cerebellum (Table 1). The observed activation in the smooth pursuit eye movements is likely to be evoked by the motion of the dot and the associated smooth pursuit response.

When we directly compared the two experiments, no difference in activation was observed. With a more lenient statistical threshold more activation was observed in the cerebellum during the smooth pursuit eye movement. This outcome suggests that smooth pursuit eye movement and fixation suppression of OKR activate overlapping cortical pathways. The difference in cerebellar activation is likely to be induced by the presence of an active eye movement component in the smooth pursuit experiment. Finally, the comparable activation of MT/V5 in

the two experiments supports the notion that the visual motion stimulation between the two experiments was indeed very similar.

Our imaging results suggest that smooth pursuit and fixation suppression of OKR activate overlapping pathways in which fixation suppression of the optokinetic reflex can be regarded as smooth pursuit on a non-homogenous background without motion of the target.

PART 3 – SACCADIC EYE MOVEMENTS

In the third part of this thesis, brain activation was studied in relation to saccadic eye movements. We focused on the cerebellum, which is involved in maintaining saccadic accuracy [8].

In **Chapter 5** we studied the differences in cerebellar, as well as cerebral activation patterns associated with reflexive and voluntary saccades. Behavioral studies on eye movement control suggest that the modification of saccadic amplitudes in a so-called saccadic adaptation paradigm can be dissociated between voluntary and reflexive saccades. It has been proposed that the generation of reflexive and voluntary saccades are mediated by independent mechanisms [9]. As the cerebellum is an important brain structure in saccadic gain control [10-14], it is argued that the cerebellum might be differently involved in maintaining the accuracy of reflexive and voluntary saccades.

We compared the brain activation related to reflexive and voluntary saccades. Reflexive saccades were evoked by suddenly appearing targets. Voluntary saccades were made between two permanent visible targets. The results showed stronger activation in the FEF, PEF, MT/V5, the precuneus (V6), the angular and the cingulate

Functional Area	Stimulus					Comparison		
	A	B	C	D	E	A vs B	C vs B	D vs E
	Single Dot 	Limited Lifetime dots 	Stripes 	Single dot with background 	Fixation suppression of OKR with background 			
Frontal Eye Field (FEF)	B	-	B	B	B	L	L	-
Supplementary Eye Field (SEF)	L	-	B	L	-	-	-	-
Parietal Eye Field (PEF)	B	-	L	B	B	-	L	-
Visual Area 5 (MT/V5)	R	-	R	R	B	R	R	-
Oculomotor Area of the cerebellum	B	R	B	B	-	B	B	-

Table 1: Summary of the activations observed during smooth pursuit of a single dot, during the optokinetic reflex with limited lifetime dots and stripes, and smooth pursuit or OKN suppression of a dot moving relative to a striped pattern (B: bilateral; R: right hemisphere; L: left hemisphere; - indicates no significant activation).

gyri during reflexive saccades than during voluntary saccades. No significant differences in activation were found in the cerebellum (Table 2). These results indicate that the alleged separate mechanisms for control of reflexive and voluntary saccades are to be found in cerebral rather than in cerebellar areas.

In **Chapter 6**, we investigated the role of the cerebrum and the cerebellum in the processing of post-saccadic visual errors. Subjects had to make saccadic eye movements to a flashed target. In the first condition of the experiment, large variable post-saccadic visual errors were induced by randomly shifting the saccade target during the saccade toward it. The random distribution of the post-saccadic errors prevented the modification of saccadic amplitudes. In the second condition of the experiment, the target did not shift when the subjects made a saccade toward it. Since post-saccadic visual errors are likely to drive the adaptation process [15, 16] which is likely to be mediated within cerebellar structures [10, 11, 14], we hypothesized that specific cerebellar regions are involved in the processing of post-saccadic visual errors.

Both saccadic conditions revealed the expected brain activation patterns in the cerebrum (FEF, MT/V5) and in the saccade-related oculomotor regions of the cerebellum (vermis and lobules VI and VII). Furthermore, we observed an increase in cerebellar activity related to larger post-saccadic visual errors (Table 2): bilaterally in lobule VIII,

Functional Area	Stimulus				Comparison			
	A	B	C	D	A versus B	B versus A	C versus D	D versus C
	Voluntary Saccades 	Reflexive Saccades 	Saccades without target step 	Saccades with random target step 	Voluntary vs. Reflexive Saccades	Reflexive vs. Voluntary Saccades	No step vs. Random step	Random step vs. No step
Frontal Eye Field (FEF)	B	B	B	B	-	B	-	-
Supplementary Eye Field (SEF)	-	-	-	-	-	-	-	-
Parietal Eye Field (PEF)	L	B	B	B	-	B	-	-
Visual Area 5 (MT/V5)	-	B	B	B	-	B	-	-
Oculomotor Area of the cerebellum	-	-	B	B	-	-	-	-

Table 2: Summary of the activations during reflexive and voluntary saccades, and during saccades without and with random target steps (B: bilateral; R: right hemisphere; L: left hemisphere; - indicates no significant activation.)

IX, X, unilaterally in the left VIIIb, and in vermis VIII. These results suggest a possible role of areas outside the oculomotor vermis in the processing of post-saccadic visual errors.

FUTURE DIRECTIONS

In this thesis we explored only a few types of eye movements that are related to visual processing of the environment. However, we did not touch on the vestibular ocular reflex (VOR), i.e. the eye movement that is evoked by vestibular stimulation. The VOR is usually evoked by rotating the subject using a rotating chair or moving platform [17]. However, rotating the subject inside the scanner bore is not feasible. Another way of evoking a proper VOR response is by inserting cold or warm water in the ear. When a subject is lying in supine position, cold water stimulation in one of the ears leads to a sensation of rotation in the direction opposite to the side of stimulation. In the dark, it also induces nystagmus, with the fast phases in the direction of the ear that is stimulated. However, when the subject has his eyes open, the sensation of being rotated is contradicted by the stable visual environment. In a pilot study we observed that this mismatch between visual and vestibular information leads to an increase in activity in the cerebellum (Figure 1). This preliminary finding is in good agreement with electrophysiological studies [18].

The study comparing reflexive and voluntary saccadic eye movements (Chapter 5), focused on differences in activation in the cerebellum. Although cognitive processes in the cortex are allegedly more involved in the control of voluntary saccades than in reflexive saccades, it is conceivable that in our specific paradigm, both saccades are being processed on a relatively low level. In other words, cognitive processes such as memory and attention were probably less

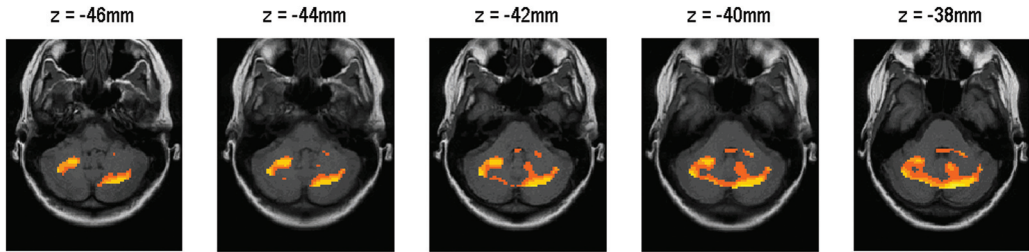


Figure 1: Activation in the cerebellum during cold water stimulation in the left ear of one subject in the light (unpublished data).

involved in that experiment. It might be worthwhile to extend the study of voluntary saccades to include memory-guided saccades (in which the subject has to remember the target location), and delayed saccades (in which the subject has to postpone the actual movement until a trigger signal is provided).

REFERENCES

1. Brandt, T., et al., Bilateral functional MRI activation of the basal ganglia and middle temporal/medial superior temporal motion-sensitive areas: optokinetic stimulation in homonymous hemianopia. *Arch Neurol*, 1998. 55(8): p. 1126-31.
2. Bucher, S.F., et al., Sensorimotor cerebral activation during optokinetic nystagmus. A functional MRI study. *Neurology*, 1997. 49(5): p. 1370-7.
3. Dieterich, M., et al., fMRI signal increases and decreases in cortical areas during small-field optokinetic stimulation and central fixation. *Exp Brain Res*, 2003. 148(1): p. 117-27.
4. Dieterich, M., et al., Horizontal or vertical optokinetic stimulation activates visual motion-sensitive, ocular motor and vestibular cortex areas with right hemispheric dominance. An fMRI study. *Brain*, 1998. 121 (Pt 8): p. 1479-95.
5. Konen, C.S., et al., An fMRI study of optokinetic nystagmus and smooth-pursuit eye movements in humans. *Exp Brain Res*, 2005. 165(2): p. 203-16.
6. Dieterich, M. and T. Brandt, Brain activation studies on visual-vestibular and ocular motor interaction. *Curr Opin Neurol*, 2000. 13(1): p. 13-8.
7. Mestre, D.R. and G.S. Masson, Ocular responses to motion parallax stimuli: the role of perceptual and attentional factors. *Vision Res*, 1997. 37(12): p. 1627-41.
8. Leigh, R.J. and D.S. Zee, *The Neurology of Eye Movements*. Third ed. 1999, New York: Oxford University Press.
9. Deubel, H., Separate adaptive mechanisms for the control of reactive and volitional saccadic eye movements. *Vision Res*, 1995. 35(23-24): p. 3529-40.
10. Barash, S., et al., Saccadic dysmetria and adaptation after lesions of the cerebellar cortex. *J Neurosci*, 1999. 19(24): p. 10931-9.
11. Desmurget, M., et al., Functional anatomy of saccadic adaptation in humans. *Nat Neurosci*, 1998. 1(6): p. 524-8.
12. Ron, S. and D.A. Robinson, Eye movements evoked by cerebellar stimulation in the alert monkey. *J Neurophysiol*, 1973. 36(6): p. 1004-22.

13. Straube, A. and H. Deubel, Rapid gain adaptation affects the dynamics of saccadic eye movements in humans. *Vision Res*, 1995. 35(23-24): p. 3451-8.
14. Straube, A., et al., Cerebellar lesions impair rapid saccade amplitude adaptation. *Neurology*, 2001. 57(11): p. 2105-8.
15. Robinson, F.R., C.T. Noto, and S.E. Bevans, Effect of visual error size on saccade adaptation in monkey. *J Neurophysiol*, 2003. 90(2): p. 1235-44.
16. Wallman, J. and A.F. Fuchs, Saccadic gain modification: visual error drives motor adaptation. *J Neurophysiol*, 1998. 80(5): p. 2405-16.
17. Houben, M.M., et al., Angular and linear vestibulo-ocular responses in humans. *Ann N Y Acad Sci*, 2005. 1039: p. 68-80.
18. Blazquez, P.M., Y. Hirata, and S.M. Highstein, The vestibulo-ocular reflex as a model system for motor learning: what is the role of the cerebellum? *Cerebellum*, 2004. 3(3): p. 188-92.

CHAPTER 8

SAMENVATTING

SAMENVATTING

In dit proefschrift hebben we de neuro-anatomische basis onderzocht van verschillende typen oogbewegingen. We hebben gebruik gemaakt van functionele magnetische resonantie “imaging” (fMRI) om afbeeldingen te maken van de hersenactiviteit die optreedt bij het maken van gladde volgbewegingen (“smooth pursuit”), de optokinetische reflex (OKR) en saccadische oogbewegingen. We hebben gekeken naar de overeenkomsten en verschillen tussen deze oogbewegingen. Hierbij is zowel gekeken naar de hersenactiviteit in de grote hersenen (het cerebrum) als in de kleine hersenen (het cerebellum).

DEEL 1 – SMOOTH PURSUIT EN OKR

In **hoofdstuk 2** hebben we de hersenactiviteit onderzocht die wordt veroorzaakt door smooth pursuit en door OKR. De beweging van een stip is gebruikt als stimulus voor smooth pursuit. Een bewegend patroon van willekeurig geplaatste stippen met een beperkte levensduur is gebruikt als stimulus voor OKR. Smooth pursuit oogbewegingen leidde tot activiteit in de corticale oogbewegingsgebieden (FEF, SEF, en PEF), het gebied MT/V5 en in het cerebellum. Vergelijking van de hersenactiviteit liet zien dat een sterkere activiteit in de frontale oogbewegingsgebieden (FEF), het MT/V5 gebied en in het cerebellum werd gezien bij smooth pursuit dan bij OKR (tabel 1). We concluderen hieruit dat het smooth pursuit oogbewegingsstelsel en het optokinetische oogbewegingsstelsel kunnen worden onderscheiden met behulp van fMRI.

In eerdere studies naar de hersenactiviteit tijdens smooth pursuit en OKR oogbewegingen werd geen verschil gevonden. In deze studies werd

de optokinetische reflex echter uitgelokt door een standaard stimulus bestaande uit bewegend patroon van strepen of vaste stippen [1-6]. Wij waren van mening dat een vast patroon van zwarte en witte strepen niet alleen het optokinetische systeem activeert vanwege de perifere stimulatie van de retina maar ook het smooth pursuit systeem vanwege de gelijktijdige stimulering van de fovea, net als wanneer de ogen een enkele bewegende stip moeten volgen.

In **hoofdstuk 3** hebben we de bijdrage van het smooth pursuit systeem bestudeerd aan de hersenactiviteit die wordt veroorzaakt door een standaard OKR stimulus. We hebben onderzocht in welke mate de hersenactiviteit die veroorzaakt wordt door smooth pursuit en door OKR, kan worden geïsoleerd door de smooth pursuit component te elimineren uit de OKR response. Hiervoor hebben we dezelfde OKR stimulus gebruikt als in hoofdstuk 2. In deze stimulus, bestaande uit een bewegend patroon van willekeurig geplaatste stippen met een beperkte levensduur wordt elke stip binnen 50 ms opnieuw gepositioneerd. Aangezien smooth pursuit een latencie heeft van meer dan 100 ms, is het onwaarschijnlijk dat het smooth pursuit systeem een rol speelt bij het vrijwillig volgen van dit bewegende patroon [1, 7]. Het is daarom aannemelijk dat deze speciale OKR stimulus met stippen met beperkte levensduur alleen het optokinetische systeem aanspreekt.

We hebben de hersenactiviteit gemeten tijdens het maken van oogbewegingen in reactie op de een standaard OKR stimulus bestaande uit een vast patroon van zwarte en witte strepen, en OKR stimulus bestaande uit een patroon van stippen met een beperkte levensduur. We vonden we een sterkere activatie in de frontale en parietale oogbewegingsgebieden (FEF, PEF), het MT/V5 gebied en in het cerebellum wanneer de standaard stimulus werd gebruikt (zie tabel 1).

Deze gebieden van de hersenen zijn dus vooral betrokken bij het vrijwillig volgen van een bewegende stimulus met behulp van het smooth pursuit systeem.

We concluderen dat het smooth pursuit oogbewegingsysteem en het optokinetische oogbewegingsysteem kunnen worden gescheiden met behulp van fMRI door gebruik te maken van een stimulus die zich alleen richt op OKR, zonder een versturende bijdrage van het smooth pursuit systeem.

DEEL 2- SMOOTH PURSUIT EN FIXATIE ONDERDRUKKING VAN DE OKR

In **hoofdstuk 4** hebben we onderzocht of er verschillen zijn in de hersenactiviteit die wordt gezien bij smooth pursuit oogbewegingen en bij fixatie onderdrukking van de OKR. In deze studie werden beide oogbewegingen opgewekt door een doel dat bewoog ten opzichte van de achtergrond. In het eerste experiment bewoog het doel waarbij smooth pursuit oogbewegingen werden opgewekt, terwijl in het tweede experiment de achtergrond bewoog waarbij de proefpersoon de opdracht kreeg om te fixeren op een punt om de OKR te onderdrukken. In beide experimenten moest de relatieve beweging van de achtergrond worden genegeerd en het doel moest worden gefixeerd. In beide experimenten was de afbeelding van de stimulus op de retina van het oog vergelijkbaar.

Net als in de experimenten in hoofdstuk 2 en 3 induceerde smooth pursuit oogbewegingen activiteit in de FEF, de SEF, de PEF, de MT/V5 en lobule VI en vermis VI van het cerebellum. Fixatie onderdrukking van de OKR leidde ook tot activatie in de FEF, de PEF, MT/V5, maar niet

in de SEF of het cerebellum (zie tabel 1). De waargenomen activiteit in het smooth pursuit systeem wordt waarschijnlijk opgewekt door de beweging van de stip en de bijbehorende smooth pursuit response.

Bij de directe vergelijking van de twee experimenten, werd geen verschil in activatie waargenomen. Bij een lagere statistische drempelwaarde werd meer activatie in het cerebellum waargenomen tijdens smooth pursuit oogbewegingen. Deze uitkomst betekent dat bij smooth pursuit oogbewegingen en fixatie onderdrukking van de OKR overlappende corticale trajecten worden geactiveerd. Het verschil in cerebellaire activatie wordt waarschijnlijk veroorzaakt door de aanwezigheid van een actieve oogbewegings component in het smooth pursuit experiment. De vergelijkbare activatie van MT/V5 in de twee experimenten ondersteunt de gedachte dat de visuele bewegings stimulatie in de beide experimenten inderdaad hetzelfde was.

Op grond van onze fMRI resultaten concluderen we dat fixatie onderdrukking van de optokinetische reflex kan worden beschouwd als smooth pursuit van een stilstaand object op een niet homogene, bewegende, achtergrond.

DEEL 3 – SACCADISCHE OOGBEWEGINGEN

In het derde deel van dit proefschrift werd de hersenactiviteit onderzocht in relatie tot de saccadische oogbewegingen. We hebben ons daarbij meer specifiek gericht op het cerebellum dat betrokken is bij de nauwkeurigheid van saccades [8].

Functioneel Gebied	Stimulus					Vergelijking		
	A	B	C	D	E	A versus B	C versus B	D versus E
	Enkele stip 	Beperkte levensduur stippen 	Strepen 	Enkele stip met achtergrond 	Fixatie onderdrukking van OKR met achtergrond 			
Frontale Ooggebieden (FEF)	B	-	B	B	B	L	L	-
Supplementaire Ooggebieden (SEF)	L	-	B	L	-	-	-	-
Parietale Ooggebieden (PEF)	B	-	L	B	B	-	L	-
Visueel Gebied 5 (MT/V5)	R	-	R	R	B	R	R	-
Oculomotorisch gebied van het cerebellum	B	R	B	B	-	B	B	-

Tabel 1: Samenvatting van de activiteiten waargenomen tijdens smooth pursuits van een enkele stip, tijdens de optokinetische reflex met beperkte levensduur stippen en strepen, tijdens smooth pursuits van een stip op een stilstaand gestreept patroon, en tijdens fixatie onderdrukking van de OKR van een bewegend gestreept patroon (B: bilateraal; R: rechter hemisfeer; L: linker hemisfeer; - geen significante activiteit).

In **hoofdstuk 5** hebben we de verschillen bestudeerd in zowel de cerebellaire als ook de cerebrale activatie patronen die worden geassocieerd met reflexmatige en vrijwillige saccades. Gedragstudies naar de controle van de nauwkeurigheid van saccades laten zien dat de aanpassing van de amplitudes van saccades niet gelijk is voor reflexmatige en vrijwillige saccades. Er werd daarom beweerd dat de nauwkeurigheid van reflexmatige en vrijwillige saccades door geschieden mechanismen gebeurt [9]. Aangezien het cerebellum een belangrijke structuur is met betrekking tot de controle van saccadische nauwkeurigheid [10-14], zou het mogelijk kunnen zijn dat het cerebellum verschillend betrokken is bij het maken van reflexmatige en vrijwillige saccades.

We hebben de hersenactiviteit die gevonden werd bij reflexmatige en vrijwillige saccades vergeleken. Reflexmatige saccades werden opgewekt door doelen die plotseling verschenen. Vrijwillige saccades werden gemaakt tussen twee altijd zichtbare doelen. Er werd een sterkere activatie in de FEF, PEF, MT/V5 de precuneus (V6), de angular en cingular gyri gezien tijdens reflexmatige saccades dan tijdens vrijwillige saccades. Er werden echter geen verschillen gevonden in de activatie van het cerebellum (zie tabel 2). Deze resultaten geven aan dat de vermeende gescheiden mechanismen voor de controle van reflexieve en vrijwillige saccades eerder te vinden zijn in het cerebrum dan in het cerebellum.

In **hoofdstuk 6** hebben we de rol van het cerebrum en cerebellum bestudeerd in het verwerken van de visuele fouten na het maken van een saccade. Proefpersonen moesten saccadische oogbewegingen maken naar een geflitst doel. In de eerste

Functioneel Gebied	Stimulus				Vergelijking				
	A	B	C	D	A versus B	B versus A	C versus D	D versus C	
	Vrijwillige Saccades 	Reflexmatige Saccades 	Saccades zonder doel stap 	Saccades met willekeurige doel stap 					
Frontale Ooggebieden (FEF)	B	B	B	B	-	B	-	-	
Supplementaire Ooggebieden (SEF)	-	-	-	-	-	-	-	-	
Parietale Ooggebieden (PEF)	L	B	B	B	-	B	-	-	
Visueel Gebied 5 (MT/V5)	-	B	B	B	-	B	-	-	
Oculomotorisch gebied van het cerebellum	-	-	B	B	-	-	-	-	

Tabel 2: Samenvatting van de activiteiten tijdens de reflexmatige en vrijwillige saccades, en tijdens saccades zonder en met willekeurige stappen van het doel tijdens de saccade er naar toe (B: bilateraal; R: rechter hemisfeer; L: linker hemisfeer; - geen significante activiteit).

conditie van het experiment werden grote variabele post-saccadische visuele fouten geïnduceerd door het willekeurig verschuiven van het doel tijdens de saccadische oogbeweging. De willekeurige verdeling van de post-saccadische fouten voorkwam de aanpassing van de saccadische amplitudes, zoals die zou optreden als het doel steeds dezelfde sprong zou maken. In de tweede conditie van het experiment verschoof het doel niet wanneer de proefpersonen een saccadische oogbeweging maakten. Aangezien post-saccadische visuele fouten waarschijnlijk de drijvende kracht zijn van het aanpassingsproces van de amplitude van saccades [15, 16] waarbij het cerebellum sterk betrokken is [10, 11, 13], veronderstelden wij dat specifieke cerebellaire gebieden betrokken zijn bij het verwerken van post-saccadische visuele fouten.

Beide saccadische toestanden lieten de verwachte activatie patronen zien in het cerebrum (FEF, MT/V5) en in de saccade gerelateerde oculomotorische gebieden van het cerebellum (vermis en lobules VI en VII). Bovendien zagen we een toename van de cerebellaire activiteit gerelateerd aan post-saccadische visuele fouten (zie tabel 2): bilateraal in lobule VIII, IX, X, unilateraal in de linker VIIb en vermis VIII. Deze resultaten suggereren een mogelijk rol van andere dan de oculomotorische gebieden in het cerebellum bij het verwerken van post-saccadische visuele fouten.

REFERENTIES

1. Brandt, T., et al., Bilateral functional MRI activation of the basal ganglia and middle temporal/medial superior temporal motion-sensitive areas: optokinetic stimulation in homonymous hemianopia. *Arch Neurol*, 1998. 55(8): p. 1126-31.
2. Bucher, S.F., et al., Sensorimotor cerebral activation during optokinetic nystagmus. A functional MRI study. *Neurology*, 1997. 49(5): p. 1370-7.
3. Dieterich, M., et al., fMRI signal increases and decreases in cortical areas during small-field optokinetic stimulation and central fixation. *Exp Brain Res*, 2003. 148(1): p. 117-27.
4. Dieterich, M., et al., Horizontal or vertical optokinetic stimulation activates visual motion-sensitive, ocular motor and vestibular cortex areas with right hemispheric dominance. An fMRI study. *Brain*, 1998. 121 (Pt 8): p. 1479-95.
5. Dieterich, M., et al., Cerebellar activation during optokinetic stimulation and saccades. *Neurology*, 2000. 54(1): p. 148-55.
6. Konen, C.S., et al., An fMRI study of optokinetic nystagmus and smooth-pursuit eye movements in humans. *Exp Brain Res*, 2005. 165(2): p. 203-16.
7. Mestre, D.R. and G.S. Masson, Ocular responses to motion parallax stimuli: the role of perceptual and attentional factors. *Vision Res*, 1997. 37(12): p. 1627-41.
8. Leigh, R.J. and D.S. Zee, *The Neurology of Eye Movements*. Third ed. 1999, New York: Oxford University Press.
9. Deubel, H., Separate adaptive mechanisms for the control of reactive and volitional saccadic eye movements. *Vision Res*, 1995. 35(23-24): p. 3529-40.
10. Barash, S., et al., Saccadic dysmetria and adaptation after lesions of the cerebellar cortex. *J Neurosci*, 1999. 19(24): p. 10931-9.
11. Desmurget, M., et al., Functional anatomy of saccadic adaptation in humans. *Nat Neurosci*, 1998. 1(6): p. 524-8.
12. Ron, S. and D.A. Robinson, Eye movements evoked by cerebellar stimulation in the alert monkey. *J Neurophysiol*, 1973. 36(6): p. 1004-22.
13. Straube, A., et al., Cerebellar lesions impair rapid saccade amplitude adaptation. *Neurology*, 2001. 57(11): p. 2105-8.
14. Straube, A., et al., Characteristics of saccadic gain adaptation in rhesus macaques. *J Neurophysiol*, 1997. 77(2): p. 874-95.
15. Robinson, F.R., C.T. Noto, and S.E. Bevans, Effect of visual error size on saccade adaptation in monkey. *J Neurophysiol*, 2003. 90(2): p. 1235-44.
16. Wallman, J. and A.F. Fuchs, Saccadic gain modification: visual error drives motor adaptation. *J Neurophysiol*, 1998. 80(5): p. 2405-16.

PART 5

APPENDIX



BART, CAROLINE,
DORIS & EMMA

伯德
頌
恩
繼
蓮

APPENDIX

List of Publications

ARTICLES

Schraa-Tam CKL, Van der Lugt A, Smits M, Frens MA, Van Broekhoven PCA, Van der Geest JN. fMRI of optokinetic eye movements with and without a contribution of smooth pursuit. *J Neuroimaging*. (*J Neuroimaging*, 2008, 18(2):158-167)

Schraa-Tam CKL, Van der Lugt A, Smits M, Van Broekhoven P, Frens M, Van der Geest JN. An fMRI study on smooth pursuit and fixation suppression of the optokinetic reflex using similar visual stimulation. (*Exp Brain Research*, 2008, 185(4):535-544)

Schraa-Tam CKL, Van Broekhoven P, Van der Geest JN, Smits M, Frens M, Van der Lugt A. Cortical and cerebellar activation induced by reflexive and voluntary saccades (*Exp Brain research*, DOI 10.1007/s00221-008-1569-4)

Schraa-Tam CKL, Van der Lugt A, Smits M, Frens M, Van Broekhoven P, Van der Geest JN. Disentangling smooth pursuit and optokinetic eye movements: a functional magnetic resonance imaging study. (Accepted by *Clinical Physiology and Functional Imaging*)

Schraa-Tam CKL, Van Broekhoven P, Van der Lugt A, Smits M, Frens M, Van der Geest JN. Cerebellar contributions to the processing of saccadic errors (submitted)

Smits M, Visch-Brink E, **Schraa-Tam CK**, Koudstaal PJ, Van der Lugt A. Functional Magnetic Resonance Imaging (fMRI) of language: an overview of easy to implement language paradigms for patient care and clinical research. (*RadioGraphics*, 2006, 26:S145-S158)

ABSTRACTS

2007

PCA van Broekhoven, **CKL Schraa-Tam**, MA Frens, A van der Lugt, M Smits, JN van der Geest. Cerebellar activation during saccadic error detection: an fMRI study. Proceedings for the 6th Dutch Endo-Neuro-Psycho Meeting, Doorwerth, Netherlands, 2007 (UAI: 55689a340330115426)

2006

Schraa-Tam CK, Van der Lugt A, Smits M, Frens MA, Van Broekhoven P, Van der Geest JN. A new stimulus for isolating optokinetic eye movement from smooth pursuit. *Proc Intl Soc Mag Reson Med*, 2006

Smits M, **Schraa-Tam CK**, Van der Geest JN, Koudstaal PJ, Van der Lugt A. Evaluation of working memory with functional Magnetic Resonance Imaging (fMRI): an overview of several paradigms and research and clinical applications. Electronic supplement European Congress of Radiology, 2005;14:2804

2005

Schraa-Tam CK, Van der Lugt A, Frens MA, Van Broekhoven P, Smits M, Van der Geest JN. Brain areas activated by bilateral caloric vestibular stimulation with visual stimuli: An fMRI study. Proceedings for the 11th Annual Meeting of the organization of human brain mapping, Toronto, Ontario, Canada, 2005;11:1421.

Schraa-Tam CK, Van der Lugt A, Frens MA, Smits M, Van Broekhoven P, Van der Geest JN. Visual-vestibular stimulation of different temperature (20OC VS 43OC): An fMRI study. Electronic supplement MAGMA, 2005;18:S210 (DOI s10334-005-0116-6).

Schraa-Tam CK, Van der Lugt A, Frens MA, Smits M, Van Broekhoven P, Van der Geest JN. A comparison of the bilateral and unilateral vestibular (caloric) stimulations: An fMRI study. Electronic supplement MAGMA, 2005;18:S211 (DOI s10334-005-0116-6).

Schraa-Tam CKL, Van der Lugt A, Frens MA, Van Broekhoven PCA, Smits M, Van der Geest JN. Brain areas activated by bilateral caloric vestibular stimulation with visual stimuli: An fMRI study. Electronic supplement NeuroImage 2005;26:1421 (DOI 10.1016/j.neurimage.2005.04.020).

2004

Schraa-Tam CK, Van der Lugt A, Frens M, Van der Geest JN. Functional MRI of Optokinetic stimulation with limited and infinite lifetime random dot patterns. Proceedings from the 34th Annual meeting of the Society for Neuroscience, Washington, DC. Program No 630.5.2004.

Van der Geest JN, **Schraa-Tam CK**, Van der Lugt A, Frens M. Functional MRI of Vestibular Cancellation. Proceedings from the 34th Annual meeting of the Society for Neuroscience, Washington, DC. Program No 712.5.2004.

Schraa-Tam CK, Smits M, Van der Lugt A, Van der Geest JN. Functional Magnetic Resonance Imaging (fMRI) of vestibular and visual interactions in caloric vestibular stimulation. Radiological Society of North America scientific assembly and annual meeting program, Oak Brook, IL. Radiological Society of North America, 2004:241.

Schraa-Tam CK, Van der Lugt A, Frens MA, Smits M, Van Broekhoven PC, Van der Geest JN. fMRI of visual and vestibular interaction. Electronic supplement MAGMA, 2004;16:S183.

Schraa-Tam CK, Van der Lugt A, Frens MA, Smits M, Van Broekhoven PC, Van der Geest JN. fMRI of smooth pursuit and optokinetic reflex eye movements. Electronic supplement MAGMA, 2004;16:S184.

Tam C, Van der Geest JN, Smits M, Van der Lugt A. Rest conditions in fMRI: exploring the differences. Proc Intl Soc Mag Reson Med, 2004;11:2542.

CONFERENCE PROCEEDINGS

2006

Schraa-Tam CK, Van der Lugt A, Smits M, Frens MA, Van Broekhoven P, Van der Geest JN. A new stimulus for isolating optokinetic eye movement from smooth pursuit. International Society of Magnetic Resonance and Medical Imaging, Seattle, Washington (USA), 6-12 May 2006: poster presentation.

Smits M, **Schraa-Tam CK**, Van der Geest JN, Koudstaal PJ, Van der Lugt A. Evaluation of working memory with functional Magnetic Resonance Imaging (fMRI): an overview of several paradigms and research and clinical applications. European Congress of Radiology, Vienna (AT), 3-7 March: educational exhibit.

2005

Smits M, Visch-Brink E, **Schraa-Tam CK**, Van der Geest JN, Koudstaal PJ, Van der Lugt A. Functional Magnetic Resonance Imaging (fMRI) of language: an overview of easy to implement language paradigms for clinical and research purposes. Radiological Society of North America 91st Scientific Assembly and Annual Meeting, Chicago (US), 27 Nov - 2 Dec 2005: education exhibit.

Schraa-Tam CK, Van der Lugt A, Frens MA, Van Broekhoven P, Smits M, Van der Geest JN. Brain areas activated by bilateral caloric vestibular stimulation with visual stimuli: An fMRI study. Proceedings for the 11th Annual Meeting of the organization of human brain mapping, Toronto, Ontario (CN), 12-16 June, 2005: poster presentation.

2004

Schraa-Tam CK, Van der Lugt A, Frens M, Van der Geest JN. Functional MRI of Optokinetic stimulation with limited and infinite lifetime random dot patterns. Proceedings from the 34th Annual meeting of the Society for Neuroscience, San Diego, California (US), October 23-27, Oct 2004: poster presentation.

Van der Geest JN, **Schraa-Tam CK**, Van der Lugt A, Frens M. Functional MRI of Vestibular Cancellation. Proceedings for the 34th Annual meeting of the Society for Neuroscience, San Diego, California (US), October 23-27, Oct 2004: oral presentation.

Schraa-Tam CK, Smits M, Van der Lugt A, Van der Geest JN. Functional Magnetic Resonance Imaging (fMRI) of vestibular and visual interactions in caloric vestibular stimulation. Radiological Society of North America 90th Scientific Assembly and Annual Meeting, Chicago (US), 27 Nov - 3 Dec 2004: poster presentation.

Curriculum Vitae - Caroline Kai Lin Schraa-Tam

EDUCATIONAL HISTORY

Doctor of Philosophy
(expecting 7 Jan 2009)
Erasmus University, Rotterdam, The Netherlands
Jan 2003 – June 2007

Master of Science in Neuroscience (2005)
Erasmus University, Rotterdam, The Netherlands
Aug 2004 – Aug 2005

Master of Science in Engineering
Business Management (2003)
The University of Warwick, UK & The Hong
Kong Polytechnic University, Hong Kong
Sept 1999 – June 2002

Master of Engineering in Electrical and
Computer Engineering (1996)
University of Alberta, Canada
Sept 1995 – Dec 1996

Bachelor of Science in Electrical
Engineering (1995)
University of Alberta, Canada
Sept 1991 – June 1995

COMPLETED COURSES

Integrity in Research, A New PhD Course
Department of Ethics and Philosophy,
ErasmusMC, Rotterdam, NL
Jan 2006 – Mar 2006

Classical Methods for Data-Analysis
Netherlands Institute for Health
Sciences, Rotterdam, NL
19 Sept – 14 Oct, 2005

Biomedical English Writing and Communication
Netherlands Institute for Health
Sciences, Rotterdam, NL
Jan 2005 – Apr 2005

fMRI Course
Organization for Human Brain Mapping, USA
12 June 2005

Statistical Parametric Mapping Course
The Institute of Neurology, London, UK
May 2004

Tool-Kit of Cognitive Neuroscience 2004:
Advanced topics in MR imaging of the brain
F.C. Donders Centre for Cognitive
Neuroimaging Nijmegen, NL
11 – 13 March 2004

Toolkit of Cognitive Neuroscience 2004:
advanced course in fMRI data analysis
F.C. Donders Centre for Cognitive
Neuroimaging Nijmegen, NL
2 - 4 Feb, 2004

The 2nd Leuven Clinical fMRI Hands-on
University Hospitals Leuven, Be
2 – 3 Oct, 2003

ISO 9000 Auditor/ Lead Auditor course
ISO 9000 Training Series

WORK EXPERIENCES

Researcher (fMRI)
Erasmus University, Rotterdam, NL
Principal investigator: Prof. Dr.Willem Verbeke
Nov 2007 – present

PhD research project: fMRI
Erasmus MC – University Medical
Centre, Rotterdam, NL
Principal investigator: Dr. Aad van der Lugt
Jan 2003 – June 2007

MRI Application Specialist
Siemens Ltd, Hong Kong
Aug 2000 – Aug 2002

IT co-ordinator, ISO co-ordinator
Sunny Chemicals (HK) Limited
Sept 1998 – Jul 2000

Student researcher
University of Alberta, Canada
Sept 1995 – Dec 1997

AWARDS

Travel award from NIH
2R13 MH062008-06
Conference on Functional Mapping
of the Human Brain

Alexander Rutherford Scholarship
Government of Alberta, Canada
1991

About the Author

Caroline was born and brought up in Hong Kong. She finished her A-level study in Melbourne, Australia. Following her family, she immigrated to Edmonton, Alberta, Canada in the 90's. There she finished her Bachelor degree in Electrical Engineering at the University of Alberta. Within the next year, she finished her first Master degree in Electrical and Computer Engineering. A year later she went back to Hong Kong to start working and there she finished her second Master degree in Business Engineering Management jointly offered by the University of Warwick and the Hong Kong Polytechnic University. Six years ago she married Bart and moved to Rotterdam, The Netherlands. Since then she started her Doctoral degree at Erasmus Medical Centre, Rotterdam. During the past six years, she also gave birth to two beautiful daughters, Doris and Emma; and finished her third Master degree in Neurosciences at Erasmus MC.

Love is patient, love is kind. It is not jealous, (love) is not pompous, it is not inflated, it is not rude, it does not seek its own interests, it is not quick-tempered, it does not brood over injury, it does not rejoice over wrongdoing but rejoices with the truth. It bears all things, believes all things, hopes all things, endures all things.

(1 Corinthians 13:4-7)

Acknowledgement

This dissertation is the result of a lot of support, help, guidance, care, energy, love and creativity from many of you. Thank you.

Department of Radiology, ErasmusMC, Rotterdam, The Netherlands

Prof. Dr. Krestin (Thanks to be my promotor, admitted me for the PhD program and approving my extension); Dr. Aad van der Lugt (Thanks to be my supervisor and helping me through especially when I was having my difficult time); Dr. Marion Smits (Thank you); Prof. Dr. Pattynama (The way you winkle your right eye to say hello is very cute ;)); Dr. Tanghe (Your warm smile and your sincere 'Hello' keep me coming to work every day); Dr. Zwenneke Flach (nice neighbour); Dr. Matheijssen (Thank you for your technical help); people of clusterbureau 7 (nice neighbour, your warm smile and your sincere 'Hello' keep me with hope); Marja, Petra, Wendy, Astrid, Brenda, Marjolein, the secretary member of radiology (Thank you for showing me all the supporting issues); Caroline, Wibeke from the trialbureau (Thank you for your support); Erik-Jan Schoonen (Thank you for arranging all the supporting letters for me); Frans, Thomas, Mika, Zhouli (Thank you for your love and care); Ton, Natasja, Simone, Belinda, Willy, Jane, Agnes, Hanneke, Sita, Annelies, Mattijs, Mijke, Hannie V, Hannie (my gossiping pal.....), Ton (Thank you for making this thesis and making all the changes for me!).

Department of Neuroscience, ErasmusMC, Rotterdam, The Netherlands

Prof. Dr. de Zeeuw (Many thanks for helping me to resolve the outrageous tuition fee that I needed to pay for my Master degree, you are cool man!); Prof. Dr. Borst, Dr. van der Steen (Thanks for admitting and passing me the Master of Neuroscience degree, you guys are like a grandfather to me, thank you.); Prof. Dr. Frens (Thank you for accepting me to your group and helping me through); Dr. van der Geest (Thank you to be my co-promotor, helping me through even though you are always busy and only have time to talk to me while you are smoking outside the building! ☺); Dr. Ruigrok (my tutor in MSc and a role model); Dr. Elgersma, Dr. Hansel, Dr. Holstege, Dr. Hoogenraad, Dr. Brecht, Dr. Jaarsma, Dr. Fekkes (my tutor in MSc); Bart, Beerend, Albertine, Samantha, Heiko, Arthur, Harm, Marc, Michiel (Great pal! Keep up the laughter!!!); Loes, Edith, Susan (Thank you for your support, care, and love); member of Neuroscience (you guys are cool); Cecile (Thank you, my friend ☺....); those who were involved in purchasing the eye-tracker (THANKS! Although it came at the very end of my study and I needed to redo all my experiments with the eye-tracker, at least this gave me a chance to prove myself.)

Institute for Sales and Account Management, Rotterdam, The Netherlands

Prof. Dr. Willem Verbeke, Ralph and Roeland
(Thanks ISAM ©)

Siemens Healthcare

Mr. Denis Leung, CEO of Siemens Ltd., Hong Kong (The best boss, a good leader), Monique Yeung, Wanda Poon, Gloria Chui, Cynthia Tse, KW Wong, Tony Yim, Frederick Chan, CC Fu, Alex Yan, KK Li, Ray Lam, Raymond Wong, Oliver Liu, Jimmy Wong, Jason Lai, Michael Wong and Members of the Department of Medical Solutions of Siemens Hong Kong, Tomas Anderson from Siemens Germany, Marivic, Wai Ling, Roy from Siemens Singapore (Greatest pal on earth!) Bart Schraa, Dr. Erik van den Bergh from Siemens Nederland (Thank you)

United Christian Hospital, Hong Kong, China

Dr. James Chi-sang Chan, Consultant Radiologist and Chief of Service, Department of Radiology and Organ Imaging, Lo, Chik Fai (PDDR), Ho, Man Ho Paul (PDDR, BSc), Ng, Tse Woon (PDDR, MSc, MBA) (Dark chocolate lovers, great Teachers! You guys are the best!)

Department of Biomedical Engineering, University of Alberta, Alberta, Canada

Prof. Dr. Peter S Allen, Prof. Dr. Richard E. Synder, Prof. Dr. Zoltan J. Koles, Ms. Maisie Goh, Ms. Carol Hartle

Canada

Father Ho, Andy and Grace Ho, Willim and Iris Fung, Doris, Mr. and Mrs Hong!

Tintern CEGGS, Oxley College, Melbourne, Australia; Sir Elles Kadoorie Secondary School, St. Clare Primary School, Hong Kong, China

Teachers of all these schools thank you for your selfishness care of teaching and to pass on the knowledge unconditionally. I am sure I was just an ordinary student but without all these basic education, I would never be able to reach the rest of my university studies.

Thank you for guiding, shaping and teaching someone like me who does not even have any significance in your life. I really do appreciate it. Thank you.

My Huisarts

Dr. R.J.M. Laschet (My Dr. Hous, thank you for taking care of Bart, Doris, Emma and me. Thank you for your emotional support also.)

My Family

Dad, Mom, Kelvin, Ivy, Margaret, Bart, Doris, Emma

Henkt, Ans, Willem, Nora, Fabiënne, Ralph, Esmeralda, Karel, Ingeborg, Lisanne, Kelly, Martijn†

Dr. Kai Cheong Diu, Mrs Sui Yan Wong, Prof. Dr. Chui Mei Tiu, Prof. Dr. Yi Hong Chou, Mr. Cheung Kui Poon, Mrs. Chui Hung Poon